THE EFFECTS OF LOW POWERED PULSED RADIO-FREQUENCIES ON WOUND HEALING USING *IN VIVO* AND *IN VITRO* MODEL SYSTEMS.

A THESIS SUBMITTED TO THE UNIVERSITY OF ST. ANDREWS FOR THE DEGREE OF MASTER OF SCIENCE

BY

FIONA CULLEN

DEPARTMENT OF ANATOMY AND
EXPERIMENTAL PATHOLOGY
UNIVERSITY OF ST ANDREWS
ST ANDREWS. SCOTLAND

AUGUST 1987

CONTENTS

SUMMARY

In vitro and *in vivo* models of wound healing were exposed to low powered pulsed radio waves at 27 MHz frequency. All experiments were carried out under blind conditions whereby the experimenter did not know which radio frequency emitting device was active and which was sham. The *in vivo* model used was the chorio-allantoic membrane (CAM) of the chicken embryo maintained in shell-less culture. Burn wounds were inflicted on the CAM and wound healing parameters (wound area, petecheal haemorrhage and ingrowth of vessels) were measured for three days after injury for active and sham exposed wounds. No differences were found between the active and sham exposed groups on any of the measures.

Bovine aorta endothelial (BAES) cells grown in culture were used as the *in vitro* model. The rate of outgrowth of a wounded monolayer of cells was recorded for 3 days for active and sham exposed cultures. No differences in the outgrowth rate were found between the groups. Moreover, cell division showed no differences between the active and sham exposed groups when measured over 5 days. The level of BAES cyclic AMP production were assayed after 2, 3 and 6 days growth. The only difference between the active and sham exposed groups in the level of cyclic AMP was found after 2 days growth.

These results are discussed in the light of clinical and experimental studies on the effects of pulsed radio frequencies, many of which have reported beneficial healing effects. Special attention is given to studies which employed field parameters similar to those used in the work presented here.

DECLARATION

I, Fiona Cullen, hereby certify that this thesis has been composed by myself, that it is a record of my own work, and that it has not been accepted in partial or complete fulfilment of any degree or professional qualification.

Signed ..... Date.29.7.87.

Certified by

Signed ..... Date.29 July 1987

COPYRIGHT

ACKNOWLEDGEMENTS

I would like to convey my appreciation to Professor D Brynmor Thomas for allowing me to use the facilities within the department to carry out my research work under the supervision of Dr C Evans who I am indebted to. I wish to extend my sincere gratitude to the director, Dr R H C Bentall, of the Institute of Bioelectric Research, Romanno Bridge, Peeblesshire for providing funds to make this thesis possible.

My thanks also to Dr J Aiton for his help and advice with the cyclic AMP assay. Special thanks to Mr A Bentall and Mr R Constable for their patient assistance with statistics, and to Mr D Ogden, Mr I Davidson, Mr D Roche, Mr J Mackie and Mr S Edwards for technical help, and to Dr C D'Arrigo, Miss V Ferro and Miss C Wigzell for their practical assistance.

Finally my hearty thanks to Mr and Mrs Nichols for their support in so many ways during my stay in St. Andrews and Dundee.

LIST OF FIGURES

LIST OF TABLES

TABLE 14: The numbers of shell-less eggs entered into the analysis per batch.

TABLE 15: An analysis of variance on the wound parameters on differences between batches.

LIST OF PLATES

PLATE 1: Oscilloscope tracing to show the output of an RFED (Parameters in Table 1). Two pulses are shown, each lasting 80usecs and separated by 920 usecs. The amplitude is arbitarily set and is not indicative of the power output.

PLATE 2: Oscilloscope tracing to show an enlargment of one of the pulses of RF energy shown in Plate 1, oscillating at the carrier frequency of 27 x 10^6 cycles per second (27MHz). The amplitude has been arbitarily set and is not indicative of the power output.

PLATE 3: RFED surrounding culture dish (5.8 cms in dimaeter) as used for cell division and monolayer outgrowth experiments.

PLATE 4: RFED surrounding culture dish (each well 3.5 cms in diameter) used for cyclic AMP measurements.

PLATE 5: RFED surrounding culture dish (6.8 cms in diameter) used for the CAM wound healing model (shell-less culture).

PLATE 6: Apparatus used for cracking the fertile eggs.

PLATE 7: Burning the CAM surface of 10.5 incubation day shell-less cultures.

PLATE 8: Growth line of BAES 90 hours after scraping. The thick arrow indicates an area of pallisading cells. The dotted line is the approximate position of the original growth line and the thin arrow indicates the direction of cell outgrowth (x700).

PLATE 9: The CAM burn wound 1 hour after injury (x20).

PLATE 10: The CAM burn wound 13 hours after injury (x20).

PLATE 11: The CAM burn wound 25 hours after injury (x20).

PLATE 12: The CAM burn wound 37 hours after injury (x20).

PLATE 13: The CAM burn wound 49 hours after injury (x20).

PLATE 14: The CAM burn wound 73 hours after injury (x20).

PLATE 15: Light Microscopy: Unwounded CAM at 10.5 incubation

days, where X marks the probable position of a lymphatic vessel (x400)

PLATE 16: Light Microscopy: Wounded CAM 1 hour after injury where Y marks an area of haemorrhage (x550)

PLATE 17: Light Microscopy: Wounded CAM 24 hours after injury. Z marks an area where some cellular components are beginning to move towards the wound margin (x450)

PLATE 18: Light Microscopy: Wounded CAM 36 hours after injury where T marks the thickened chorionic epithelium (x450)

PLATE 19: Light Microscopy: Wounded CAM 48 hours after injury where T and Z are as given in Plates 17 and 18 (x250)

PLATE 20: Light Microscopy: Wounded CAM 48 hours after injury (wound centre x250)

PLATE 21: Light Microscopy: Wounded CAM 73 hours after injury. Note the extensive inflammatory and necrotic material (purple area) (x250)

PLATE 22: Scanning Electron Microscopy: Wounded CAM 24 hours after injury (wound margin x700)

PLATE 23: Scanning Electron Microscopy: Wounded CAM 48 hours after injury (wound margin x700)

PLATE 24: Scanning Electron Microscopy: Wounded CAM 73 hours after injury (complete wound x45)

PLATE 25: Scanning Electron Microscopy: Wounded CAM 73 hours after injury (wound margin x700)

INTRODUCTION

1. ELECTRICITY AND HEALING

Special electrical events have been associated with tissue injury for a considerable amount of time. Inflammatory skin conditions were noted by Adam in 1799 to respond to Faradic and Galvanic stimulation (Adam, 1799). Dubois-Reymond (1860) showed that near an injury, nerves are externally electronegative with respect to the uninjured portions, and he inferred a flow of current around a wound. Over a century later potential differences from 51-64mV (inside negative) were measured in the human skin (Barker et al, 1982) and wound electrical fields of 100-200mV/mm were measured in the cavie glabrous epidermis (Barker et al, 1982). Barker proposed that these fields help guide the cellular movements that close wounds. Electrical fields have also been found to be associated with developing organisms, as exemplified by the oocytes of the *Xenopus* toad, which have a current of 0.9uA/cm^2 entering at the animal pole and leaving at the vegetable pole (Jaffe, 1979). These currents have been measured in plants as well as animal cells and Nuccitelli (1984) suggests that they are caused by the spatial separation of ion leaks and pumps in the plasma membrane. Regenerating newt limbs (*Triturus viridescens*), moreover, have a current from 30-100 uA/cm ^{2} which leaves the regenerating end of the limb and enters through the proximal end and shoulder throughout regeneration (Borgens, 1982). Most of

these measurements, of both intercellular and intracellular fields, have been achieved using the vibrating probe technique (Jaffe and Nuccitelli, 1977). All of the above mentioned fields are of endogenous origin, and it has been proposed that in areas of intense cell division and growth, as seen in both development and repair, they are mobilised to aid the formation of new tissues (Borgens, 1982).

2. THE ELECTROMAGNETIC FIELD

The modulation of an electrical field produces an associated magnetic field, and together these are referred to as an electromagnetic field. Electromagnetic fields have frequencies ranging from $0-10^{18}$Hertz (where 1 Hertz (Hz)= 1 cycle per second) as shown in Figure 1. Both the magnetic and electric fields vary sinusoidally in amplitude at a rate equal to the frequency of the wave. The direction of the electric and magnetic fields are perpendicular to each other and to the direction of propagation. The electric field or field strength is measured in volts/metre (V/m) and the magnetic field in amperes/metre (A/m). The magnetic field strength is related to a further quantity, the magnetic flux density, measured in Teslas (T) so that;

(see over)

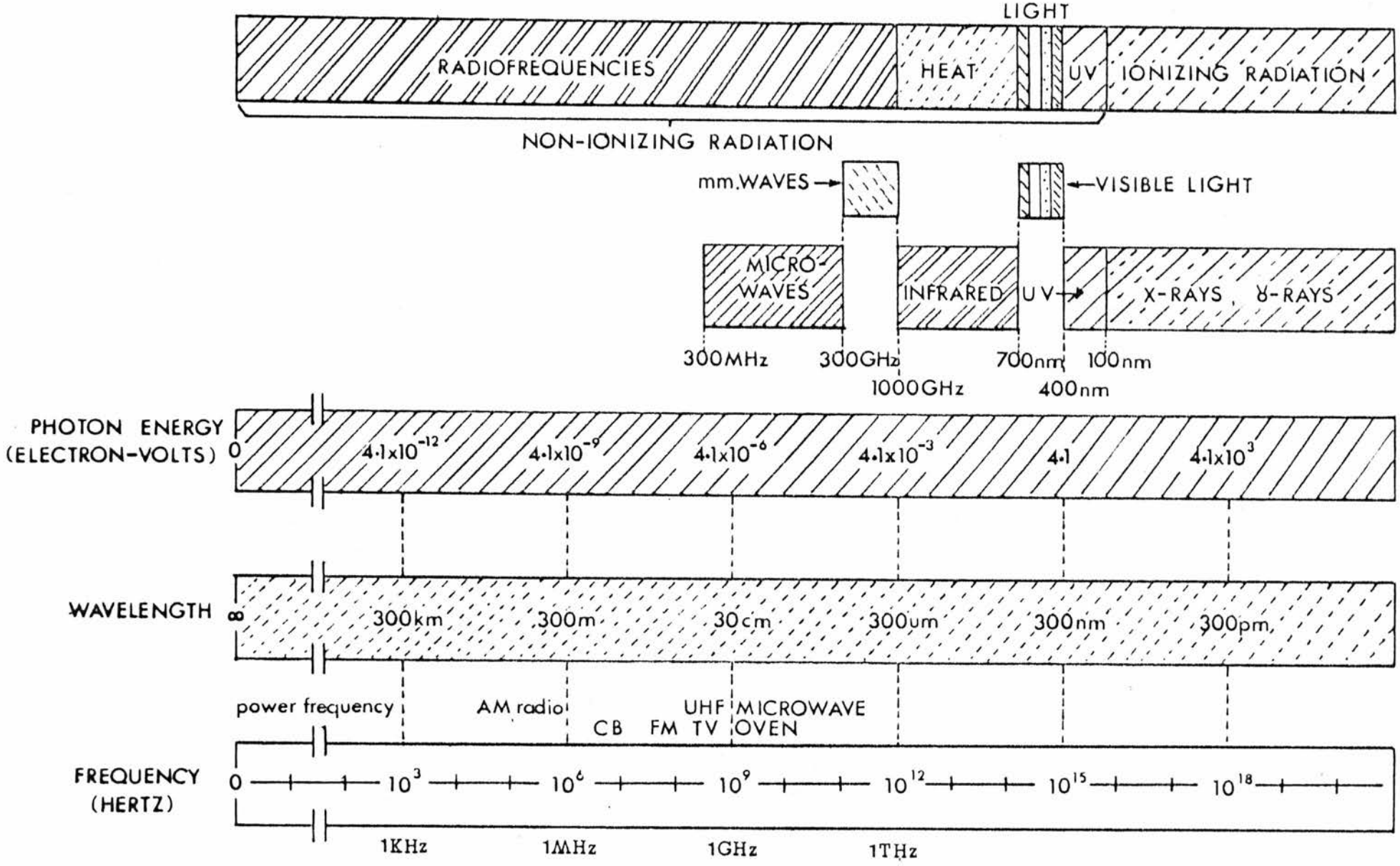

FIGURE 1 : Electromagnetic spectrum in terms of frequency, wavelength and photon energy (from Petersen 1983)

TABLE 1

The division of the radio frequency spectrum into bands (from Adey 1981).

BAND FREQUENCY	NAME	ABBREV.
DC-300Hz	Extremely Low Frequencies	ELF
300Hz-10KHz	Very Low Frequencies	VLF
10KHz-1MHz	Low Frequencies	LF
1MHz-30MHZ	High Frequencies	HF
30MHz-300MHz	Very High Frequencies	VHF
300MHz-300GHz	Microwave Frequencies	MW

$B=u_oH$

where B = magnetic flux density

H = magnetic field strength

u_o= 4 pi x 10^{-7} H/m (permeability of free space).

The vector product of the electric and magnetic field strengths represents the rate of electromagetic energy transported per unit area and is called the power density, which is measured in Watts/m^2 or W/cm^2. Biological effects are usually related to the energy absorbed per unit mass of absorbing material, referred to as the specific absorbtion rate (SAR) expressed in Watts per kg (W/kg). The SAR is a purely dosimetric quantity and presupposes no particular interaction mechanism.

The electromagnetic spectrum is divided by frequency and wavelength into a number of bands (Figure 1) and radio-frequencies (RF) have been further subdivided for convenience when used for communication purposes (Table 1). The spectrum is also divided by the effect of a given frequency when interacting with biological material, namely whether or not it is ionising. An ionising field is one which can alter the intramolecular structure or break intermolecular bonds of a substance so forming ions. Only frequencies possessing energy above a certain threshold are able to produce ionization and the

threshold is described in photon energies. The photon is used as a means of describing electromagnetic waves in terms of a flux of particles, and whose energy is related to the wavelength and frequency by Plank's constant (4.13×10^{-15} electron volt seconds (eVs)). In standard atmospheric conditions photon energies of approximately 10-12 eV are needed to produce ionization in simple atoms. Hence RF is not capable of directly causing ionization and is therefore considered as non-ionizing (Figure 1).

Electromagnetic waves occur naturally besides being formed from man made sources. Natural sources include emittence from the sun, galaxies and the earth, but the highest field strengths are electric fields as experienced during thunder storms which reach from $10-10^5$ V/m. Ordinarily the natural background is 10^{-5} uW/cm^2 maximum (5×10^{-5} T magnetic flux density). Man made sources of RF are widespread and ever increasing, but the sources responsible for the largest percentage of environmental RF energy are communication systems. The field strength may reach $0.005 uW/cm^2$ and $1-97 uW/cm^2$ near antennae (Repacholi, 1983). Other man made sources include heating devices (microwave ovens, diathermy, blood warmers, hyperthermic heaters), radars, welding equipment and other industrial appliances. Since this rapid increase in the use of RF equipment, the investigation of the biological effects of RF

TABLE 2

The categories of reports selected from the experimental literature used in the setting of exposure levels by the ANSI report (1982) (from Petersen 1982)

1. Environmental
2. Behaviour and physiology
3. Immunology
4. Teratology
5. Central Nervous System/ blood brain barrier
6. Cataracts
7. Genetics
8. Human studies
8. Thermoregulation and metabolism
10. Biorhythms
11. Endocrinology
12. Developmental
13. Evoked auditory response
14. Haematology
15. Cardiovascular

fields to enable the setting of exposure safety levels has been intense. At least 130 categories of effects have been reported (Glaser, 1971), but only the 15 given in Table 2 were employed by the American National Standard Institute (ANSI) in 1982. Their report (ANSI, 1982) resulted in the setting of an exposure level of up to 0.4W/kg whole body exposure. The lowest SAR at which positive bioeffects were observed was 0.003W/kg, (calcium ion flux perturbation in excised brain tissue: Bawin, 1978), and although effects agreed to be 'hazardous' by the panel were not seen at SARs lower than 5W/kg, the 0.4W/kg standard allowed for a safety margin. Each effect was found to have a defined threshold below which the effect was no longer observed, unlike the linear dose response usually assumed with ionizing radiation. Upper, as well as lower thresholds for bioeffects have been observed producing 'window effects', for frequency (Hisenkamp, 1978; DeHaas, 1979), magnetic flux density (Delgado et al, 1982) and pulse repetition frequencies (Delport et al, 1985). The lowest thresholds (as measured in power density) at which bioeffects were observed were found to be associated with pulsed electromagnetic fields (PEMF) rather than continuous wave fields (Bawin, 1978). More comprehensive limits separating occupational (left at 0.4W/kg) and public exposure (reduced to 0.08W/kg) were set by the World Health Organization, the United Nations Environmental Programme and the International Non-Ionizing Radiation Committee of the International Radiation

Protection Association (WHO/UNEP/INIRC-IRPA, 1981) and reference was made to the existence of possible non-thermal effects of RF.

The thermal versus non-thermal approaches in the effects of non-ionizing electromagnetic fields has been an area of much controversy. A thermal effect is one in which the same effect can be produced alternatively through heating the system in a different way. Conversly, a non-thermal or athermal effect, is one in which the irradiated sytem changes its properites in a way that cannot be achieved by heating (ie when its response is nonlinear) and has been referred to as a direct effect (Frohlich, 1982). Excluding the use of diathermy ("deep heat" treatment using continuous wave RF of frequency 27.12MHz), it has been generally supposed that it is the action of direct non-thermal effects which are responsible for the reported beneficial effects of RF. Most of the studies have been carried out at power densities less than 10mW/cm^2 and with SARs of less than 5W/kg.

(P.T.O)

The last 20 years has seen an increase of interest in the possible clinical applications of electrical and electromagnetic fields in a variety of forms (Illinger, 1981). Most of the work has been on hard tissue which has yielded impressive positive findings and provided impetus for investigations on soft tissues as well as cell and tissue culture.

3. HARD TISSUE HEALING

Bone potentials of piezoelectric nature which are directly related to compression effects were observed by Yasuda (1953). He reported that the compressed parts of the long bones of rabbits showed negative electric potentials, and parts under tension showed positive potentials. Cochran (1968) measured potentials from 0.05 to 20mV across strips of bone *in vitro* between two electrodes placed 15mm apart on opposite sides of the sample. Bassett and Becker (1971) suggested that the observed stress related potentials might influence the activity of osseous cells directly. This concept led to numerous clinical and experimental studies on fracture healing in which efforts were made to artificially stimulate bone growth. The way in which electromagnetic fields have been applied to bones in the clinical setting can be divided as follows;

a. implanted electrodes

b. surface electrodes: capacitive plate

c. surface electrodes: inductive coils.

a. Implanted Electrodes

The early work on the formation of bone growth in broken bones using implanted electrodes was carried out in animals and has been reviewed by Cochran (1972). Bone was formed at the cathode using direct current and Cochran (1972) quotes an optimal current range of 5-20 uA with little effect below 2uA. The threshold at which the bone was formed varied between experimenters probably due to the wide variation in the electrode materials. There are, however, fundamental problems with the use of implanted electrodes; the tissue at the anode can become necrosed, electrolytic by-products and foreign chemical species are formed, the electrodes become polarized and the electrode-stimulated bone formation is limited spatially. Moreover, surgery is needed for both the implantation and extraction of electrodes, and most fractures will heal without the need for surgery.

b. Surface Electrodes: Capacitive plates

The capacitive field is fundamentally electrical and is present when a tissue is placed between two insulated metal plates which carry a pulsed or time dependent (AC) voltage. The peak electric field is uniform throughout the specimen placed between the plates and is frequency independent. The magnetic field is circumferentially directed and increases as you move out

radially. The magnetic field peak increases linearly with frequency. The capacitive device needs a larger voltage than implanted electrodes and hence a large power pack, and is correspondingly likely to be more hazardous in the clinical environment. Few clinical trials have been carried out using capacitive fields (Martin and Gutman, 1978, McElhaney et al, 1968), and once it was found that results from the use of capacitive devices were no better than those obtained using the inductive device, much more of the research effort was directed towards the use of inductive coils.

c. Surface Electrodes: Inductive coils.

The inductive field is fundamentally magnetic and is produced when a coil of metal wire carrying a pulsed current is placed over the tissue sample. A pair of coils can be used, one either side of the specimen; this creates a more uniform field and tissue coupling is enhanced. The magnetic field is uniform with the peak value inversely proportional to frequency. The electric field is circumferentially directed and the peak value is independent of frequency.

The most prolific output of studies, and certainly the most impressive positive findings in the use of inductive devices on hard tissue healing, have been achieved by Bassett's group. After their early work with static fields on bone healing

(Bassett et al, 1964) Bassett and his group employed pulsed electromagnetic fields (PEMFs) and theorized that the detail of the pulse rise time, shape, duration and repetition rates are crucial in exerting an influence on ionic species in the vicinity of the cell. They aimed to mimic the characteristics of strain generated pulses arising in living bone due to physiological deformation. An early study on dogs using PEMFs (Bassett et al, 1974) with surgically produced bilateral osteotomies made use of two stimuli from a single coil placed over the wound; one consisted of 1.5ms pulses repeated at 1Hz (said to induce a maximum voltage of 2mV/cm in the bone), while the other consisted of 0.15ms pulses repeated at 65Hz. No changes in stiffness or histology were found in the 1Hz group, but changes were found in the 65 Hz group. There were 21 animals studied in this group and results from 8 were not analysed due to infection or because the devices delivered the wrong pulse form. Ten of the remaining 13 dogs demonstrated greater stiffness for the stimulated legs with histological and radiological changes suggestive of healing.

From 1977 onward the Bassett group changed the waveform parameters they used to a 300us pulse repeated at 75Hz giving a peak magnetic field at the centre of the coil of 16mT. A

successfully treated (Bassett et al, 1977). However, surgical intervention was necessary in 4 cases and some patients had longer treatment times than the 12-16 hours a day for 3-6 months normal treatment. Of the 14 acquired non-unions, 10 achieved final function and another was making slow progress; this gave a success rate of 76%. A study on 220 patients with acquired non-unions (Bassett et al, 1978) used a pair of coils, one placed on either side of the leg so producing a more uniform field. Two waveforms were used, one as in the 1977 study, while the other was a 5ms pulse burst repeated at 10-14Hz. The individual pulses were 30us wide, repeated every 200us (further details of the magetic field strength were not given). Of the 220 patients 108 had their results analysed and no discussion was made of the eliminated 112. Over 80% of the 108 achieved functional union. This work was extended (Bassett et al, 1979) for a further treatment of 318 fractures of which 249 reached a definable end point which the authors failed to define. Further reports quoted gave successful treatments of over 80% of cases (Bassett et al, 1981a, 1981b), and a review of 1078 cases from studies carried out world wide gave a success rate of 80%. Most of this work used a 15Hz pulse burst waveform. A summary of the waveforms used by Bassett's group quoted here together with those of Barker et al (1984) are given in Appendix 1 (page 81).

Of the clinical trials quoted above, none have been carried out in a double blind manner, whereby both active and sham devices are used and where the clinical experimenter and the patient are

ignorant of the state of the device used. Furthermore, Bassett layed great stress on detailed orthopaedic care, which was different to the treatment given to patients not in the study. In fact his group stated, "Non-unions heal rapidly with pulsing electromagnetic coils if the coils are central to a total orthopaedic care system" (Bassett et al, 1979). The care included improved immobilization and stricter emphasis on non-weightbearing. Perhaps not surprisingly, independent studies carried out using the same methods as established by Bassett with equal attention to orthopaedic care, proved equally as successful (Sutcliffe et al, 1980; O'Conner, 1980; Sedel et al, 1981). In the absence of an appropriately controlled study it still remains open to question as to whether the success was due to electromagnetic effects or to increased patient care or some other effect.

In order to clarify the clinical situation a double blind study was designed, and an interim report on 16 patients who had completed 24 weeks of treatment has been published (Barker et al, 1984). The patients suffered from fractures of the tibia which had remained un-united at least 12 months after injury. The irradiation equipment was similar to that developed by Bassett and as described by Barker and Lunt (1983); it had parameters of 1.5mT peak, 5ms burst waveform repeated at 15Hz. Five of the 9 patients allocated active treatment had clinically

united fractures at the end of the trial, but 5 of the 7 controls also had united fractures. In each treatment group all fractures which had become clinically united by week 24 remained so at week 48. The authors (Barker et al, 1984) concluded that, "the possible explanations for this result include high efficacy of long term immobilization of the limb and avoidance of weight bearing, the placebo effect of the patients "treating" themselves for extended periods each day, the limits on patient activity during waking hours caused by being connected to the machine with a cable approximately 2 metres long, the additional attention they receive on their frequent visits to the clinic or any combination of the above." (Barker et al, 1984).

Hard tissue healing studies using inductive coils on animals have included more controls and the work of Bassett's group on dogs (Bassett et al, 1974) was repeated independently yielding negative results (Enzler et al, 1980). Hisenkamp (1978b), using rat tibial osteotomies, tested three waveforms with 2Hz, 11Hz and 20Hz in group sizes of 5-9 animals and bursts of positive potential peaks 5ms wide (the magnetic intensity value was not given). Mechanical progress was measured by the attachment of weights to a support fixed to the rat leg in the area of the osteotomy, and which incorporated a hinge system when a set of pins were removed. The force required to reproduce the deformation was proportional to the bone

consolidation. He found a window effect in that only the 11Hz treated group showed increased mechanical progress and only in the early stages. DeHaas (1979) studied the effect of 0.1Hz, 1Hz and 4Hz sine wave magnetic fields on the healing of osteotomised rabbit radius using fields of 25mT. Accelerated healing rates were found in the early stages (first 2 weeks) but these differences which were not sustained over 4 weeks.

4. SOFT TISSUE HEALING

Virtually all 'normal' soft tissue healing proceeds through progressive stages of blood clotting, inflammation, (to remove damaged materials), proliferation (to replace damaged cells and their products), and remodelling (to recreate the normal structure as closely as possible). Inadequate healing may result from any number of factors that have interfered at one or more levels in the healing process, and similarly, the action of electromagnetic fields on soft tissue healing may be at one or more levels. The effects of electromagnetic fields on soft tissue healing have not been as widely studied as hard tissue, either clinically or experimentally.

As mentioned earlier, electric fields from 100 to 200mV/mm have been measured at a wound edge (Barker et al, 1982), and if

natural fields at the wound edges affect the healing process, then it may be possible to accelerate healing by enhancing them through the application of external sources. Some studies have employed RF parameters as used in bone healing trials while others have used the same frequency as in the technique of diathermy ('deep heat' treatment); namely 27MHz, but at a reduced power density. Diathermy treatment is thought to increase the blood flow resulting from the thermal action. Vasodilation is generally beneficial to the healing of soft tissue injuries through the actions of increased oxygen, nutrition and a better inflammatory response. However, in the last 20 years there have been claims for healing effects which are non-theraml acting at reduced power densities.

Successes of up to 50% were reported in the healing of ulcers of various types by the application of DC electrical stimulation (Wolcott et al, 1969; Gault and Gatens, 1976). Stress was placed on meticulous nursing care including attention to external pressure, friction, heating, moisture, hygiene, nutrition and circulation during the period of stimulation. No sham devices were used to act as controls. A double blind study (Wilson, 1972) was carried out using PEMF on 20 pairs of patients matched for age and sex suffering from inversion of the ankle (assumed to be a sprained ankle although no further details are given). This study employed an irradiation device

referred to as 'Diapulse', with a peak power of 975 Watts, pulsed at 27MHz and with a pulse duration of 65 microseconds. No figure is given for the power received by the tissue. The treatment was for one hour for each of three days and the patients were assessed for swelling, pain and disability before and after treatment. The active treatment was found to be preferable to the sham on all scores and significant differences were demonstrated for pain and disability scores. A further double blind study was carried out using the Diapulse machine on medium-thickness split-skin graft wounds in man (Goldin et al, 1981). A mean energy output was given of 25.3 Watts with a 3 cms depth penetration. The patients were assessed on the degree of pain and the state of healing. 17 out of 29 patients with active machines had donor site wounds that were 90% or more healed at seven days compared with 11 out of 38 patients using the sham machine (59% and 29% healing respectively).

Another clinical trial was implemented on the postoperative reaction after cosmetic surgery to remove excess skin from the upper and /or lower eyelids, referred to as a blepharoplasty (Nicolle and Bentall, 1982). The RF devices used had the same parameters as those used in the present study (see Table 3), but were fitted into spectacles which had had the lenses removed. Only one device in each pair of glasses was active, and the patient and experimenter did not know the nature of the devices.

The spectacles were worn by 21 patients for 24 hours after bilateral blepharoplasty. The patients were assessed for oedema and bruising, at 1, 3 and 6 days post operatively. In 11 cases, improvement (paricularly at 24 hours) was apparent in patients with the active as compared with the sham device.

Animal models used for the study of soft tissue wound healing in response to PEMFs are few. The tensile strength of 25 rat abdominal wounds was measured after the animals had been killed at 2 and 8 days after injury. The volume of water needed to be added into a plastic bag placed in the peritoneal cavity, so causing the wound to burst, was measured (Bentall, 1981). A placebo group was compared with two irradiated groups using the same electromagnetic parameters given in Table 3, but at two power levels (2mW and 15W) above. Both of the power levels were found to increase the wound tensile strength after 2 and 8 days of healing as compared with that in the placebo group. Rabbits were used in the investigation of the healing of ligaments using PEMF at 1Hz, 350mA square wave for up to 6 weeks (Frank et al, 1983); earlier recovery was observed based on histological, chemical and mechanical indices.

5. CELLULAR AND BIOCHEMICAL EFFECTS

Indirect indices of wound healing have been measured in rat skin

flaps maintained in culture and fixed on a perspex frame during PEMF irradiation (Delport et al 1985). Protein incorporation, DNA synthesis, membrane transport of amino acids and the cellular levels of cyclic AMP and ATP were assessed after the skin flaps had been irradiated for 30-60 minutes using an active or sham device. The irradiation used a driving voltage of 5-20 V, had a pulse frequency of 0.5-10KHz, a pulse width of 150usec, pulse-burst frequency from 1-70 Hz and the number of pulses per burst from 1-100. The authors reported a stimulatory effect of the PEMF on protein synthesis and on the transport of amino acids across the membrane, both of which increased from 20-52% as compared with controls. No stimulatory effects were reported on DNA synthesis, cyclic AMP or ATP levels. From this it was suggested that the PEMF enhanced the transport of precursors across the cell membrane. The effects were dependent on specific electromagnetic parameters. The fields needed to be applied perpendicularly to the skin flaps and the following parameter ranges were needed: pulse frequencies from 1-5KHz, pulse widths of 10-20usecs and pulse burst frequencies from 10-30. Similar but more persistent results were obtained when, instead of pulse bursts, continuously running pulses with otherwise identical parameters were used.

Contrary to the negative results of Delport et al (1985) on DNA synthesis and cyclic AMP, other studies based on cell culture

work did show changes in these and other parameters. RNA synthesis in salivary gland chromosomes of the dipteran *Sciara coprophila* was found to be stimulated as reflected in transcriptional autoradiography and by analysis of (^{3}H) uridine uptake (Goodman et al, 1983; Goodman and Henderson, 1986). A sinusoidal and a quasi-rectangular wave form (repetitive single pulses and repetitive pulse bursts) were used in this study. The frequencies ranged from 1.5-72Hz, the magnetic field strengths from 1.2-3.6x10^{-3} T, and the electric field strengths from 1.6-15mV. Transcriptional uptake was most pronounced at 72Hz and from 3.5-3.8x10^{-3} T in the single pulse and sinusoidal waveforms, and to a lesser extent in the pulse burst waveforms. The chromosomes were irradiated for up to an hour and peak responses were seen at 15-30 minutes. From the results the authors were unable to conclude whether any one field parameter was responsible for the effectiveness of the PEMF in inducing transcription. Enhanced DNA synthesis was found in human fibroblasts when they were exposed to sinusoidally varying magnetic fields for a wide range of frequencies (15Hz to 4kHz) and magnetic fluxes (2.3 x 10^{-6} to 5.6 x 10^{-4} T), which are similar to the levels used clinically (Liboff et al, 1984). Peak responses were seen at 20 hours in 10 different combinations of field parameters. However, Takahashi et al (1986) tested the effect of pulse width, magnetic flux and frequency on DNA systhesis in Chinese hamster V79 cells, and

found enhancement at more specific parameters. Only pulse widths of 25us, frequencies of 10 and 100Hz and magnetic flux densities from 2-8 $\times 10^{-5}$ T gave enhanced DNA synthesis.

An enhancement of DNA synthesis in embryonic chick epiphyseal cartilage cells in response to a 5Hz oscillating electric field of 1166 V/cm was reduced when sodium and calcium fluxes were inhibited (Rodan et al 1978). This suggests that the ionic fluxes generated by the field perturbations trigger DNA synthesis in the cells. Interestingly, the enhancement appeared to be tissue specific as no effect was seen using the same field parameters on chick fibroblasts and rat spleen lymphocytes.

Cell proliferation, besides being associated with an increase in DNA and RNA synthesis, is also accompanied by membrane depolarization (Jaffe, 1976) and changes in cyclic AMP levels. Cyclic AMP acts as an information vehicle carrying messages at the cellular level and its production is controlled by the membrane bound enzyme, adenylate cyclase. The primary site of action of PEMF is thought to be at the cell membrane, causing either a perturbation of ion-transport phenomena (Pilla, 1979), or a change in the level of cyclic AMP (Luben et al, 1982). The hypothesis that cell membrane dependent cyclic AMP changes convey and mediate the electrogenically induced effects on bone remodelling has been investigated by Norton et al (1977). They

employed an *in-vitro* model of both intact and isolated cells from chick embryo epiphyseal cartilage. The isolated cells were simulated using potential differences from 0-1500 V oscillating at 5Hz, giving a suggested cell exposure in the order of millivolts. The optimal exposure time was found to be 10 minutes and voltages above approximately 600V decreased the cyclic AMP cell content. A similar dose response was carried out on 52 pairs of intact tibia which were irradiated for up to 25 minutes. In this instance the level of cyclic AMP was found to rise significantly above the controls when the voltages were above 900V. The peak response was found to be at 5 minutes and the differences were seen only when the tibiai were placed parallel to the field. Thus, the effects on the intact epiphysis and on the isolated cells were opposite, a situation postulated to result from the state of maturation of the cells. In partial agreement with these findings are those of Farndale (1984) who found increased levels of basal cyclic AMP in rabbit bone marrow cells. However, these results were not repeated by Farndale and Murray (1986) who found no significant differences in basal cellular levels in the same cells. Measurements made of the response of chicken tendon fibroblasts cells to prostaglandin E_2 at times of up to 10 minutes showed lower levels of cyclic AMP were found in the PEMF treated cultures than in the controls. The PEMF was of the same parameters as used by Bassett et al (1977): 75Hz with a pulse width of 300usec and peak induced

current density of 10uA/cm^2. Prostaglandin E_2 activates adenylate cyclase and is involved in bone resorption; the authors proposed that the adenylate cyclase complex was temporarily inactivated by prolonged exposure to PEMF by a process of desensitization.

6. THE PRESENT STUDY

The work presented here uses both an *in vitro* and *in vivo* wound healing models to test the effects of low powered PEMFs on soft tissue healing. The hypothesis that the division and outgrowth of endothelial cells could be enhanced is derived from the beneficial results seen using low powered RF on soft tissue healing (Goldin et al, 1981; Wilson, 1972; Nicolle and Bentall, 1982). The response could be due in part to an increase in the microcirculatory system reflected in an increase in surrounding wound capillaries. Bovine aorta endothelial (BAES) cells are used here to test this hypothesis and also to observe whether the basal cellular levels of cyclic AMP are changed on exposure to PEMFs. It has been suggested that the effects of RF are not only tissue specific but are also dependent on the maturation of the cells and on the presence or absence of the cellular matrix (Delport et al 1985), so it is particularly pertinent to use an *in vivo* as well as an *in vitro* model. The *in vivo* model used is the wounded chorio-allantoic membrane (CAM) of the chicken embryo. It has been chosen because it represents a reproducible

model system providing a multilayered soft tissue in association with a complete physiological system in a form suitable for experimentation.

The RF parameters used have the same frequency as that of the 'Diapulse' machine which has shown some positive effects (Wilson, 1972; Goldin et al, 1981). The repetition frequency was set arbitrarily at 1Hz on the basis of results having been obtained over a wide range of frequencies (Liboff et al, 1984), and the power levels and magnetic fluxes were set in the same range (Table 3) as those used by Bentall (1981). The particular parameters used in this study were selected in the light of beneficial effects reported by Nicolle and Bentall (1982).

METHODS AND MATERIALS

6. IRRADIATION DEVICES

Radio frequency emitting devices (RFEDs) were supplied by Medical Electronics (Scotland) Ltd. They consisted of an elastomer module containing the circuitry necessary to convert battery energy into pulsed electromagnetic energy which was transmitted from an attached coil. The coil (a coaxial loop antenna) was made to fit around the size of dish used. There were three different RFED designs used in this study, all of which emitted low power, pulsed electromagnetic frequencies (PEMF) of the parameters as given in Table 3 (unless otherwise stated) and depicted in oscilloscope tracings in Plates 1 and 2. The three types of RFEDs used are demonstrated in Plates 3, 4 and 5. The RFEDs of any of the three designs were paired such that one of each pair was an actively irradiating device while the other was a sham device. Both types (active and sham) were identical in appearance and content but the battery connection in the sham device was broken. The strongest region of electrical influence of an active RFED is in the area encompassed by the coaxial cable and within the plane of the loop of cable. This electrical influence within the loop possesses rotational symmetry about the axis of the loop. Therefore, specimens or regions at the same distance from the centre of the loop, and with the same orientation to the centre of the loop, will experience the same electrical influence. Guidelines for the use of the RFEDs were supplied by Dr T Cox

TABLE 3

Parameters of the RFEDs

carrier frequency	:26MHz
pulse repetition frequency	:1000Hz
pulse duration	:80usec
power output	:400uWatts
central magnetic flux	:1uTesla

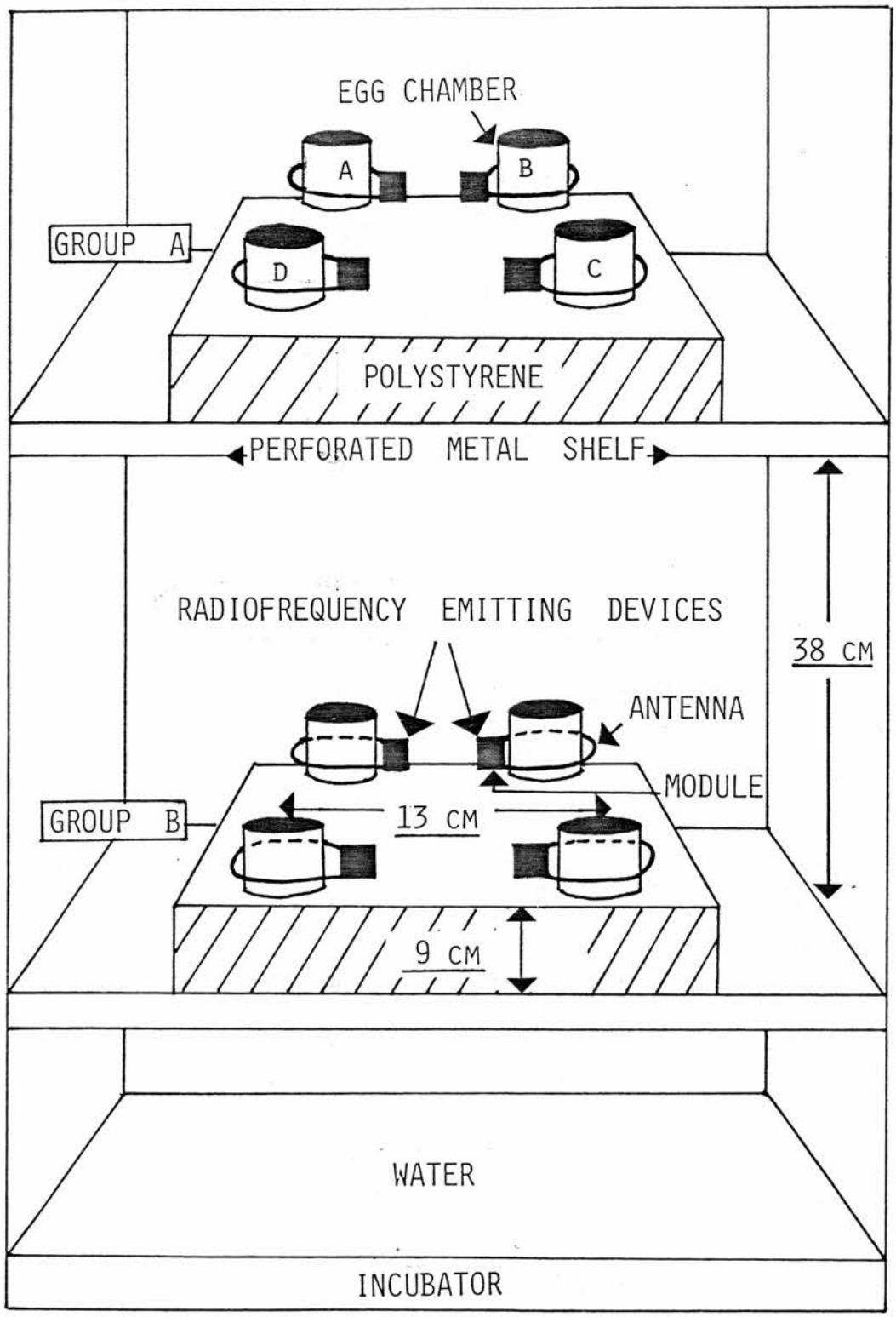

FIGURE 5 : RFED arrangement inside the incubator as used for the CAM wound model.

TABLE 4

Interference factors between RFEDs A, B, C, and D (Fig. 5)

COILS INTERACTING	INTERFERENCE FACTORS
AB	6.7%
BC	4.5%
BD	2.3%

(Medical Electronics, Scotland). Owing to a stray electrical influence around the outside of the cable loop, and above and below it, a distance of at least 25cms between active and sham devices was recommended. Moreover, active devices needed to be from 10 to 15cms from any metal object to maintain interference at a minimum. The incubator used for the *in vitro* studies had metal sides but glass shelves, and its size dictated that only one pair of RFEDs could be used at any given time. In the case of the *in vivo* study a larger incubator was used but a degree of interference was still experienced (see Table 4). In each study the experimenter was blind at all times to the nature of the RFEDs, which were coded and tested for activity by an impartial colleague at the start and finish of each experiment.

The two designs of RFED used for the *in vitro* studies are illustrated in Plates 3 and 4. Plate 3 shows the RFED which was made to encompass a 58mm petri-dish as used in both the cell division and the wounded monolayer studies. The RFED in Plate 4 was designed to encompass a six well square plate as used in measurements of cellular levels of cyclic AMP. The magnetic flux pattern in the area encompassed by the RFED fitting the 58mm dishes is the same as that shown in Figure 2. The magnetic flux values in the centre of each of the six wells when encompassed by the RFED shown in Plate 4 ranged from 0.66-0.73uT and the frequency was 22.3MHz, otherwise the

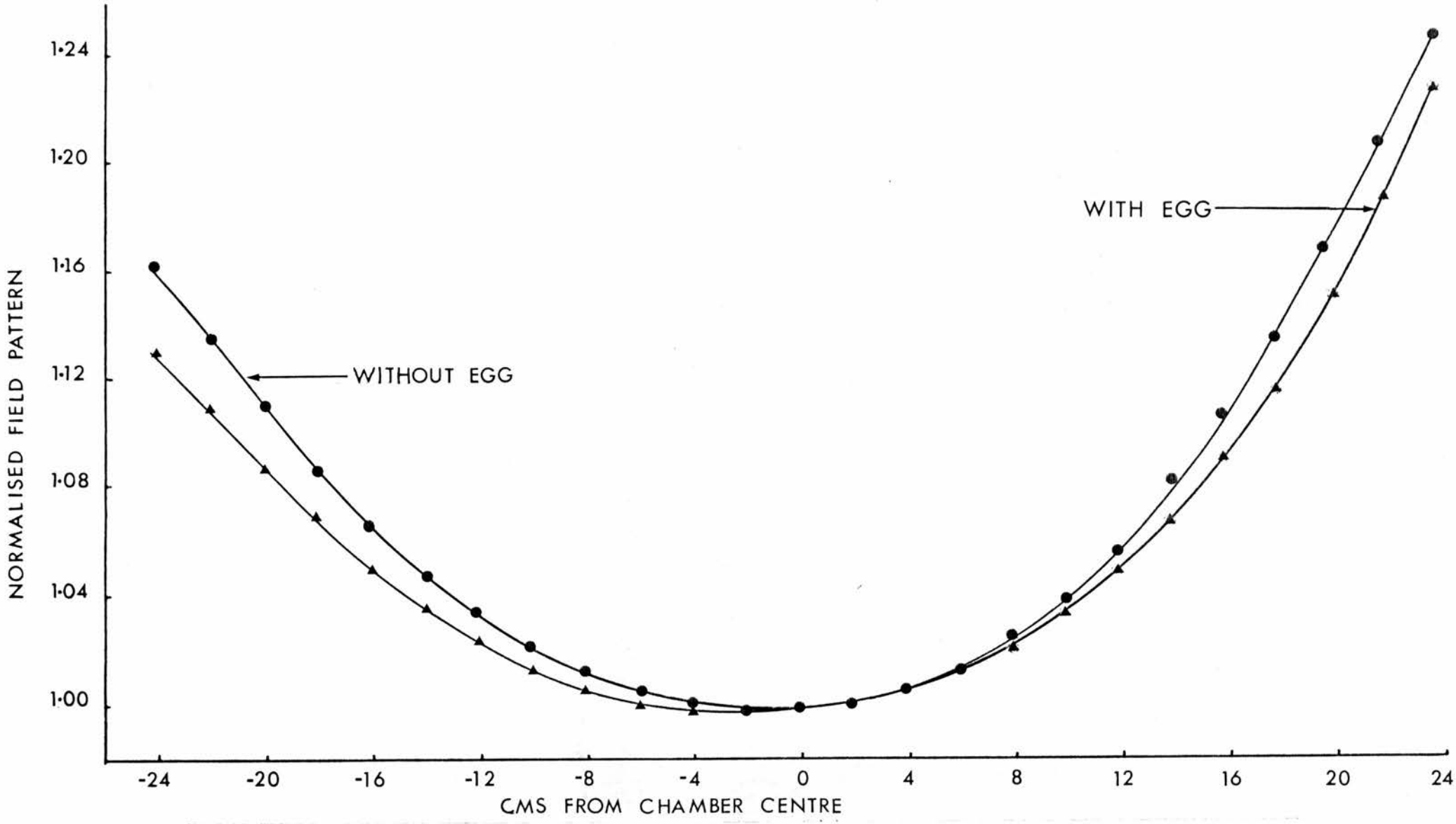

FIGURE 2 : Normalised field patterns along the diameter of an egg chamber when fitted with an active RFED. Measurements taken just above the surface of the egg and at the same height without the egg in place.

parameters are as given in Table 3. All of the RFEDs had a jack plug which, when removed from the module, activated the device.

An RFED used for the *in vivo* study is illustrated in Plate 5 and it is shown fitted around an egg chamber of diameter 68mm. The coaxial cable was positioned to be at the height of the chorio-allantoic membrane. Figure 2 shows the variation of the magnetic flux, as detected by a search coil, both with and without an infertile egg in postion. Eight devices were positioned in a cabinet incubator as shown in Figure 5, with the active and sham devices kept on separate shelves on top of blocks of polystyrene to reduce field interference. The coupling factor from the active to the sham device (defined as the search coil output at the sham device due to induction by the active device, divided by the search coil output of active device x100) was less than 0.27%. Interference factors between active devices A, B, C, and D shown in Figure 5 (defined as the search coil output at the centre of de-activated coil B due to active coil A divided by the search coil output of activated coil B x100) are given in Table 4.

7. *IN VITRO* MODELS

7.1 Cells and Media

Bovine aorta endothelial cells, derived originally by Schwartz (1978) were the gift of Dr J Starkey (Washington State University). These cells, referred to as BAES cells, were seeded onto 90mm petri-dishes (Nunclon) at a density of $6x10^5$ in 10mls of complete Eagle's medium (CEM), from which they were harvested and reseeded for experimentation. CEM was prepared by supplementing Eagle's minimum essential medium with the following:

benzyl penicillin	:50IU/ml
streptomycin	:50ug/ml
glutamine	:2mM
insulin	:0.125IU/ml
endothelial growth factor	:5ug/ml
fetal calf serum (Gibco)	:10%
sodium pyruvate	:1mM
essential vitamins	:1%
amino acids	:1%

The cells were maintained at 37°C in a humid environment of 5% carbon dioxide in air. After three days growth the cells were harvested, counted and replated. The medium was removed and the cells washed with 10mls of Dulbecco's calcium and magnesium free phosphate buffered saline (CMF-PBS). The CMF-PBS was removed and 2mls of 2mM EDTA and 0.1% trypsin in CMF-PBS were added. The cells were returned to the incubator at 37°C for 5 minutes, after which time the trypsin action was stopped by the addition of CEM. The suspension was spun down at 240g for three minutes

and the resultant cell pellet resuspended in a known quantity of CEM. The cell suspension was counted in a Coulter counter (Coulter Electronics Ltd.) set at an aperture current of 0.177mA, with an amplification of 64 and lower and upper thresholds at 10 and 86. The counter was fitted with a Channelyzer set on external count control, with the base channel threshold at 5, window width of 99.6 and a count range of 100. Cells were then replated onto appropriate dishes for experimentation or onto the 90mm dishes to provide an ongoing supply of cells. The cells were not used beyond passage 25 and were brought up from frozen supplies when necessary.

7.2 The effect of radio frequecies on BAES cell division.

BAES cells were seeded onto 58mm petri-dishes (Nunclon) at a density of 2.2×10^5 cells per plate in 3.5mls of CEM. Immediately after seeding, two dishes were fitted with RFEDs (paired as described in section 1) which were activated as soon as the dishes were put onto separate shelves of an incubator at 37°C. The dishes were left in the incubator for one of the following times: 24, 48, 72, 96 and 120 hours with a medium change at 72 hours. The cells were examined daily under an inverted microscope using phase contrast optics (Olympus, model IMT). After the completion of the growth time the cells from each dish were counted as described in section 7.1. Each of the five growth time intervals were

repeated four times. The RFEDs used were interchanged between the two shelves of the incubator on alternate experiments.

7.3 The effect of radio frequencies on the outgrowth of a wounded BAES monolayer.

BAES cells were seeded onto 58mm petri-dishes (Nunclon) at a density of 2.2×10^5 and left to grow to confluence for three days. Half of the monolayer of cells was then scraped from the surface of two dishes using a rubber policeman, with the aim of forming as straight a line as possible across the central diameter of each dish. The cells were washed three times with CEM after scraping and left with 3.5mls CEM in the dish. The monolayer left *in situ* on the dish was looked upon as being 'wounded' and the line of cells so formed is referred to as the growth line. The dishes were marked at right angles to the growth line for the purpose of re-alignment on the microscope stage. Five locations were chosen at approximately equal intervals along the length of the growth line and their positions were determined using the microscope stage vernier scale. All recordings were taken with the microscope set at x100 magnifications. Each of the two dishes was fitted with an RFED and positioned in the incubator as described in section 6. Six hours later the dishes were removed from the incubator and set on the microscope stage and the previous measurement points relocated. The horizontal vernier scale, which was running

parallel with the growth line, was positioned at each of the five previous readings and the vertical vernier was read after being set at the front of the growth line. Only one criterion was employed to define the leading edge of the moving growth line: this was to discount the presence of a single isolated cell from qualifying. The measurments were made for four days at either six or twelve hourly intervals. The medium was replaced approximately 60 hours after the first reading to remove cells which were rounding up due to over crowding from behind the growth line.

7.4 The effect of radio frequecies on the BAES cellular level of cyclic adenosine 3',5' -monophosphate (cyclic AMP).

The cellular level of cyclic AMP was measured under the influence of the RFEDs both on confluent and sub-confluent BAES cells using a method based on the technique of Brown et al (1971). The cells, seeded at a denstiy of $1x10^5$ on 35mm petri-dishes (Nunclon) were left to grow for 2, 3, or 6 days.

i) Stimulation of the cultures.

The irradiation from the RFED was the source of stimulation, and the cyclic AMP was prevented from being broken down by the addition of 1mM IBMX (Isobutyl-methyl-xanthine) in the incubation fluid (Kreb's solution with 1% BSA).

Twelve 35mm dishes of BAES cells, grown for 2, 3 or 6 days were placed into the wells of two, six well plates (Nunclon) and held

in place by a drop of water in the base of each well. The six well plates were fitted with an RFED each as shown in Plate 4 and described in section 6. Both plates were transferred to the hot room where the medium was removed from the twelve dishes and the cells washed with warm Kreb's solution (pH 7.4). This was then aspirated and 2mls of Kreb's solution with 1% BSA and 1mM IBMX were added to each of the twelve dishes. The RFEDs were immediately activated, the two plates placed at least 40cms apart, and the incubation fluid left in contact for 15 minutes. At the finish of the incubation period the two six well plates were lifted away from the RFEDs and put on ice. The cyclic AMP was extracted from the cells by the addition of 300ul of 0.2M hydrochloric acid to each dish. The acid was left in contact with the cells for 15 minutes after which time its action was stopped by neutralization with 210ul of 0.5M TRIS, making the final pH 7.5. The cells were subsequently scraped from the dishes with a rubber policeman and spun at 950g at 4°C for 15 minutes. The supernatant, once decanted, formed the sample in the radioimmunoassay. Two plates without cells acted as plate blanks and were taken through the assay procedure. A further two 35mm dishes which had been seeded at the same concentration of BAES cells were used for establishing cell counts. In control experiments, to show that the system was functioning, the cultures were stimulated with Forskolin (10uM) with or without IBMX (1mM). The resulting stimulation was compared with the effects seen in the absence of Forskolin (with or without IBMX). A significant response was always seen in the presence of Forskolin and IBMX (from 0.75 to 1.6 x 10^{-4} pMole cyclic AMP per cell).

ii) *The competitive binding radioimmunoassay.*

The assay is based on the competition between unlabelled cyclic AMP (in the samples) and a known quantity of (^{3}H)-cyclic AMP for high affinity sites on a binding protein from bovine adrenals. The amount of (^{3}H)-labelled binding complex formed is inversely related to the amount of unlabelled cyclic AMP in the sample added to the assay tube. Measurement of the protein bound radioactivity enables the amount of unlabelled cyclic AMP present in the sample to be calculated. Separation of the protein-bound nucleotide from the free nucleotide is achieved by absorbing the free nucleotide on to charcoal and precipitating this charcoal complex by centrifugation. The supernatant is decanted and assayed for its (^{3}H) content by liquid scintillation counting. The concentration of cyclic AMP in the sample is then determined from the standard curve.

Standards of unlabelled cyclic AMP were made from 0.625 to 20pM cyclic AMP (diluted in assay buffer: 50mM TRIS buffered water with 4mM EDTA at pH 7.5). A 100ul aliquot of each standard was added to assay tubes in triplicate. The rest of the assay tubes were made up with 100ul of the 14 samples (12 from the two multiwell plates and the two plate blanks). Three assay tubes containing 100ul of 1mM unlabelled cyclic AMP provided a measure of the non-specific binding or background scintillation counts.

A further three, containing 100ul of the assay buffer only, provided a measure of the maximum binding of labelled cyclic AMP in the absence of unlabelled cyclic AMP plus background counts.

50ul of (^{3}H)-cyclic AMP (5uCi/10mls) was added to all of the tubes followed by 200ul of the binding protein (bovine adrenal homogenate diluted in 15mls of Kreb's solution). Immediately after adding the binding protein, the tubes were vortexed for 5 seconds and incubated for a minimum of 1.5 hours at 4°C. The assay tubes were transferred to Coolspin holders and 500ul of the charcoal suspension (2 grams of charcoal in 100mls of distilled water and 0.2 grams of BSA) was added to each assay tube. The tubes were immediately spun in a Coolspin at 950g for 15 minutes, so separating the bound cyclic AMP from the free. The supernatant was decanted into scintillation vials with 5mls of scintillant (Optiphase Safe, LBK Ltd.). Scintillations were counted for 5 minutes in a liquid scintillation counter (1214 Rackbeta: LKB Wallace) .

iii) Treatment of results

Replicate assays were performed for each growth time; 5 for 2 days growth, 3 for 3 days growth and 4 for the 6 day growth measurements. The background counts per minute (cpm) obtained from the 1mM cyclic AMP were subtracted from the cpm obtained from the assay buffer only, giving a measure of cpm bound in the absence of any added, unlabelled cyclic AMP (Co). The background cpm obtained from the 1mM cyclic AMP were subtracted

from the cpm obtained from the assay buffer only, giving a measure of cpm bound in the absence of any added, unlabelled cyclic AMP (Co). The background cpm was also subtracted from all other cpm (standards and samples) to give Cx. The values of Co/Cx were calculated for each of the standard concentrations from which the regression equation was obtained (with R^2 values ranging from 96.6% to 98.7%). The unknown concentrations of cyclic AMP were derived from the regression equation by entering the Co/Cx values. From the cell counts and measures of the cell volumes (obtained from the Coulter Counter with the following values, 122um^3 at 2 days, 129um^3 at 3 days and 87um^3 at 6 days growth) calculation of the cyclic AMP released per cubic micron of cell was determined for active and sham irradiated cells grown for 2, 3, and 6 days. T-tests were performed to test for differences between the two groups at each growth time.

8. *IN VIVO* CAM WOUND MODEL.

8.1 Incubation prior to the shell-less preparation

Fertile White Leghorn eggs from the Poultry Research Centre, Edinburgh (average weight 60.5 + or - 5 grams), were incubated at 37.5°C and 60% relative humidity. After 24 hours of incubation the eggs were turned three times a day and at four days incubation their contents were cultured.

8.2 Shell-less preparation

The technique for maintaining the fertile egg contents in a shell-less form was based on that of Dunn, Fitzharris and

Barnett (1981). The eggs were taken from the incubator in batches of six, washed in 70% alcohol and placed in a laminar flow cabinet. After allowing 5 minutes for the embryo to float to the upper surface, the egg was placed on a piece of low density polythene film (Handi-Wrap from Dow Chemicals) beneath a G-clamp as shown in Plate 6. An aluminium strip moulded to fit the curvature of the egg was placed between the G-clamp pressure pad and the egg shell surface to spread the pressure so preventing the formation of a starburst crack. The G-clamp pressure pad was brought down on top of the egg until the shell was heard to crack. In most cases a single crack around the short axis of the egg was formed. Reverse action forceps were inserted into the lower portion of the crack (Plate 6) to avoid damaging the embryo, and gently opened, so pushing the two shell halves apart. As soon as the egg contents started to flow from between the crack, the aluminium strip and forceps were removed. The shell halves were lifted out making sure the sharp edges did not puncture the embryonic structures. The egg contents, now lying in the polythene film, were placed in a chamber constructed from a 50mm deep section of 96mm diameter plastic down piping, secured with a rubber band and enclosed in a petri-dish (Plates 5 and 7). Figures 3 and 4 show the differences in the arrangement of the egg contents when in shell-less culture and when *in ovo* at 11-13 days incubation age. The shell-less eggs (SL eggs) were maintained in a Forma 3336

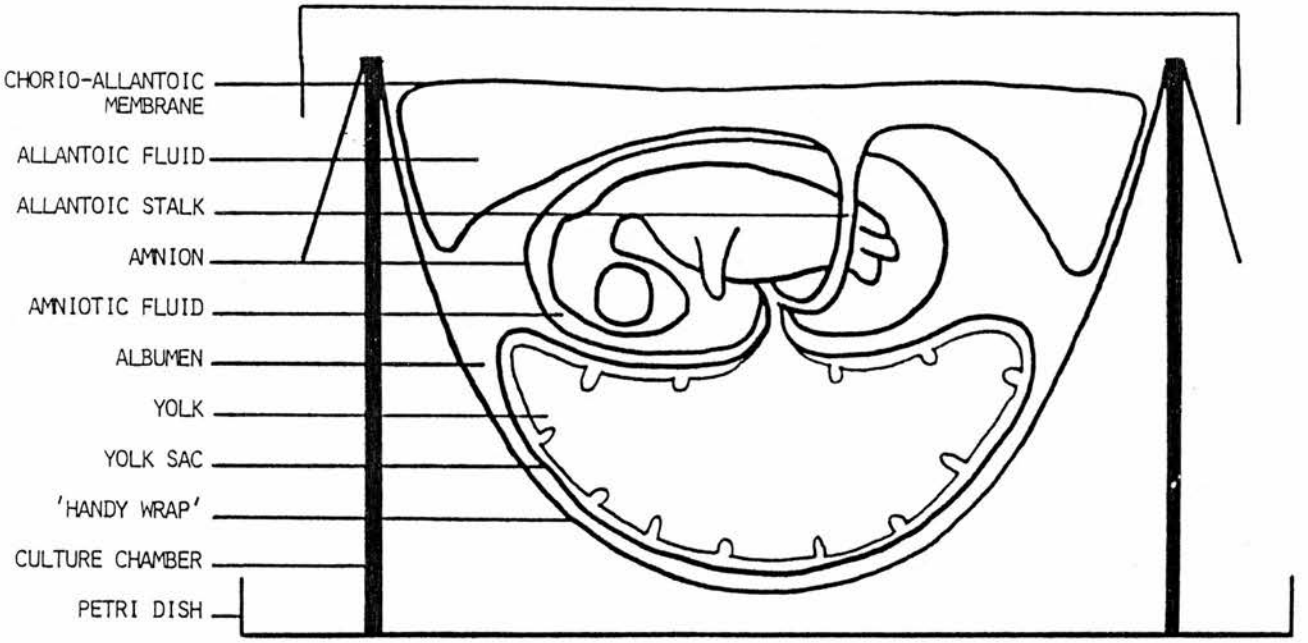

FIGURE 3 : The chicken embryo and associated structures as seen in shell-less culture at approximately 13 incubation days.

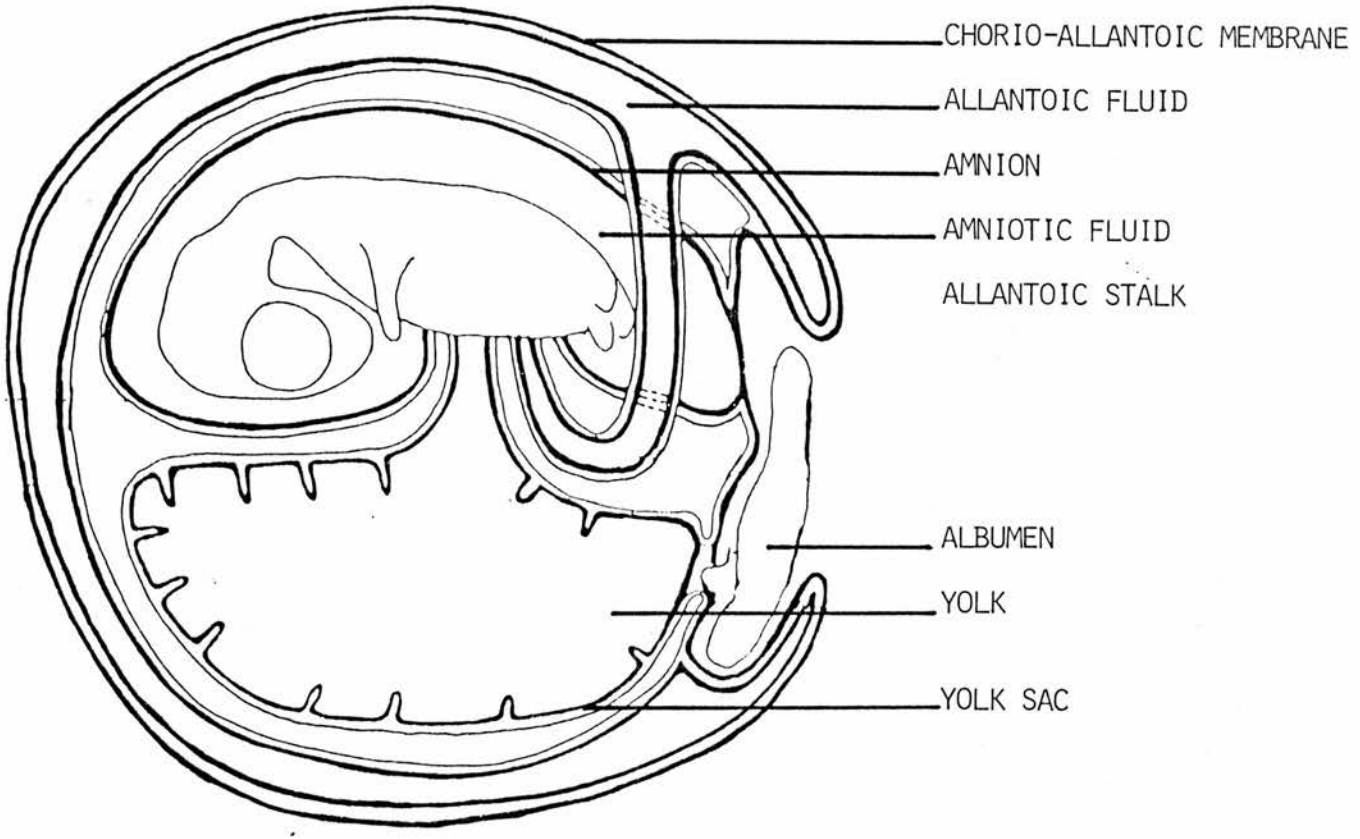

FIGURE 4 : The chicken embryo and associated structures as seen in ovo at approximately 13 incubation days (from Freeman and Vince 1974)

incubator at 37.5°C, 90-100% relative humidity, 1.5-2.5% carbon dioxide and a flow of fresh filtered air at 0.9l/min. The incubation time was calculated from four hours after transfer of the last egg to the incubator to allow conditions to settle. The shell-less eggs were maintained for 6.5 days (10.5 days total incubation age) by which time the CAM had grown to reach the chamber perimenter and was sufficiently developed to tolerate wounding. Six batches of eight eggs each were wounded and entered into the experiment.

8.3 Wounding and irradiating the CAM of shell-less eggs.

A burner, constructed from a 5mm diameter coil of resistance wire (650 milli ohms) attached to a heat resistant handle and supplied with 6-7 amps via a DC power supply, was used to burn the CAM surface. After pre-heating for approximately 5 seconds the burner was held as near as possible to the surface of the CAM without touching for 3.0-3.5 seconds (Plate 7). This resulted in a discrete, medium to severe burn. The wounding procedure was carried out in a laminar flow cabinet and the eight SL eggs from any given batch were wounded at two minute intervals. Embryo trauma was minimised by wounding an area of the CAM away from major blood vessels and from the embryo. Immediately after wounding, the eight egg chambers were fitted with RFEDs as described in section 1 and arranged as shown in Figure 5.

8.4 Photography of the CAM wound

The SL eggs were taken from the incubator in pairs for photography of the wounds one hour after wounding and subsequently at three hourly intervals for three days. A Kyowa Techniscope fitted with fibre optic light guides and camera (Cannon AE1) containing 160 ASA Kodak Ektachrome film, was used to take wound photographs at x7 magnifications.

8.5 Bacteriological swabs

At 73 hours post wounding, when the last photograph had been taken, swabs for routine bacteriology were taken from the eggs in Batches 3,5 and 6 (see Table 14 for egg numbers in each batch). The swabs were incubated in Stuart's and Broth media and sent to the Edinburgh Royal Infirmary Bacteriological Department.

8.6 Histology of the wounded and unwounded CAM: Light Microscopy.

Samples of the wounded CAM were obtained for light microscopy from SL eggs other than the experimentals at 1, 24, 36, 48 and 73 hours after injury, together with unwounded samples at 1 hour post wounding (10.5 days incubation age). To prevent distortion of the CAM, a piece of filter paper (8x8mm approximately) was

floated beneath the CAM in the allantoic fluid (Figure 3) and lifted up under the desired sample area. After cutting the CAM around the filter paper allowing for a large margin, the tissue was pinned to the paper and immediately immersed in 10% neutral buffered formalin after which the following procedure was carried out:

1. dehydration in 75% alcohol over night,
2. 30 mins in second 75% alcohol,
3. 30 mins in each of two 96% alcohols followed by 20 mins in each of two absolute alcohols,
4. 30 mins in chloroform 1,
5. 1.5 mins in chloroform 2,
6. 0.5 min in Paraplast wax 1,
7. 45 mins in Paraplast wax 2,
8. 45 mins in Paraplast wax 3,
9. the tissue was blocked out in wax and cut transversely at 6 microns,
10. the sections were floated out on subbed slides (ie. the slides were covered in a film of gelatin to enable the tissue to adhere) in a water bath at 45°C.
11. the slides were transferred to an oven set at 45°C and left overnight,
12. the wax was dissolved (in preparation for staining) in xylene for 2 mins and the tissue rehydrated in the

following series of alcohols,

13. absolute alcohol for 1 min., 0.5 min. in 96% alcohol, 0.5 min. in 75% and distilled water for 0.5 min.,
14. stained in Celestine Blue for 10 mins,
15. washed in distilled water,
16. stained in Meyer's Haemalum,
17. washed in alkaline tap water for 5 mins,
18. stained in Van Gieson's for 1min.,
19. washed quickly in 96% alcohol,
20. dehydrated in absolute alcohol for 1 min.,
21. cleared in xylene for 1 min. after which the edges of the tissues were dried,
22. mounted in DPX (plastic in xylene from BDH).

The slides were observed and photographed under a Zeiss Photomicroscope.

8.7 Histology of the wounded CAM: Scanning Electron Microscopy

Samples of the CAM for SEM at 24, 48 and 72 hours after injury were obtained as described above but using smaller pieces of filter paper (3x3 mm or 5x3 mm). Unwounded samples at the equivalent incubation ages (11.5, 12.5, and 13.5 days) were also obtained. The samples were fixed immediately in 4%

paraformaldehyde/glutaraldehyde in 0.08M sodium cacodylate buffer (pH 7.3) for 2 hours followed by washing for 2 hours. Post fixation in 1% osmium tetroxide for one hour was then followed with three washes in 0.08M sodium cacodylate, each lasting 15 minutes. The samples were then dehydrated in 50, 75, and 95% alcohol for 15 minutes in each solution. Three changes in absolute alcohol each of 15 minutes followed with the filter paper being replaced prior to the last wash. The samples were critical point dried with liquid carbon dioxide, attached to a metal block with silver conducting paint and rotary sputter coated with gold to a depth of 12um. The samples were observed and photographed on a Scanning Electron Microscope (JOEL, model-JSM35CF).

8.8 Parameters Measured for Wound Evaluation

i) Wound area

The wound area measurements were made directly from the slides using a semi automatic image analyser (System iii. Micro Measurements Ltd.) to give the results in square cms. The criteria found necessary to determine the wound edge were:

a. to exclude areas of dense capillaries which became blurred

b. to include the oedematous surround

c. to include half a blood vessel when it abutted up to the wound edge.

ii) Changes in the vessels surrounding the wounds

Each slide was projected and a circle was drawn around the wound at a distance of 5mm from the wound edge (equivalent to 0.2mm on the CAM). The circle diameter was taken from the widest part of the wound. All vessels intersecting the circle were counted with no attempt to distinguish between CAM vessels and the underlying allantoic vessels. If the capillaries became a blurr or were not clearly defined owing to a dark background, then the vessel count was made over a sector of the circle over which they were counted. After accounting for a magnification factor of x25, counts were converted to counts per centimetre of circumference.

A further series of vessel counts were taken from the CAM of 5 unwounded SL eggs over the same time period and time intervals. A small piece of plastic placed on the CAM acted as a guide to relocate the exact area of CAM to be photographed. The marker was positioned at least 1.5 cms from the area which was photographed to exclude the recording of vessels possibly formed in response to pressure from the weight of the marker. The circle diameter from which these control vessel counts were made was fixed at the mean of the diameters used for the experimental eggs at 37 hours after wounding (ie. half way through the experimental time.

iii) Petecheal haemorrhage

Petecheal haemorrhage was defined as any redness within the confines of the wound area. The slides were projected and all red areas blocked in on a sheet of paper placed ontop of the projected picture. The areas were obtained from the image analyser to give the results in square cms. Only the first eight slides of each wound (the first 25 hours) had petecheal haemorrhage scores calculated as most haemorrhage had been absorbed by this time.

The experiments performed on chick embryos during the course of this thesis were carried out within Home Office regulations.

RESULTS

9. *IN VITRO* RESULTS

9.1 BAES Cell Division.

Table 5 shows cell counts which have been meaned from the four replicates of each of the five growth times together with S.E.M values, regression equations and R^2 values for both active and sham exposed groups. The results are represented graphically in Figure 6. An analysis of variance with repeated measures was carried out on the data which showed that there was no significant difference in cell division between the RF and sham irradiated groups ($F = 1.97$ where $n1 = 4$, $n2 = 30$; NS).

9.2 Outgrowth of a wounded monolayer

Table 6 shows the mean distances travelled by the wounded monolayer together with the S.E.Ms, regression equations and R^2 values for the active and sham exposed groups. The measurements taken from each of the five positions across the growth line were meaned for the six replicates in both groups. The results are represented graphically in Figure 7. Plate 8 shows the growth line 90 hours after scraping. The cells can be seen to be pallisading behind the growth line; this pallisading reached up to a depth of 35 cells.

An analysis of variance with repeated measures and with two

TABLE 5

A) Cell counts for active and sham exposed groups after 24-120 hours growth.

GROWTH TIME (HOURS)	ACTIVE GROUP		SHAM GROUP	
	CELL COUNT $X10^5$	S.E.M (n=4)	CELL COUNT $X10^5$	S.E.M (n=4)
24	5.233	0.679	5.775	0.559
48	7.253	0.131	7.735	0.559
72	10.975	0.736	10.65	0.532
96	11.465	0.685	12.922	0.631
120	15.700	0.897	14.530	1.022

B) Regression analysis for the data in Part A) above.

GROUP	EQUATION	R^2
ACTIVE	COUNT = 2.58 + 0.105 X TIME	94.8%
SHAM	COUNT = 3.51 + 0.0946 X TIME	98.9%

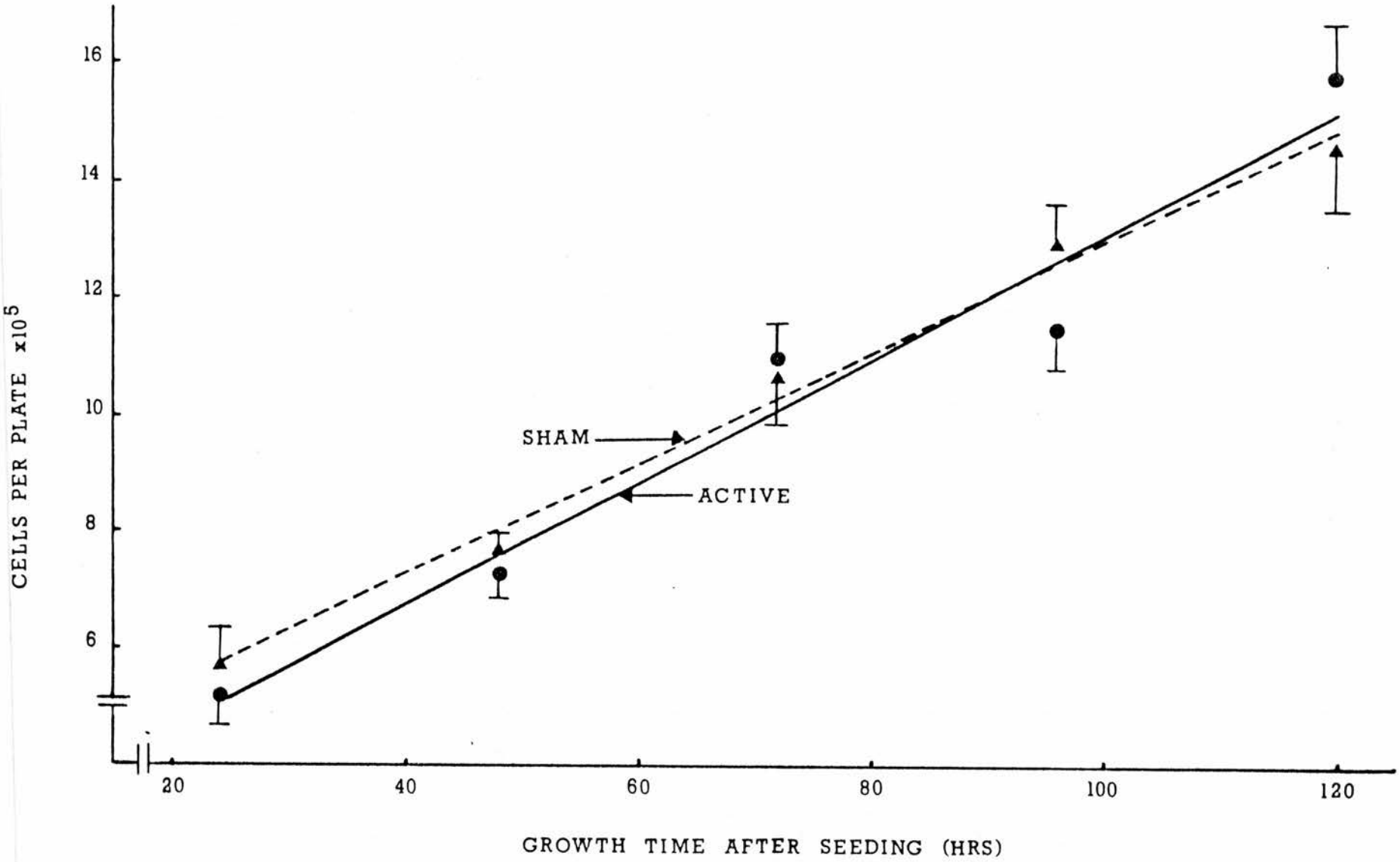

FIGURE 6 : Graph to show cell numbers against growth time for active (●) and sham (▲) exposed groups (Means + or - S.E.M where n(active) = 4 and n(sham) = 4).

TABLE 6

A) The mean distance travelled by a wounded BAES monolayer for active and sham exposed groups.

TIME POST WOUND (HOURS)	ACTIVE GROUP		SHAM GROUP	
	DISTANCE um	S.E.M n=30	DISTANCE um	S.E.M n=30
12	276.6	35.1	253.0	26.6
24	503.4	28.2	441.8	36.9
36	653.4	37.8	700.0	39.8
48	930.0	50.3	906.8	37.4
60	1140.0	64.4	1133.2	58.0
72	1493.4	71.7	1500.0	61.4
84	1806.8	77.3	1836.6	68.4
96	2050.0	85.7	2049.8	88.9

B) Regression Equations

GROUP	EQUATION	R^2
ACTIVE	DISTANCE = -53.7 + 21.5 TIME	98.9%
SHAM	DISTANCE = -85.5 + 22.0 TIME	99.0%

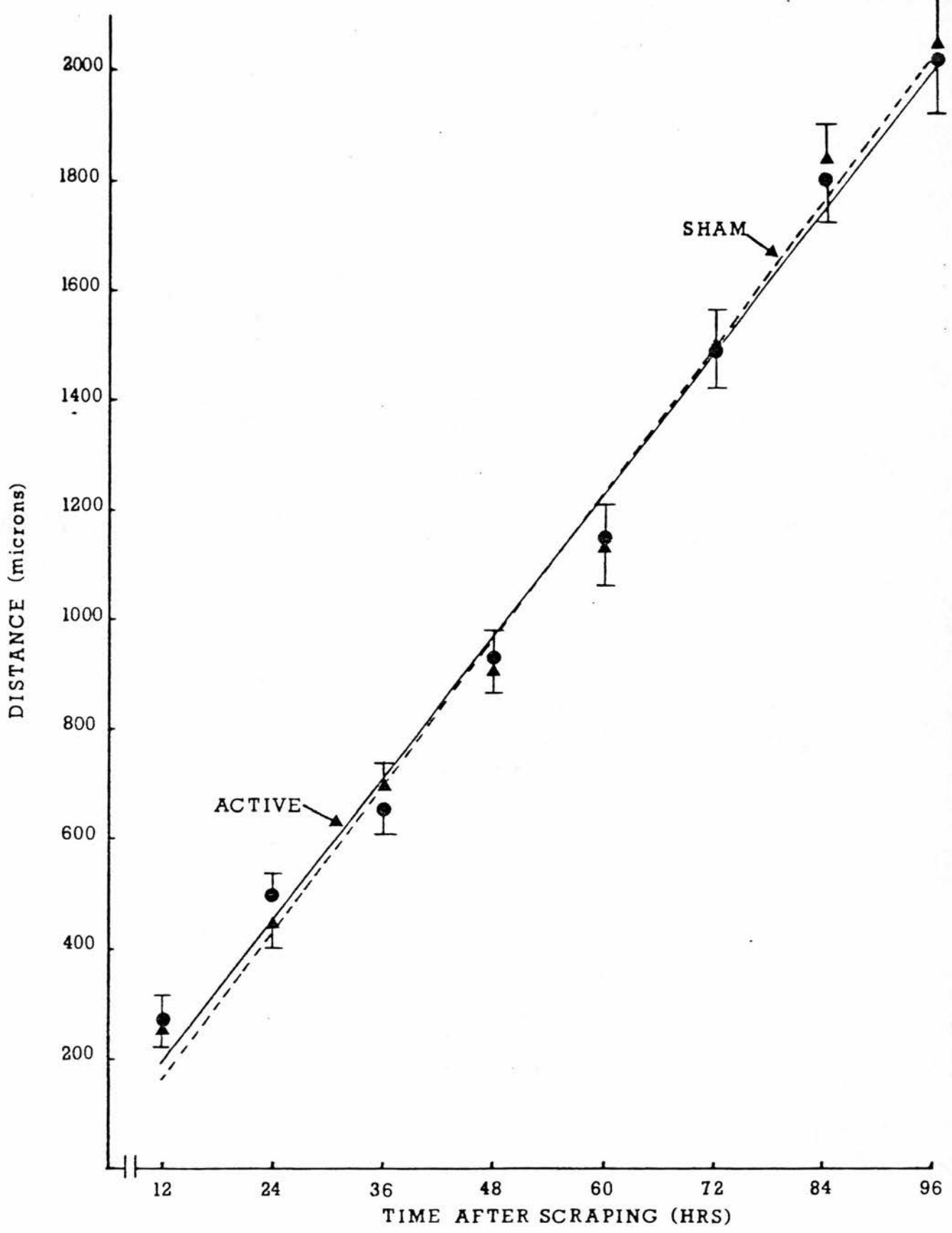

FIGURE 7 : Graph to show the rate of outgrowth of a wounded cell monolayer for active (●) and sham (▲) exposed groups (Means + or - S.E.M where n(active) = 30 and n(sham) = 30).

within subject factors (namely, the position across the growth line and the RF or sham exposed groupings) was carried out to test the null hypothesis that there was no difference between sham and FR exposed groups. The growth lines were largely linear (Table 6). There was no difference demonstrated between the active and sham exposed groups in the rate of outgrowth of the monolayer ($F = 0.05$, $df = 7/70$ $p = 0.9$ NS) which averaged 21.7um/hr for both groups. The five positions across the growth line were different within each group ($F = 3.32$, $df = 4/40$ $p = 0.02$), but the interaction of measurement position and groups showed no differences ($F = 0.13$ $df = 4/40$ $p = 0.97$ NS). The rate of the monolayer outgrowth was no different between the two groups when taking into consideration the measurement positions ($F = 0.65$, $df = 28/280$ $p = 0.92$ NS).

9.3 Production of cyclic AMP in BAES cells.

The results of the replicate assays for cells grown for 2, 3, and 6 days are shown in Table 7 together with the results of Student's T-test analysis to test for differences between the active and sham irradiated groups. The results are represented in Figure 8, where the n values given for each point are the number of replicates x6 minus the sub-threshold values. A sub-threshold value was obtained when the release of cyclic AMP, as measured in the 100ul aliquot of sample, was lower than 0.625 pMole (ie the smallest standard value). Such values were removed as they were known to be inaccurate. The percentages of

TABLE 7

Student's T-Test analysis on the cellular levels of cyclic AMP from active and sham exposed groups.

GROWTH TIME (days)	cAMP RELEASE (pMole/um^3 x 10^{-7})				T	N	p
	ACTIVE GROUP		SHAM GROUP				
	MEAN	SEM	MEAN	SEM			
2	0.3208	0.0376	0.1991	0.144	3.22	50	0.0023
3	0.3782	0.0400	0.2703	0.0464	1.76	24	0.092
6	0.1156	0.0505	0.1137	0.0305	0.03	11	0.970

TABLE 8

The percentage of sub-threshold values obtained in the cyclic AMP measurements for active and sham exposed groups.

GROWTH TIME (days)	% OF SUB-THRESHOLD VALUES	
	ACTIVE	SHAM
2	27.8	30.6
3	52.8	47.2
6	79.2	75.0

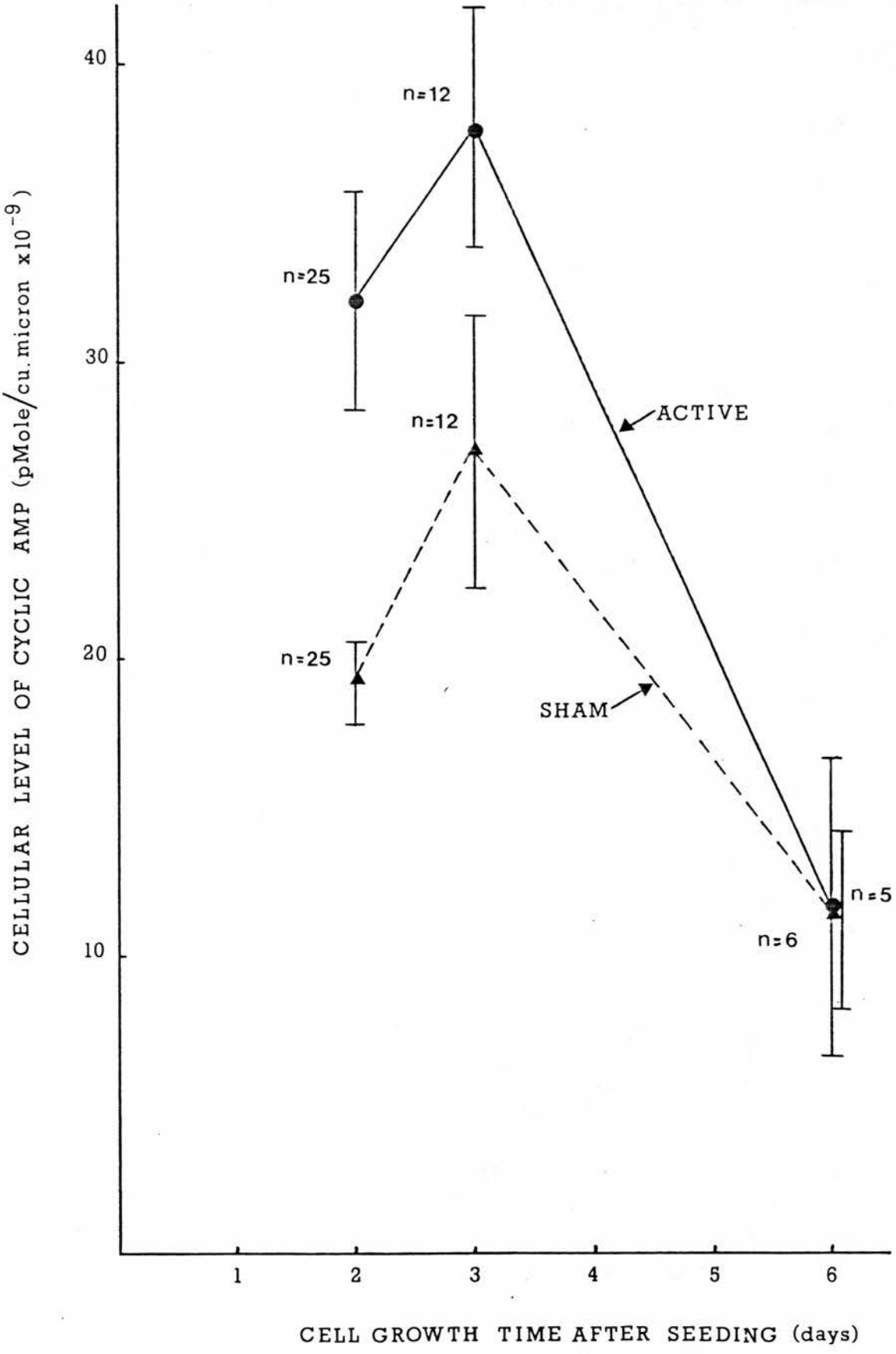

FIGURE 8 : Graph to show the cellular level of cyclic AMP in active (●) and sham (▲) exposed groups at 3 growth times (Means + or − S.E.M and n values given in Table 7).

sub-threshold values for each growth time are given in Table 8.

10. *IN VIVO* CAM WOUND MODEL RESULTS

10.1 Description of the Wounds from the Parameters Measured.

From the six batches of eight eggs, 28 were entered into the analysis. The remaining 20 died from between the time of wounding and the end of the experiment. The results of the three wound parameters from the 28 eggs took the general form as shown in Figure 9, the data for which is taken from an individual actively irradiated egg. Plates 9-14 show the wound at 1,13,25,37,49 and 73 hours after injury and are taken from the same egg whose data are depicted in Figure 9. The wound area displayed an initial rapid decrease from 45 to 35 sq.mm in the first 4 hours after wounding which was followed by a plateau for the next 9 hours. The wound area then rapidly decreased over the next 24 hours and levelled off by 46 hours post wounding to 4 sq.mm. This area remained to the end of the measuring time (73 hours). The surrounding vessel counts increased from an initial 13 vessels/cm at 1 hour post wounding up to 35 vessels/cm at 73 hours post wounding (Figure 9). The individual vessel counts showed a levelling off towards the end of the measurement time. The area of haemorrhage decreased from

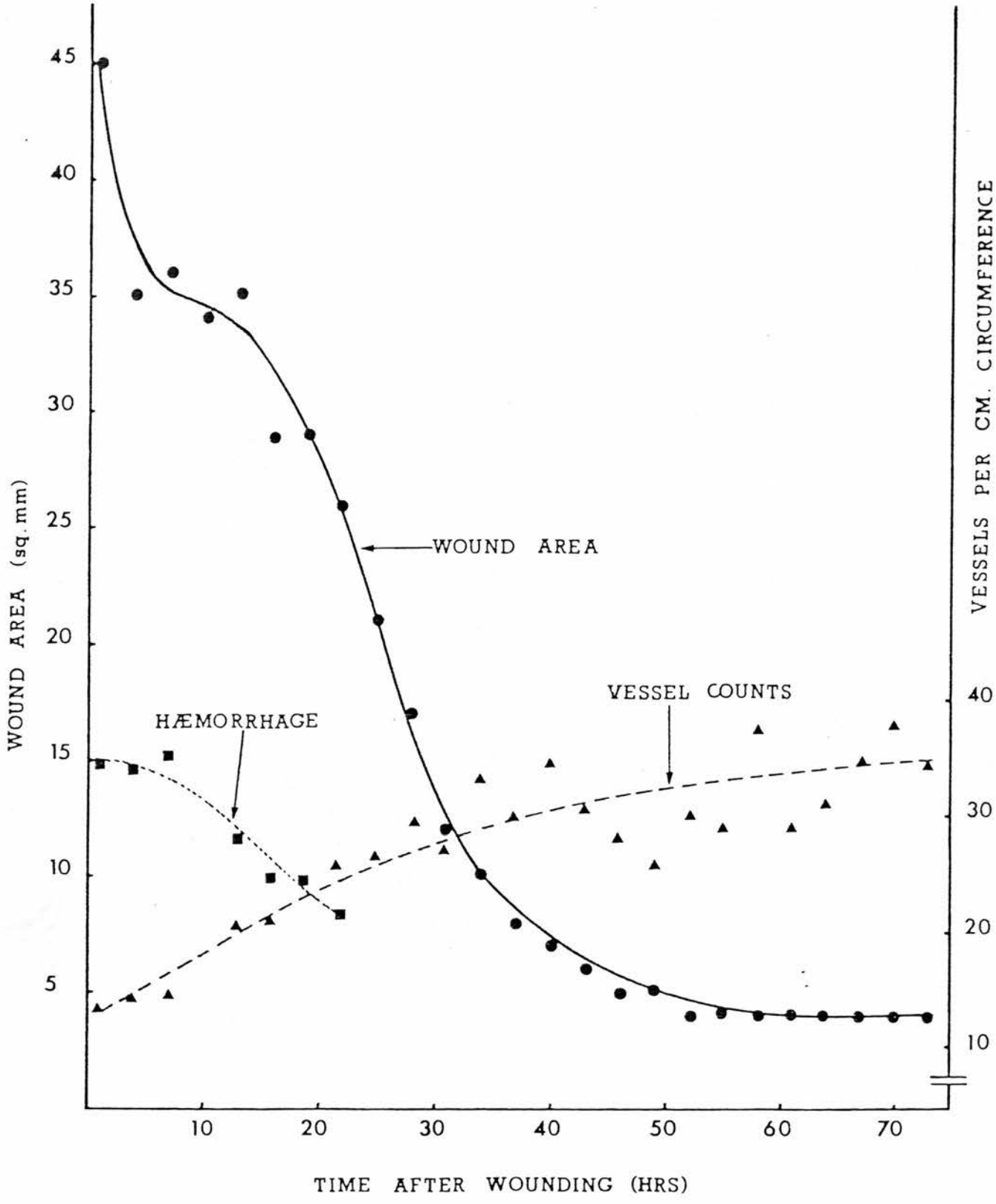

FIGURE 9 : Graph to show the CAM wound area (●), petecheal haemorrhage (■) and vessel counts (▲) for a single shell- less egg.

about 33% of the wound area at one hour post wounding (15 mm^2) to 27% (8.4 mm^2) by 25 hours post wounding.

10.2 Wound Area

The mean wound areas for both the active and sham exposed groups are given in Table 9 and represented graphically in Figure 10. Both the sham and actively irradiated groups followed the same sigmoid shaped curve for reduction of wound area. A fourth degree polynomial of the standard form:

$$y = ax^4 + bx^3 + cx^2 + dx + e$$

was fitted to the data of each individual embryo and the parameters derived from this equation were analysed using Student's T-test. The steepest slope of the rate of wound reduction (taken from 13 to 34 hours post wounding), the time of occurrence of the steepest slope and the time at which the wound area was reduced by 50%, showed no significant differences between the two groups. The results are shown in Table 10.

10.3 Surrounding Wound Vasculature Changes

The mean numbers of vessels per centimetre which crossed a circle positioned 0.2mm from the wound edge (5mm as projected) for active sham and control groups are given in Table 11 and represented graphically in Figures 11 and 12. Both sham and

TABLE 9

CAM mean wound areas for active and sham exposed groups.

TIME POST WOUND (HOURS)	ACTIVE GROUP		SHAM GROUP	
	WOUND AREA mm^2	S.E.M n=12	WOUND AREA mm^2	S.E.M n=16
1	55.3	3.0	54.0	2.5
4	49.4	3.6	48.5	2.7
7	49.8	3.5	49.6	2.6
10	49.4	3.5	48.3	2.6
13	49.1	3.8	48.1	3.2
16	46.9	4.0	45.3	3.2
19	44.3	3.6	42.7	3.1
22	41.3	3.6	39.6	3.1
25	39.3	3.9	36.3	3.2
28	35.3	4.1	32.9	3.1
31	31.2	4.0	29.6	3.1
34	28.3	4.1	26.2	3.2
37	23.8	3.7	23.1	2.9
40	21.5	3.6	20.6	2.7
43	18.8	3.2	17.9	2.6
46	16.6	3.0	15.9	2.5
49	14.8	2.8	14.0	2.3
52	13.3	2.7	12.5	2.2
55	11.7	2.4	11.0	2.0
58	10.9	2.4	9.9	1.9
61	9.3	1.2	8.7	1.6
64	8.8	1.9	8.1	1.6
67	7.7	1.6	7.1	1.3
70	6.6	1.3	7.0	1.8
73	5.8	1.0	6.5	1.5

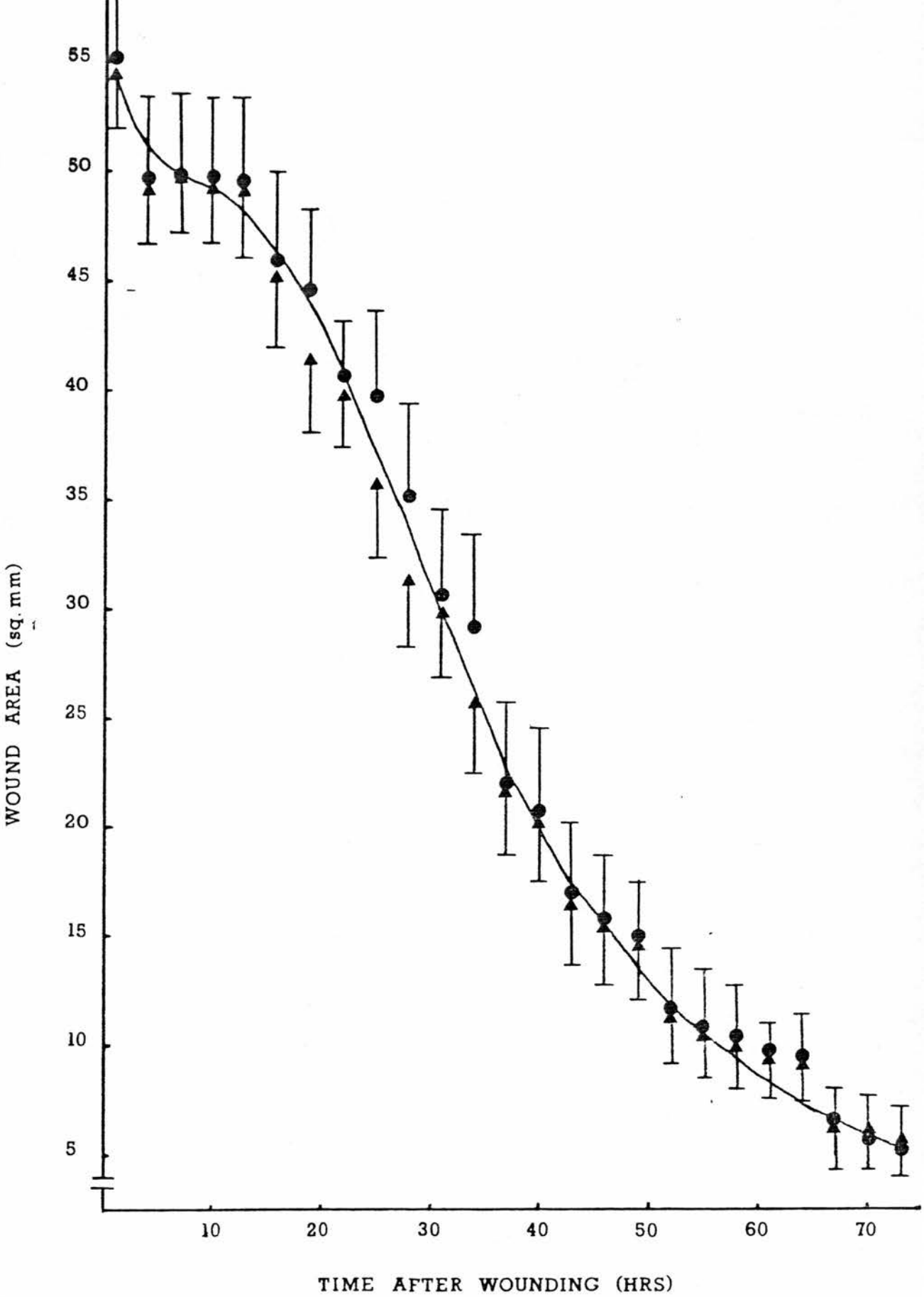

FIGURE 10: Graph to show the CAM wound area contraction over time for active (●) and sham (▲) exposed groups (Means + or - S.E.M where n(active) = 12 and n(sham) = 16).

TABLE 10

Student's T-Test analysis on the paramenters derived from cam wound area measurements

Parameter	Active	Sham	T	N	p
Steepest slope (x)	-0.0120	-0.0117	-0.25	28	0.8073
Time of (x)*	27.5	28.1	-0.26	28	0.9956
Tx50%	34.3	33.2	0.41	28	0.6849

* (hrs post wounding)

Tx50% = the time (hours) taken for the wounds to reduce to 50% of their size at 1hour post wounding.

TABLE 11

A) The mean number of vessels surrounding active and sham exposed groups and unwounded controls, expressed as the number of vessels per cm (VES/CM)of wound circumference (see Section 8.8ii for control vessel counting method).

TIME POST WOUNDING (HOURS)	ACTIVE GROUP VES/CM	ACTIVE GROUP S.E.M n=12	SHAM GROUP VES/CM	SHAM GROUP S.E.M n=16	CONTROL GROUP VES/CM	CONTROL GROUP S.E.M n=5
1	15.3	1.5	16.5	0.7	13.8	0.3
4	14.9	1.3	14.8	1.0	15.5	1.0
7	14.6	1.2	15.2	1.0	14.2	0.7
10	15.7	1.1	15.5	0.9	14.6	1.0
13	17.1	1.0	16.3	0.8	17.1	0.6
16	18.3	0.9	17.9	1.0	14.6	0.8
19	19.4	1.3	20.6	1.0	*	*
22	20.0	1.6	20.9	0.9	14.7	0.6
25	21.6	1.6	22.5	1.2	14.2	1.3
28	22.6	2.1	23.3	1.1	14.5	0.9
31	23.6	2.3	25.3	1.6	18.1	1.1
34	22.2	2.1	24.3	1.9	16.3	1.6
37	23.4	1.9	25.9	1.3	17.0	0.8
40	23.3	1.8	26.4	1.4	*	*
43	25.1	1.7	26.2	1.4	*	*
46	27.2	2.0	27.7	1.6	16.9	0.7
49	27.9	2.2	29.2	2.2	15.8	0.9
52	27.2	2.4	27.8	2.0	16.9	1.1
55	28.2	2.8	28.9	2.2	16.5	0.5
58	29.8	2.2	30.2	1.7	17.4	0.9
61	30.5	2.0	30.7	1.8	16.7	1.1
64	32.1	2.1	32.4	2.2	15.7	0.6
67	34.4	2.1	31.3	2.0	*	*
70	35.3	2.0	33.8	2.3	16.4	0.6
73	34.2	2.6	33.7	2.4	16.4	0.7

B) Regression equations for the above data omitting 1 hour post wounding for active and sham groups where a decrease is seen prior to the increase.

GROUP	EQUATION	R^2
ACTIVE	DISTANCE = 13.3 + 0.292 X TIME	97.8%
SHAM	DISTANCE = 14.4 + 0.277 X TIME	96.5%
CONTROL	DISTANCE = 14.8 + 0.031 X TIME	21.5%

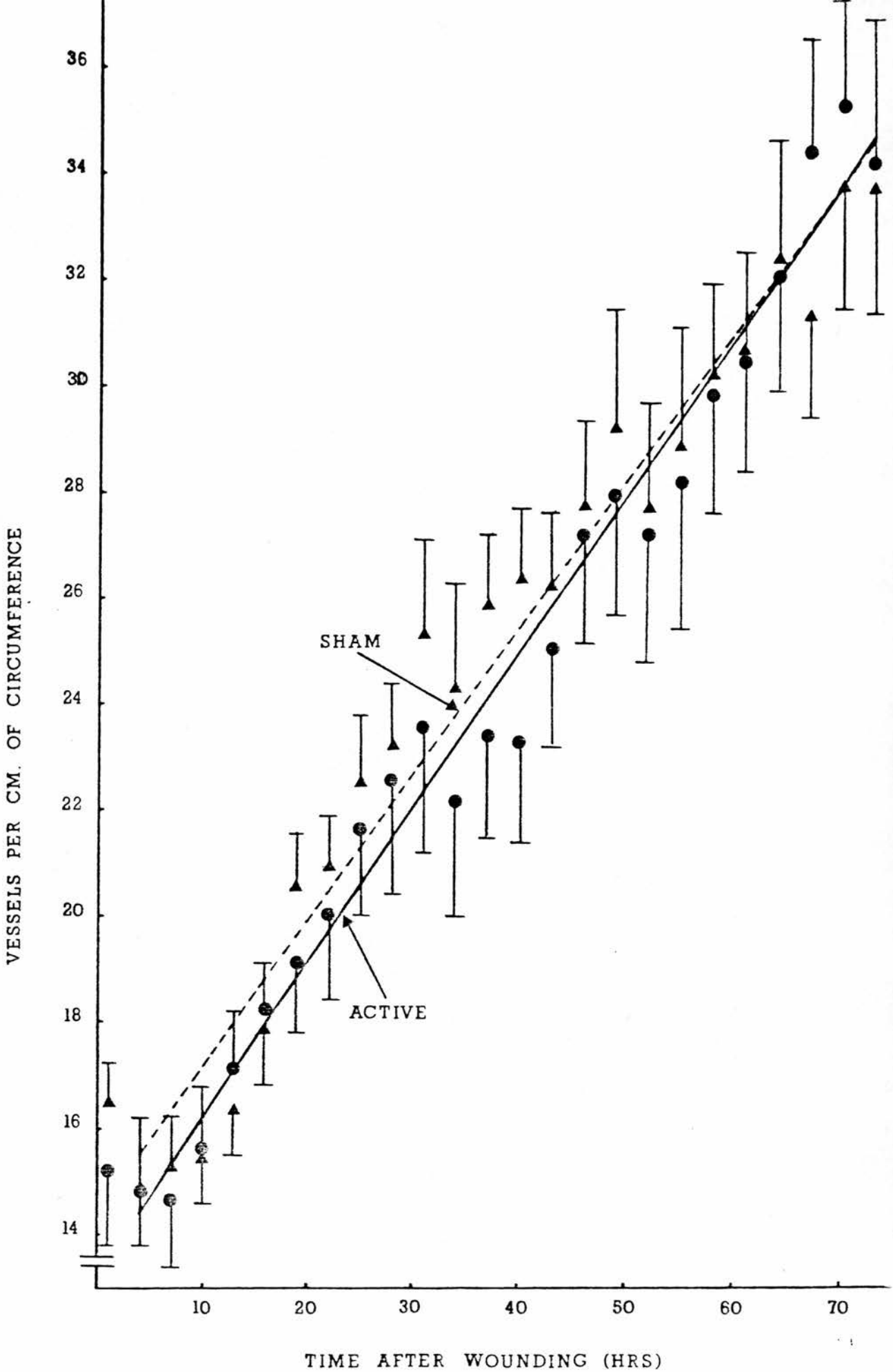

FIGURE 11: Graph to show the change over time in the number of vessels surrounding active (●) and sham (▲) exposed CAM burn wounds (Means + or - S.E.M where n(active) = 12 and n(sham) = 16).

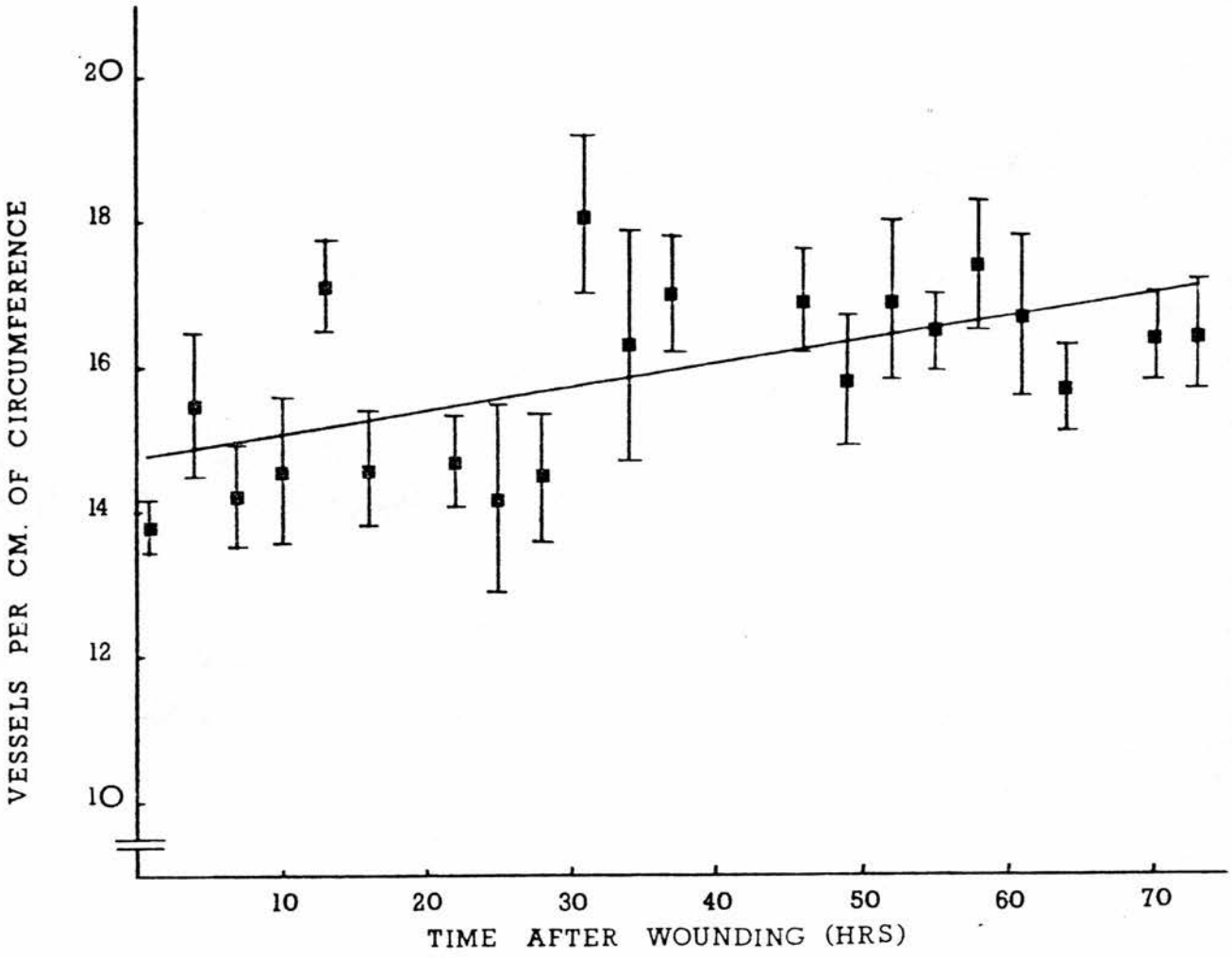

FIGURE 12: Graph to show unwounded CAM control vessel counts (Means + or - S.E.M where n = 5).

active groups (Figure 11) displayed a consistent increase from 15 to approximately 36 vessels per centimetre of wound circumference, while the unwounded control CAM vessel counts (Figure 12) ranged from about 14 - 18 vessels/cm over the period of measurement without a marked increase with time. The data were submitted to an analysis of variance which showed no difference in the vessel counts between the active and sham groups ($F = 0.01$, $n1 = 28$, $n2 = 2$, non-significant). Student's T-test analysis was performed on the initial mean angiogenesis counts from the RF and sham irradiated groups. Further T-test analysese were carried out on the beginning, mid and end sections which were obtained by dividing the data from the total time span of 73 hours into three near equal periods. The results (Table 12) show that there was no significant difference between the active and sham groups within each section.

10.4 Petecheal Haemorrhage

The mean areas of petecheal haemorrhage for active and sham exposed groups are given in Table 13 and represented graphically in Figure 13. A steady decrease of haemorrhage from 22 to 8 mm^2 was seen during the 25 hours over which the measurements were made. The data were submitted to an analysis of variance which showed no difference between the two groups ($F = 1.16$, $n1 = 28$, $n2 = 2$, non-significant).

TABLE 12

Student's T-Test analysis on the initial vessel counts and beginning, mid and end sections of the active and sham exposed groups.

PARAMETER	ACTIVE	SHAM	T	N	SIG
Initial ves.count	15.27	16.31	0.62	28	NS
Beginning section	0.95	0.57	0.90	28	NS
Mid section	0.55	1.00	1.95	28	NS
End section	0.90	0.94	0.14	28	NS

NS = Non-significant

TABLE 13

A) The mean areas of petecheal haemorrhage (area pet.) in the wounds of active and sham exposed groups.

TIME POST WOUNDING (HOURS)	ACTIVE GROUP		SHAM GROUP	
	AREA PET. mm^2	S.E.M n=12	AREA PET. mm^2	S.E.M n=16
1	23.9	2.0	23.5	1.5
4	21.8	1.7	21.7	1.3
7	21.0	2.0	22.2	1.3
10	16.8	1.6	17.4	1.5
13	13.7	1.8	15.8	1.8
16	10.3	1.7	13.3	1.8
19	8.5	1.3	11.1	1.6
22	7.3	1.1	9.4	1.5

B) Regression equations for the above data.

GROUP	EQUATION	R^2
ACTIVE	DISTANCE = 25.4 - 0.865 X TIME	97.6%
SHAM	DISTANCE = 25.0 - 0.714 X TIME	96.4%

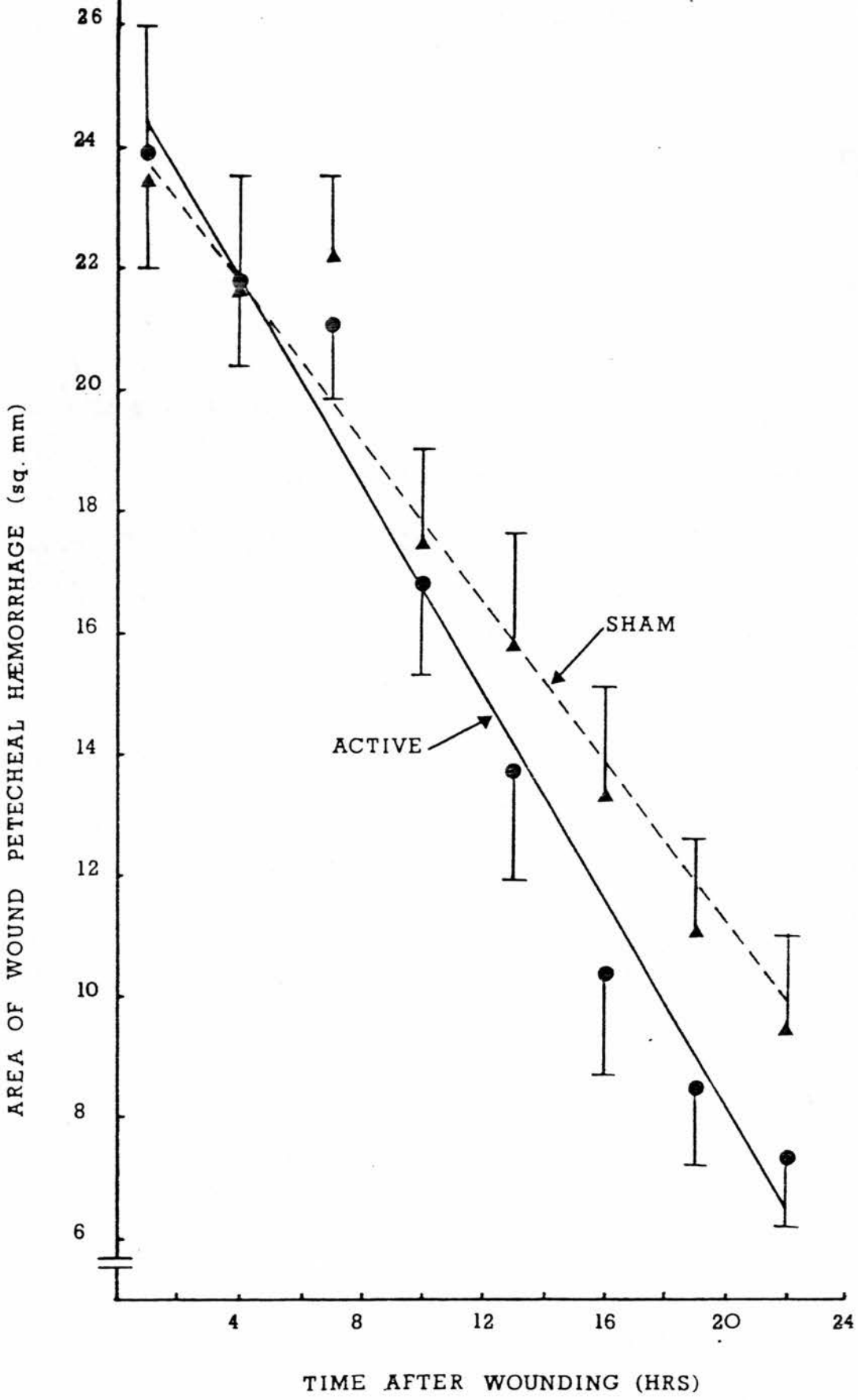

FIGURE 13: Graph to show the clearance of petecheal haemorrhage in active (●) and sham (▲) exposed CAM wounds (Means + or − S.E.M where n(active) = 12 and n(sham) = 16).

10.5 Batch Analysis

The 28 eggs entered into the analysis were from 6 batches of eggs as shown in Table 14. An analysis of variance was performed on the data from batches 1,3,5 and 6 to test for differences BETWEEN the batches on the three wound parameters (wound area, vessel counts and petecheal haemorrhage). Significant differences were found on all three of the parameters (Table 15). However, data from the analysis of variance showed that there were no significant group-within-batch differences (Table 15).

10.6 Wound Bacteriology

Swabs taken from the wounds of the 18 eggs in batches 3, 5 and 6, produced growths of subtiloid organisms in 12 (6 in each group), *Staphylococcus albus* in 3 (2 in the active group and 1 in the sham), and the remaining 3 showed no bacterial growths (all in the sham group). All the eggs appeared healthy and there was no visible bacterial growth.

10.7 Histological observations: Light Microscopy

Unwounded tissue (10.5 days incubation age)

After 10.5 days incubation the CAM is a well differentiated tissue as seen in Plate 15. The tissue is divided into three

TABLE 14

The numbers of eggs entered into the analysis per batch.

	BATCH NO.	ACTIVE GROUP	SHAM GROUP	TOTAL EGGS PER BATCH
	1	2	2	4
	2	0	2	2
	3	4	4	8
	4	0	1	1
	5	4	4	8
	6	2	3	5
TOTALS	6	12	16	28

TABLE 15

An analysis of variance on the wound parameter data (wound area, petecheal haemorrhage and angiogenesis) from batches 1,3,5 and 6 to test for between and within batch differences (where n = 25 for all parameters).

	WOUND AREA		PETECHEAL		ANGIOGENESIS	
	F	P	F	P	F	P
BATCH	15.65	0.0001	3.40	0.04	13.4	0.0001
GROUPS	0.10	NS	1.16	NS	0.01	NS
BXT*	3.02	0.02	2.49	0.06	3.10	0.0001
GXT**	0.16	NS	0.36	NS	0.82	NS

* the interaction of Batch X Time.

** the interaction of Group X Time

distinct layers, the outer chorionic epithelium, the mesenchyme and the inner facing allantoic endothelium. The chorionic epithelium is composed of a double layer of squamous epithelial cells with a central blood sinus inbetween. True endothelial cells are not evident in the chorionc epithelium (Flummerfelt and Gibson 1969), but the blood sinuses interconnect with the blood vessels in the tissue below. The mesenchyme is composed of loose connective tissue, blood vessels, lymphatic vessels and intercellular fine collagen fibres. In Plate 15 the central blood vessel is probably an artery as the wall is thicker than the surrounding vessels some of which may be lymphatic vessels as evidenced by both their position and empty lumens (marked by X on Plate 15). Smooth muscle fibres will be present in the cells surrounding the arteries. The allantoic epithelium faces into the allantoic fluid (Figures 3 and 4) and is composed of a single layer of squamous epithelial cells. These cells take on a secretory function and after approximately 13 incubation days release mucus which acts as a protection against the increasing alkalinity of the allantoic fluid (Flummerfelt and Gibson 1969). From 10-12 days incubation the cells stain more darkly owing to the accumulation of granules prior to the secretory phase. The cross sectional thickness of the CAM varies as seen in Plate 15. The tissue in the centre of the plate is nearly double the thickness of that to the left. This variation in healthy CAM tissue is due to the position of blood vessels, although as shown in subsequent

plates, the CAM responds to injury with an increase in thickness.

1 hour after injury.

The entire tissue is greatly swollen as seen in Plate 16 showing the wound edge one hour after injury. The venules have increased in permeability resulting in a loss of protein and fluid into the tissues so increasing both tissue pressure and the concentration of cells in the blood plasma. These result in the slowing of blood flow and eventual stasis. Local haemorrhage is seen in the area above the allantoic epithelium (marked by Y on Plate 16).

24 hours after injury.

Plate 17 shows the wound margin 24 hours after injury. The tissue remains swollen, numerous capillaries have grown into the area of the wound margin (C on Plate 17) and the cellular components (Z on Plate 17) appear to be streaming towards the junction of viable and non-viable tissue. This junction, the wound margin, is now an area of intense activity. Blood clots are digested by enzymes from disintegrated neutrophils, as well as by increasing numbers of macrophages which further digest debris, red cells and the dead neutrophils. The majority of cells present will probably be the longer living macrophages. This phase of healing is often referred to as the 'demolition

phase'. The numerous capillaries near the wound margin suggest the formation of granulation tissue which is made up by vascular and fibroblastic proliferation. It is thought that the fibroblasts are derived from local fibrocytes or from undifferentiated mesenchymal cells around blood vessels.

36 hours after injury.

Plate 18 shows the wound margin 36 hours after injury. The layer of chorionic epithelium is greatly thickened (T on Plate 18). Cells from the epithelium begin to migrate over the wound and contribute to the wound closure together with proliferation of cells further back from the wound edge. Further into the wound (CB on Plate 18) the tissue remains engulfed with coagulated blood vessels and debris.

48 hours after injury.

Plate 19 shows the wound margin 48 hours after injury. The chorionic and the allantoic epithelial layers have both become thickened at the wound margin (marked by T on Plate 19). Numerous capillaries can be seen (C on Plate 19) and these are probably forming loops prior to the formation of further granulation tissue. The new capillary sprouts are formed partly by rearrangement and migration of pre-existing endothelial cells and partly by division of cells in the tip of the advancing capillary sprout. These sprouts are more permeable than normal

and so release fluid and permit the escape of leukocytes and red cells. The cellular components of the mesenchyme are still seen to be streaming towards the wound margin (marked by Z on Plate 19). The central area of the wound at 48 hours (Plate 20) is highly convuluted: the tissue is gathered up and is in the process of being encapsulated by the ingrowing healthy tissue.

73 hours after injury.

Plate 21 shows the wound margin 73 hours after injury. The chorionic epithelium has grown to cover a large area of the wound and most of the debris and coagulated blood has been absorbed. Numerous blood vessels still surround the wounded area (C on Plate 21) which remains swollen. When the newly formed tissue is fully functioning many of the newly formed capillaries will not be required and will be absorbed.

10.8 Histological Observations: Scanning Electron Microscopy

24 hours after injury

At 24 hours post wounding the wounded tissue has a dehydrated appearance (Plate 22) and has formed crevices. The wounded surface (to the right of W on Plate 22) has a rough appearance due to the drying and cracking of the chorionic epithelium. The

large ellipsoidal spheres are red blood cells while the smaller spheres may be intercellular components from damaged cells or surface contaminants.

48 hours after injury.

By 48 hours after injury larger folds (Plate 23) than those seen at 24 hours post injury are apparent, possibly as a result of forcing by wound contraction. The tissue to the left of W on Plate 23 is the wounded area. The chorionic epithelium is fragmented revealing the underlying mesenchyme.

73 hours after injury.

Plates 24 and 25 show the wound and wound margin 73 hours after injury. The wound has further contracted and thickened. Plate 24 shows that the wound has two distinct 'margins'; the outer margin (X on Plate 24) demarcating the oedematous extent of the wound, and the inner margin (Y on Plate 24) demarcating the extent of ingrowth of the chorionic epithelium. The centre of the wound in Plate 24 shows the highly convoluted dead tissue and just inside the inner margin is the area of repair, depicted at a higher magnification in Plate 25.

DISCUSSION

A number of different methods of field application have been employed in studying the effects of electromagnetism on biological tissue. Invasive methods, requiring the implantation of electrodes into the tissue, stimulate the production of bone (Cochran, 1972). However, surgery is necessary for the implantation and extraction of the electrodes, and bone formation is restricted to the area immediately around the electrode. Non-invasive methods include conductive and inductive techniques as described by Martin (1979). Of the two, the inductive method has been more widely used as it requires smaller voltages and is consequently less likely to be hazardous in the clinical environment. Clinical trials using the non-invasive method first employed continuous wave radio frequencies (Bassett et al, 1964) but later began experimenting with pulsed electromagnetic fields (PEMFs) from 1.0 to 1.5mV/cm (Bassett et al, 1974). By 1979 the Bassett group had produced a commercially available and patented 'stimulator' releasing PEMFs at about 70Hz. This transmitter has since been tested by other clinicians on non-unions and congenital pseudoarthroses (Sutcliffe et al, 1980; O'Connor, 1980; Sedel et al, 1980) and reported to give up to 80% success in healing. However, only one clinical trial using similar field parameters to Bassett has used double blind controls (Barker, 1984) which are essential in the light of the possible

beneficial effects of Bassett's detailed orthopaedic care regime (Bassett et al, 1979). Barker (1984) found healing in as many controls as in actively exposed non-unions and concluded that some other factor/s in Bassett's work was providing the increased healing of non-unions.

Fewer clinical trials have been carried out to investigate the effects of PEMFs on soft tissue healing. The studies particularly relevant to the present work are those that used the same electromagnetic parameters. Two such studies, one clinical employing double blind controls (Nicholle and Bentall, 1982) and one experimental (Bentall, 1981), suggested beneficial effects in the healing of soft tissue wounds and are discussed later.

The chorioallantoic membrane (CAM) of the chicken embryo was used in this study to investigate the effects of the PEMF as used by Bentall (1981) on soft tissue healing. The CAM presents an easily available, multilayered soft tissue surface for experimentation. The same PEMF was also applied to an *in vitro* model system, bovine aorta endothelial cells (BAES cells) growing in culture, in order to enable some parameters relevant to wound healing to be measured. All experiments were carried out under blind conditions, and the following were measured in response to low level PEMFs:

IN VIVO

i) changes in area of a mild burn wound on the chick embryo CAM

ii) changes in the number of surrounding vessels in association with the burn wound

iii) changes in petecheal haemorrhage within the burn wound area.

IN VITRO

i) the division of BAES cells

ii) the outgrowth of a wounded monolayer of BAES cells

iii) the cellular levels of cyclic AMP of BAES cells after 2, 3 and 6 days growth.

The CAM burn wound areas decreased consistently in a sigmoid shaped curve (Figure 10). The initial rapid decrease from 1 - 4 hours after wounding probably represents the removal of fluid. This early onset of contraction could not originate from granulation tissue as it has not yet been formed. Changes in the structure of collagen around the wound may also contribute to wound closure, but although collagen contracts to one third of its length when boiled there is no evidence that it is capable of contraction *in vivo* (Walter and Israel, 1974). Plate 9 shows that by 1 hour after wounding there is widespread haemorrhage within the wound area. At this stage capillary flow is likely to have

stopped and coagulation of cellular and tissue components occurs. The inflammatory reaction, including the absorbtion of denatured tissue components, proceeds throughout the period from 10 - 13 hours after wounding, in which a reduced rate of wound area decrease is noted (Figure 10). The cells at the wound margin start to divide and the epithelial cells migrate over the wound resulting in a sharp decrease in wound area as represented by the decline from 13 - 45 hours after wounding (Figure 10). The increased mitotic division is believed to take place 300 - 500 cells behind the epithelial wound margin (Block et al, 1963). Capillaries and fibroblasts together form new immature/granulation tissue (Plate 18), so providing replacement of lost tissue. Wound contraction and the resultant infolding of the wound centre is seen in Plates 20 and 24.

The increase in vessels surrounding the wound appeared to be due to angiogenesis associated with tissue damage rather than as a result of normal developmental processes. This is demonstrated in Figure 12, where the number of vessels counted from unwounded controls increased only slightly, whereas those surrounding a wound increased to a greater extent throughout the period of measurement (Figure 11). The first vessel count made at 1 hour after wounding was followed by a drop at 4 hours in both the active and sham

exposed groups but no consistent differences were seen for the effects of PEMFs (Figure 11). This decrease could represent vessels which are no longer visible due to the drainage of blood.

Petecheal haemorrhage within the wound decreased linearly (Figure 13) over the 22 hours after wounding, although some haemorrhagic material persisted. None of the three parameters measured from the CAM burn wounds (wound area, blood vessels and haemorrhage) showed any differences between the active and sham exposed groups (Tables 10 and 12 and Section 10.4). However, there were significant differences between batches in each of the three above mentioned parameters (Table 15). This could be due to seasonal variations as the experiments were run from January to July. Variations in the wounding procedure or in the incubation conditions could also account for such between batch differences. It cannot be fully excluded that the presence of subtiloid organisms or *Staphylococcus albus* was responsible for the observed batch differences since not all the egg batches were able to be tested bacteriologically.

The measurement of BAES cell division after seeding showed a linear growth line over the first 120 hours (Figure.6).

Over these five days, cell numbers per plate increased from the seeding concentration of 2.2×10^5 to 15×10^5. Similarly, the migration of the wounded monolayer of BAES cells was linear over 96 hours after wounding, showing an average migration rate of 21.7um/hr. Neither of these measures showed any differences between the active and sham exposed groups ($p > 0.2$ and $p = 0.9$ for the cell division and monolayer experiments respectively). The levels of BAES cell cyclic AMP measured after 2, 3 and 6 days growth showed that cyclic AMP levels decreased with increasing confluence of the cells, and hence with decreasing cell division (Figure 8). The actively exposed group showed a consistently higher level of cyclic AMP for the three growth times measured with a significant difference between the groups at 2 days growth ($p = 0.0023$). However, there were no significant differences between the groups at 3 and 6 days growth ($p = 0.092$ and $p = 0.970$ respectively). It should be noted that fewer data points were entered into the analysis at 6 days growth compared with the 2 and 3 days growth time, because an increasing number of experiments yielded cyclic AMP values which were sub-threshold (Table 6). All the levels measured were extremely low and a difference of 11×10^{-9} pMole/um^{2}between the means for active and sham exposed groups after 3 days growth (this being the largest difference) is questionable in the light

of such small measures (Table 7). They could represent temperature or handling differences. The role of cyclic nucleotides in the control of the proliferative response of quiescent cells has been an area of controversy. However, it is agreed that a sustained increase in cyclic AMP acts as a growth promoting signal for Swiss 3T3 cells (Rozengurt, 1982) and that it acts as a cell mediator for hormones. One such hormone, parathormone, acts in the resorption of bone (Chase and Aurbach, 1970). With this in mind, experimenters interested in bone formation in response to PEMFs have measured either cellular levels of cyclic AMP or changes in response to hormones. Norton (1977) found a decrease in the basal levels of cyclic AMP in isolated epiphyseal cartilage cells after exposure to alternating electric fields up to 1500 Volts for 5-25 minutes. The cyclic AMP results obtained here are not in aggreement, although a PEMF was used instead of an alternating electric field. Farndale (1984) showed significant elevations in the basal levels of cyclic AMP in rabbit bone marrow fibroblast cells after 1 and 4 hours of exposure to PEMF of the type used by the Bassett group. These results, however, were not repeatable (Farndale and Murray, 1986). These authors found a decrease in cyclic AMP levels in cultures which had previously been exposed to a PEMF for up to 9 days. From this it was hypothesised that the PEMF was acting in a fashion similar to a hormone;

activation and subsequent desentization of adenylate cyclase. The increase observed in the present study after 15 minutes exposure to PEMF is of such a small magnitude as not to lend support to the hypothesis. Such considerations together with the negative results from the wounded monolayer and cell division experiments, suggest that the results are not robust enough to lend support to the hypothesis that the PEMFs are responsible for the differences in the cyclic AMP levels. Further work needs to be done to substantiate any possible relationship.

In conclusion, the present study using pulsed electromagnetic fields of the type used by Bentall (1981), showed no differences between active and sham groups in the following measures: the rate of reduction of burn wound area on the chicken CAM, the number of vessels surrounding the wounds, the petecheal haemorrhage decrease within the wounds, the rate of division of bovine aorta endothelial cells in culture, the rate of outgrowth of a wounded monolayer of BAEs, and the levels of cyclic AMP in BAE cells after 3 and 6 days growth. Although a significant difference was found in the level of cyclic AMP at 2 days growth, the measures were small and suspect in the light of the rest of the results.

The experiments carried out in this study employed double blind control conditions. The negative results presented cause further questioning of the work of Bassett's group. The success in healing of non-unions of up to 80% must be looked on in the light of the fact that blinded controls were not employed, and that a stringent orthopaedic care regime was followed. Surgical intervention was employed on occasions in addition to the PEMFs (Bassett et al, 1977), and of 220 patients treated in another study (Bassett et al, 1978) results were presented for only 108 with no explanation given concerning the eliminated 112. The functional union in this study was reported as being 80%, but if all 112 of the unaccounted for patients failed to heal, then the success rate is brought down to 40%. In a further study (Bassett et al, 1979) there was no definition of the end point of healing. Similar criticism can be levelled at the work of independent experimenters using the same PEMFs as Bassett (Sutcliffe et al, 1980; O'Connor, 1980) but who also employed similar care regimes and did not use double blind controls.

The one double blind study carried out to date on the effect of PEMFs on non-unions (Barker et al, 1984) studied only 16 patients. Five of the 9 patients allocated active treatment had clinically united fractures but 5 of the 7 controls also

had united fratures. No clear conclusion can be made from such small patient numbers and there was a lack of mention of other prognostic factors before the allocation of patients to the treatment or control group.

Any study which used PEMFs of the same parameters as employed here is of particular interest. One such study is that of Nicolle and Bentall (1982) on 21 patients after cosmetic eye surgery. Each patient acted as his/her own control after both eyes had been operated on. Spectacles fitted with two RF emitting devices, one active and one sham were worn for 24 hours post operatively. Six of the 21 patients had insufficient swelling to provide an indication of an altered heling rate, but 11 of the remaining 15 showed a decrease on clinical assessment of bruising and swelling on the RF exposed eye as compared with the control. It could be the case that there was an amount of interference from the active to the placebo device, and this coupled with the small number of patients entered into the study, means that no conclusion concerning the effects of PEMFs can be made.

Slightly different field parameters were applied to the abdominal wounds of rats which were subsequently tested for wound tensile strength 2 and 8 days later (Bentall, 1981).

Few details of the study are given as the report is an abstract from a meeting proceedings. The group number was 25 but this could have been referring to the total of the three groups (placebo, 15 Watts, 2 mWatt groups). The amounts of fluid needed in each group to burst the abdominal wounds is higher in both of the RF exposed groups. However, the method causes concern in respect to its lack of sensitivity and to the final destination of the carefully measured fluid injected into the peritoneal cavity. It must always be of concern as to whether or not the needle has punctured the intestines, so allowing fluid to flow into the intestines rather than into the peritoneal cavity.

Finally, there is no substantial evidence from which to conclude that the PEMFs of the type used in this study have beneficial effects on the healing of wounds, as demonstrated in both *in vitro* and *in vivo* model systems.

REFERENCES

ADAMS G (1799) An essay on electricity explaining the principles of the useful science and describing the instruments. Dillon and Co. London. pp 482 - 575.

ADEY W R (1981) Tissue interactions with non-ionzing electromagnetic fields. Physiological Rev. Vol.61 No.2:pp 435 - 514.

ANSI C95.1 (1982) (American National Standards Institute). American national standard safety levels with respect of human exposure to radio-frequency electromagnetic fields, 300kHz to 100GHz, IEEE New York.

BARKER A T, DIXON R A, SHARRARD W J W, SUTCLIFFE M L. (1984) Pulsed magnetic field therapy for tibial non-union: Interim results of a doule blind trial. The Lancet. 1 May 1984. pp 994 - 996.

BARKER A T, JAFFE L F, VANABLES W (1982). The glabrous epidermis of cavies contains a powerful battery. Am. Physiol. Soc. Vol.242: R358 - R366.

BARKER A T, LUNT M J (1983). The effects of pulsed magnetic fields of the type used in the stimulation of fracture healing. Clin. Phys. Physiol. Meas. Vol.4: pp 1 - 27.

BASSETT C A L (1971) Biophysical principles affecting bone structure. In: The Biochemistry and Physiology of Bone. Vol.3 ed. G H Bourne (N.Y: Academic Press) pp 1 -69.

BASSETT C A L, CAULO N, KORT J. (1981a) Congenital "pseudoarthroses" of the tibia: treatment with pulsing electromagnetic fields. Clin. Orthop. Vol.154: pp 136 - 149.

BASSETT C A L, MITCHELL S N, GASTON S R (1981b) Treatment of ununited tibial diaphyseal fractures with pulsing electromagnetic fields. J. Bone Jt. Surg. Vol.63A: pp 511 - 523.

BASSETT C A L, MITCHELL S N, NORTON L, CAULO N, GASTON S R. (1979) Electromagnetic repairs of non-unions. In: Electrical properties of bone and cartilage ed. C T Brighton, J Black, S R Pollack. N.Y: Grune and Stratton pp 605 - 630.

BASSETT C A L, MITCHELL S N, NORTON L, PILLA A A . (1978) Repair of non-unions by pulsing electromagnetic fields. Acta Orthop. Belg. Vol.44: 706 - 724.

BASSETT C A L, PAWLUK R J, BECKER R O. (1964) Effects of electric currents on bone formation *in vivo* Nature (London) Vol.204: p 652.

BASSETT C A L, PAWLUK R J, PILLA A A. (1974) Augmentation of bone repair by inductively coupled electromagnetic fields. Science Vol.184: pp 575 - 577.

BASSETT C A L, PILLA A A, PAWLUK R J. (1977) A non-operative salvage of surgically resistant pseudoarthrosis and non-unions by pulsing electromagnetic fields. Clin. Orthop. Vol.124: 128 - 143.

BAWIN S M, ADEY W R, SABBOT I M. (1978) Ionic factors in release of $^{45}Ca^{2+}$ from chicken cerebral tissue by electromagnetic fields. Proc. Natl. Acad. Sci. Vol.75 No.12: pp 6314 - 6318.

BENTALL R H C (1981) Effect of a 15 Watt 27.12 MHz and a 2 mWatt pulsed 3 MHz device on the tensile strength of rat abdominal wall incisions. Trans. Bioelec. Repair and Growth Soc. Vol.1: pp 22.

BLOCK M, SEITER I, OETHLERT W (1963). Autoradiographic studies of the initial cellular response to injury. Exp. Cell Res. Vol.30: pp 311 - 321.

BORGENS R B (1982) What is the role of naturally produced electric current in vertebrate regeneration healing? Internatl. Rev. of Cytol. Vol.76: pp 245 - 298.

BRIGHTON C T (1981) The treatment of non-unions with electricity. J. Bone Jt. Surg. Vol.63A: pp 847 - 851.

BROWN B L, et al (1971) Preparation on cyclic AMP binding protein from bovine adrenal glands. Biochem. J. Vol.121 pp 561 - 562.

CHASE L R, AURBACH G D (1970) The effect of parathyroid hormone on the concentration of adenosine 3'5' monophosphate in skeletal tissue *in vitro* . J. Biol. Chem. Vol.245: pp 1520.

COCHRAN G B (1972) Experimental methods for stimulation of bone healing by means of electrical energy. Bull N.Y Acad. Med. Vol.48: pp 899 - 911.

COCHRAN G B, PAWLUK R J, BASSETT C A L (1968) Electromechanical characteristics of bone under physiologic moisture conditions. Clin. Orthop. Vol.58: pp 249 - 270.

DEALLER S F (1981) Electrical phenomena associated with bones and fractures and the therapeutic use of electricity in

fracture healing. J. Med. Eng. Tech.Vol.5: pp 73 - 79.

DeHAAS W G, LAZAROVICI M A, MORRISON D M. (1979) The effect of low frequency magnetic fields on the healing of the osteotomised rabbit radius. Clin. Orth. Rel. Res. Vol.145: pp 245 - 251.

DELGADO J M R, LEAL J, MONTEGO J L, GRACIA M G (1982) Embryological changes induced by weak, extremely low frequency electromagnetic fields. J. Anat. Vol.134 No.3: pp 533 - 551.

DELPORT P H, CHENG N, MULIER J C, SANSENW, DE LOECKER W (1985) The effect of pulsed electromagnetic fields on metabolism in rat skin. Bioelectrochemistry and Bioenergetics. Vol.14: pp 93 - 98.

DUBOIS-REYMOND E (1860) "Untersuchungen ueber tierche elektrizitaet". Vol.2: 2 Reimer Berlin.

DUNN B E, FITZHARRIS T P, BARNETT B D. (1981) Effects of varying chamber construction and embryo incubation age on survival and growth of chick embryos in shell-less culture. The Anat. Rec. Vol.199 No.1: pp 33 - 43.

ENZLER M A, WAELCHLI-SUTER C, PERREN S M (1980) Prevention of non-unions by means of magnetic stimulation. Ulfallheilkunde Vol.83: pp 188 - 194.

FARNDALE R W (1984) Ph.D thesis (CNAA)

FARNDALE R W, MURRAY J C (1986) The action of pulsed magnetic fields on cyclic AMP levels in cultured fibroblasts. Biochem. and Biophysica. Acta. Vol.881: pp 46 - 53.

FLUMMERFELT B A, GIBSON M A (1969) The histology of the developing chorioallantoic membrane in the chicken (*Gallus domesticus*) Can. J. of Zool. Vol.47: pp323-331.

FRANK C, SCHACHAR N, DITTRICH D, SACHRIVEN, deHAAS W, EDWARDS W (1983) Electromagnetic stimuation of ligament healing in rabbits. Clin. Orthop. Vol.175: 263-272.

FREEMAN B M, VINCE M A (1974) Development of the avian embryo. Chapman and Hall, London. pp 129.

FROHLICH H (1982) What are non-thermal electric biological effects? Bioelectromagnetics. Vol.3: pp 45 - 46.

GAULT W R, GATENS P F (1976) Use of low intensity direct

current in management of ischaemic skin ulcers. Phys. Ther. Vol.56: pp 265 - 268.

GLASER Z R (1971) Bibliography of reported phenomena ("Effects") on clinical manifestation attributed to microwave and radio-frequency radiation. Naval Medical Research Institute Research Report, project 12-524-015-004B, report No. 2.

GOLDIN J H, BROADBENT N R G, NANCARROW J D, MARSHALL J (1981) The effects of diapulse on the healing of wounds: a double blind randomised controlled trial in man. Brit. J. of Plastic Surg. Vol.34: pp 267 - 270.

GOODMAN R, BASSETT C A L, HENDERSON A S (1983) Pulsing electromagnetic fields induce cellular transcription. Science Vol.220: pp 1283 - 1285.

GOODMAN R, HENDERSON A S (1986) Some biological effects of electromagnetic fields. Bioelectrochemistry and Bioenergetics. Vol.15: pp 39 - 55. A section of J. Electroanal. Chem. constituting Vol.221.

HISENKAMP M, BOURGOIS R, BASSETT C A L, CHIABERRA A , BURNY F, RYABY J (1978b) Electromagnetic stimulation of fracture repair. Influence on healing of fresh fractures. Acta Orthop. Belg. Vol.44: pp 671 - 698.

ILLINGER K H (1981) Biological effects of non-ionizing radiation - ACS Symposium Series 157. American Chemical Society.

JAFFE L A (1976) Evidence for an electrically mediated fast block to polyspermy in sea urchin eggs. J. Cell Biol. Vol.70:229a.

JAFFE L A, NUCCITELLI R (1977) Electrical controls of development. Ann. Rev. Biophys. Bioeng. Vol.6: pp445 - 476.

JAFFE L F (1979) Control and development of ionic currents in membrane transduction mechanics. Ed. R A Cone, J E Dowling. Press N.Y. pp 199 - 231.

LEVY D D, RUBIN B (1972) Inducing bone growth in vivo by pulse stimulation. Clin.Orthop. Vol.88: pp 218 - 222.

LIBOFF A R, WILLIAMS T Jr, STRONG D M, WISTAR R Jr (1984) Time varying magnetic fields: effects on DNA synthesis . Science Vol.223: pp 818 - 820.

LUBEN R A, CAIN C D, CHEN M C Y, ROSEN D M, ADEY W R (1982) Effects of electromagnetic stimuli on bone and bone cells *in vitro* : Inhibition of responses to parathyroid hormone by low energy low frequency fields. Proc. of the Natl. Acad. of Science. Vol.79: pp 4180 - 4184.

McELHANEY J H, STALNAKER R L, BULLARD R (1968) Electric fields and bone loss of disuse. J. Biomech. Vol.1: pp 47 - 52.

MARTIN R B (1979) Comparison of capacitive and inductive bone stimulation devices. Annals of Biomed. Eng. Vol.7: pp 387 - 409.

MARTIN R B, GUTMAN W (1978) The effect of electric fields on osteoporosis of disuse. Calcif. Tissue Res. Vol.25: pp 23 - 27.

NICOLLE F V B, BENTALL R H C (1982) Use of radio frequency pulsed energy in the control of postoperative reaction in blepharoplasty. Aesth. Plast. Surg. Vol.6: pp 169 - 171.

NORTON L A, RODAN G A, BOURRETT L A (1977) Epiphyseal cartilage cAMP changes produced by electrical and mechanical perturbations. Clin. Orthop. and Related Res. Vol.124: pp 59 - 68.

NUCCITELLI R (1984) The involvement of transcellular ion current and electric fields in pattern formation. In: Pattern Formation. Ed. G M Malacinski, S V Bryant. Macmillan Pub. Co.N.Y.

O'CONNER B T (1980) The bone growth stimulator. J. Bone Jt. Surg. Vol.62B: pp 266.

PETERSEN R C (1983) Bioeffects of microwaves: A review of current knowledge. J. of Occupational Med. Vol.25 No.2: pp 103 - 111.

PILLA A A (1979) Electrochemical information transfer and its role in the control of cell function. In: Electrical Properties of Bone and Cartilage. Eds; Brighton C T, Black J, Pollack S R. Grune and Stratton N.Y. (1979) pp 455 - 489.

REPACHOLI M H (1983) Sources of application of radio-frequency (RF) and microwave energy. In: Biological Effects and Dosimetry of Nonionizing Radiation. Ed. M Grandolfo, S M Michaelson, A Rindi. Plenum Press N.Y and Lond. pp 19 - 41.

RODAN G A, BOURRET L A, NORTON L A (1978) DNA synthesis in cartilage cells is stimulated by oscillating electric fields. Science Vol.199 pp 690 - 692.

ROZENGURT E (1982) Adenosine receptor activation in quiescent Swiss 3T3 cells. Exp. Cell Res. Vol.139 pp 71 - 78.

SCHWARTZ S M (1978) Selection and charaterization of Bovine Aortic Endothelial cells. In Vitro. Vol.14 pp 666 - 680

SEDEL L, CHRISTEL P, DURIEZ J, DURIEZ R, ERRARD J, FICAT C, CANCHOIX J, WITVOET J (1981) Resultats de la stimulation par champ electromagnetique de la consolidation des pseudoarthroses. Rev. Clin. Orthop. Vol.67: pp 11 - 23.

SUTCLIFFE M L, SHARRARD W J W, MacEACHERN A G (1980) The treatment of congenital pseudoarthrosis of the tibia with pulsing electromagnetic fields (A survey of 52 cases) J. Bone Jt. Surg. Vol.62B: pp 123.

TAKAHASHI K, KANEKO I, DATE M, FAKUDA E (1986) Effect of pulsing electromagnetic fields on DNA synthesis in mammalian cells in culture. Experientia Vol.42: pp 185 - 186.

WALTER J B, ISRAEL M S (1974) General Pathology. 4th Edition. Churchill Livingstone.

WHO/UNEP/IRIRC-IRPA (1981) (World Health Organization/ United Nations Environmental Programme/ International Non-Ionizing Radiation Committee of the International Radiation Protection Association), Environmental health criteria 16, Radiofrequency and Microwaves WHO, Geneva, Switzerland.

WILSON D H (1972) Treatment of soft tissue by pulsed electrical energy. Brit. Med. J. Vol.2: pp 269 - 270.

WOLCOTT L E, WHEELER P C, HARDWICK H M, ROWLEY B A (1969) Accelerated healing of skin ulcers by electrotherapy. Southern Medical Journal. Vol.66: pp 795 - 801.

YASUDA I (1953) The classic fundamental aspects of fracture treatment. J. Kyoto Med. Soc. Vol.4 pp 395-406 English translation in 1977. Clin. Orthop. and Related Res. Vol.124: pp 5 - 8.

APPENDIX 1

TABLE OF EXPOSURE PARAMETERS AS USED BY BASSETT'S GROUP AND BARKER ET AL (1984) (AND REFERRED TO IN THIS THESIS)

REFERENCE NO.	1+	2a	2b	3	4
SINGLE (S) OR PULSE BURST (PB) WAVEFORM	NA	S	S	S	PB
SINGLE PULSE DURATION	NA	1ms	150us	300us	30us
PULSE RISE TIME	NA	-	-	$<10^{-6}$s	-
PAUSE TIME BETWEEN SINGLE PULSES	NA	999ms*	15.4ms*	13.2ms*	200us*
PULSE BURST REPETITION FREQUENCY	NA	NA	NA	NA	12HZ
PAUSE TIME BETWEEN PULSE BURSTS	NA	NA	NA	NA	91ms*
PULSE BURST DURATION	NA	NA	NA	NA	5ms
CARRIER FREQUENCY	NA	NA	NA	NA	4.4MHz*
MAGNETIC FLUX	-	-	-	-	-
ELECTRIC FIELD	-	-	-	-	-
SAR (WKg^{-1})	-	-	-	-	-
DRIVING VOLTAGE	-	24V	24V	110V	-
INDUCED VOLTAGE ($mVcm^{-1}$)	-	2	20	1-2	-
POWER (Wcm^{-1})	-	10^{-4}	$1-^{-4}$	10^{-10}	-
CURRENT	10-100uA	-	-	-	-
CURRENT DENSITY ($uAcm^{-2}$	-	-	-	10	-

SEE PAGE 83 FOR REFERENCE LIST AND PAGE 84 FOR PULSE DIAGRAM

NA - Not applicable
* - Calculated by author of this thesis.
\+ - Direct Current used.
Reference 2a and 2b the same, but two sets of parameters used.

REFERENCE NO.	5+	6a	6b$	7++	8
SINGLE (S) OR PULSE BURST (PB) WAVEFORM	-	S	PB	-	PB
SINGLE PULSE DURATION	-	380us	200us	-	28us
PULSE RISE TIME	-	$<10^{-6}$	-	-	-
PAUSE TIME BETWEEN SINGLE PULSES	-	13.7ms*	40us*	-	200us
PULSE BURST REPETITION FREQUENCY	-	NA	15Hz	-	15Hz
PAUSE TIME BETWEEN PULSE BURSTS	-	NA	66ms	-	71ms
PULSE BURST DURATION	-	NA	5ms	-	5ms
CARRIER FREQUENCY	-	NA	4.2MHz*	-	4.4MHz*
MAGNETIC FLUX	-	-	-	-	1.9uT
ELECTRIC FIELD	-	-	-	-	125mV
SAR (WKg^{-1})	-	-	-	-	-
DRIVING VOLTAGE (V)	10-18	110	-	110	-
INDUCED VOLTAGE (mV/cm)	1-1.5	1-1.5	1-1.5	-	-
POWER (Wcm^{-1})	-	-	-	-	-
CURRENT	-	-	-	-	-
CURRENT DENSITY $uAcm^{-2}$	-	-	-	-	-

SEE PAGE 83 FOR REFERENCE LIST AND PAGE 84 FOR PULSE DIAGRAMS.

NA - Not applicable
* - Calculated by author of this thesis.
$ - used if device described in 6a failed.
\+ - quoted as available as a prescription from Electro-Biology Inc., 300 Fairfield Rd, Fairfield, New Jersey 07006 (patented). No details otherwise given.
++ - Equipment referred to as BiOsteogen System 204 (above address for purchace).
Reference 6a and 6b the same, but two sets of parameters used.

APPENDIX 1 (CONTINUED)

REFERENCES USED IN APPENDIX 1 TABLE

1 - Basset C A L, Pawluk R J, Becker R O (1964)

2 - Bassett C A L, Pawluk R J, Pilla A A (1974)

3 - Bassett C A L, Pilla A A, Pawluk R J (1977)

4 - Bassett C A L, Mitchell S N, Norton L, Pilla A A (1978)

5 - Bassett C A L, Mitchell S N, Norton L, Caulo N, Gaston S R (1979)

6 - Bassett C A L, Caulo N, Kort J (1981a)

7 - Bassett C A L, Mitchell S N, Gaston S R (1981b)

8 - Barker A T, Dixon R A, Sharrard W J W, Sutcliffe M L (1984)

(Further details from Barker A T and Lunt M J (1983))

APPENDIX 1 (CONTINUED)

DIAGRAMMATIC REPRESENTATION OF PULSED ELECTROMAGNETIC WAVES: SINGLE AND PULSE BURST.

SINGLE PULSE

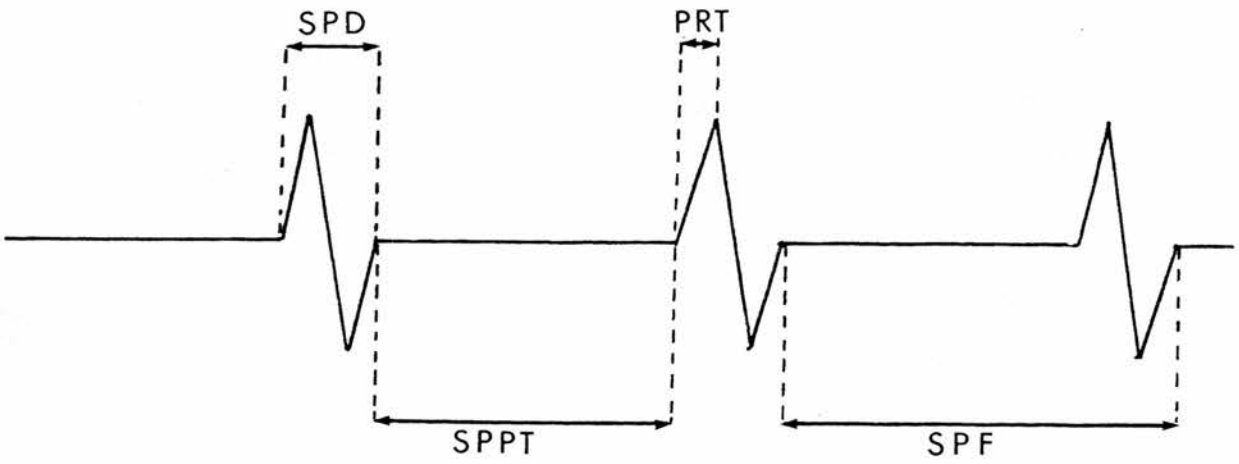

PULSE BURST

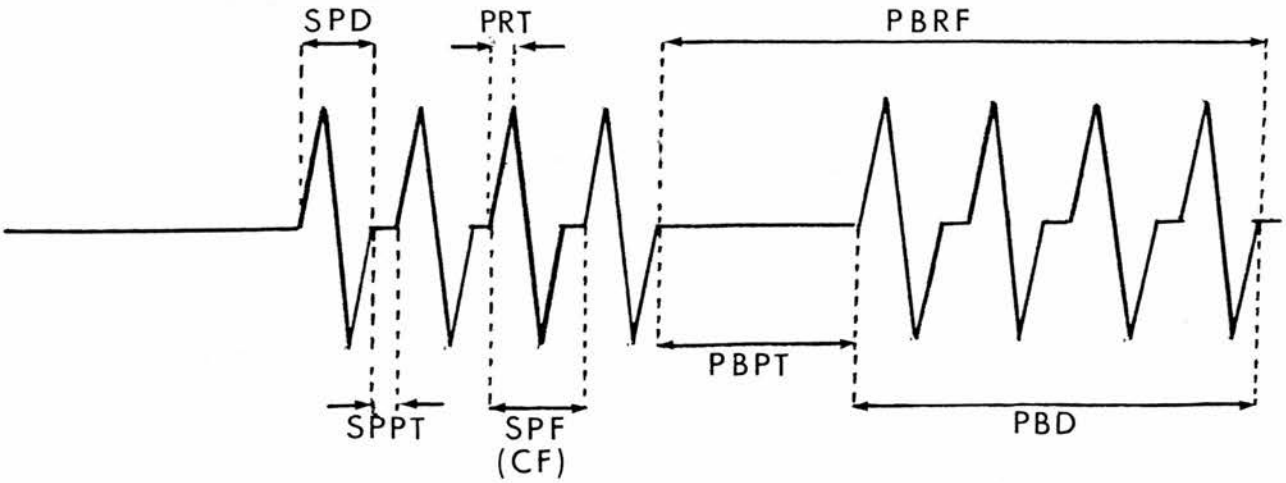

(P.T.O FOR KEY)

PLATE 1: Oscilloscope tracing to show the output of an RFED (Parameters in Table 1). Two pulses are shown, each lasting 80usecs and separated by 920 usecs. The amplitude is arbitarily set and is not indicative of the power output.

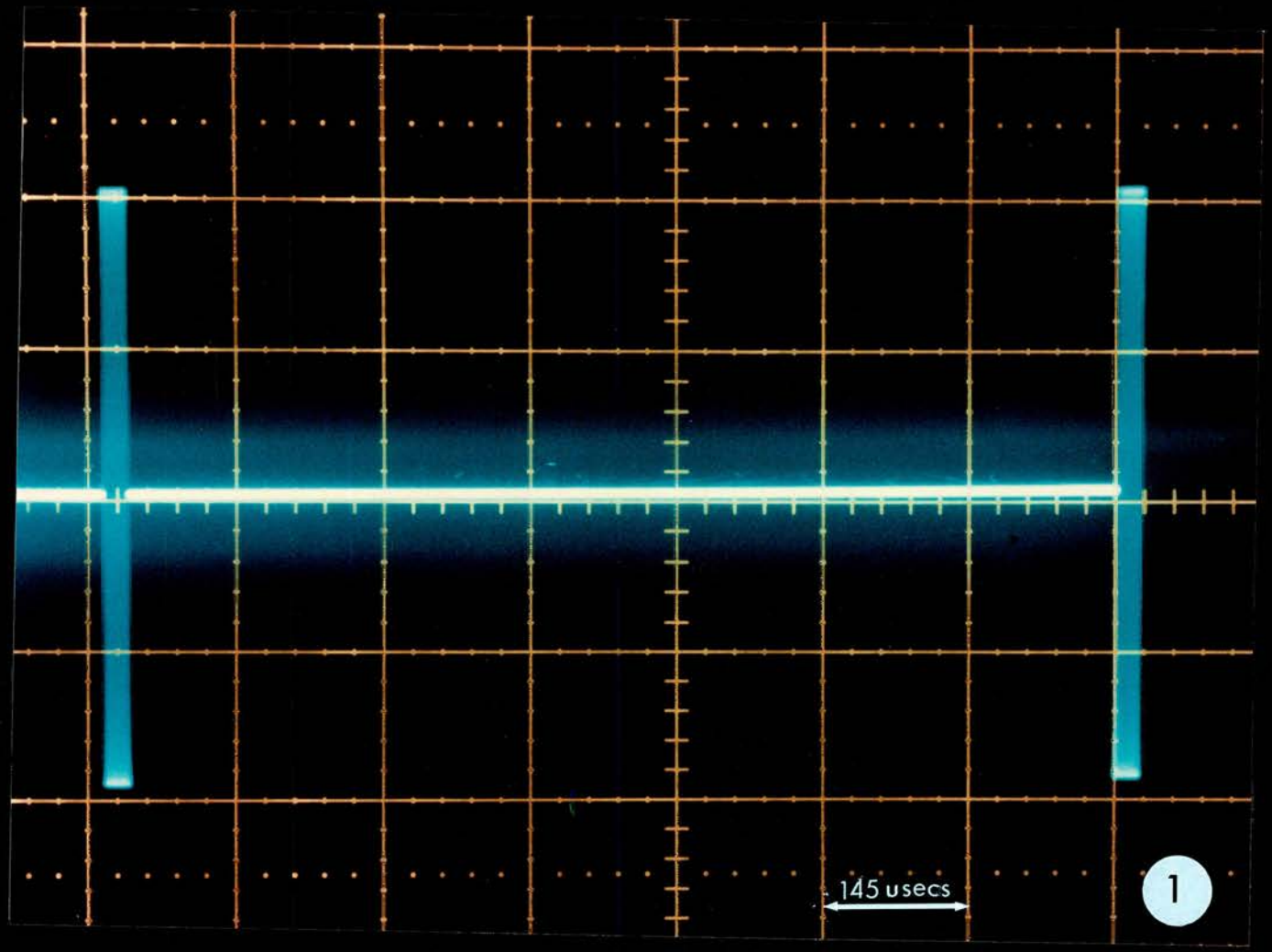
145 usecs
1

PLATE 2: Oscilloscope tracing to show an enlargment of one of the pulses of RF energy shown in Plate 1, oscillating at the carrier frequency of 27 x 10^6 cycles per second (27MHz). The amplitude has been arbitarily set and is not indicative of the power output.

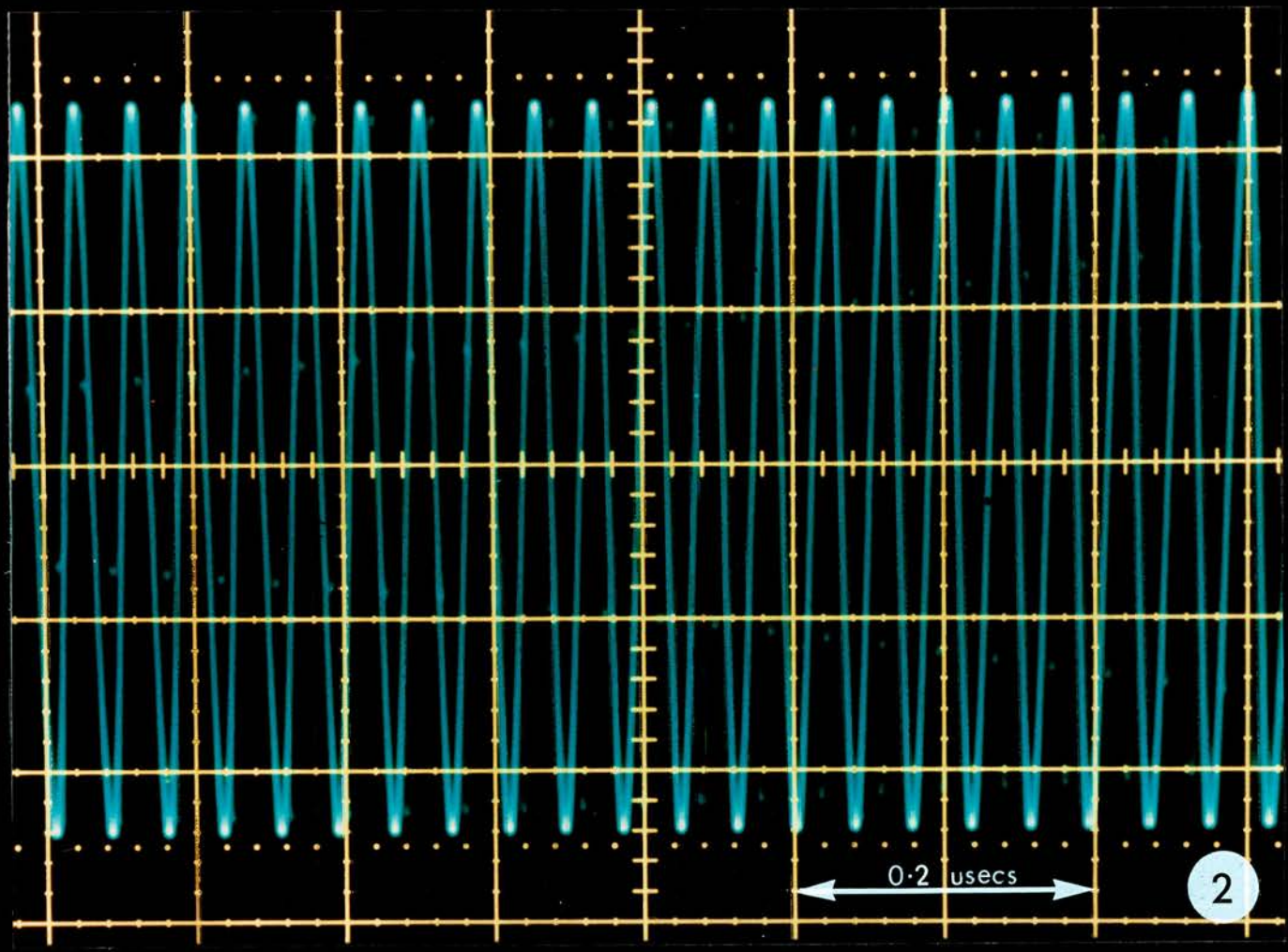
0·2 usecs
2

PLATE 3: RFED surrounding culture dish (5.8 cms in diameter) as used for cell division and monolayer outgrowth experiments.

PLATE 4: RFED surrounding culture dish (each well 3.5 cms in diameter) used for cyclic AMP measurements.

3

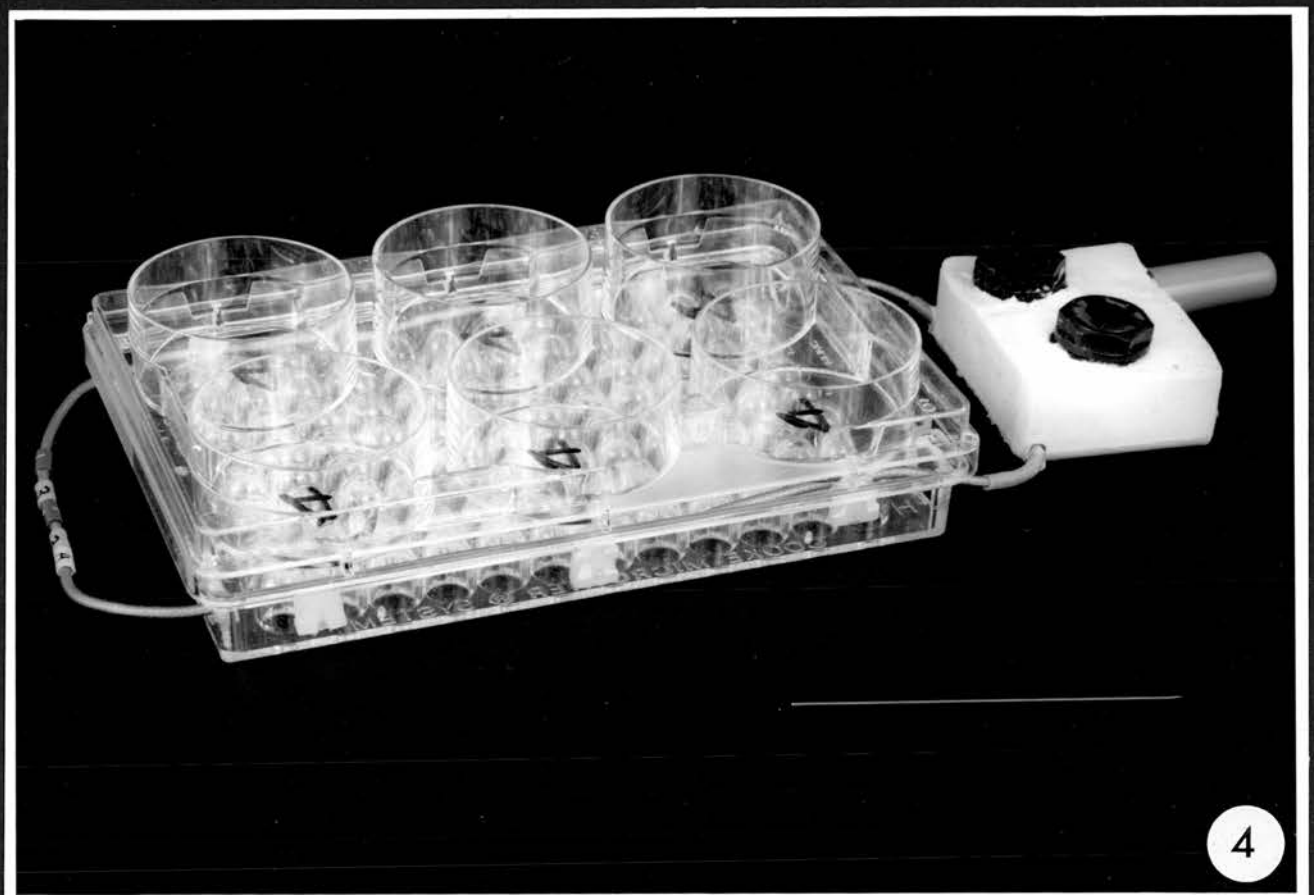

4

PLATE 5: RFED surrounding culture dish (6.8 cms in diameter) used for the CAM wound healing model (shell-less culture).

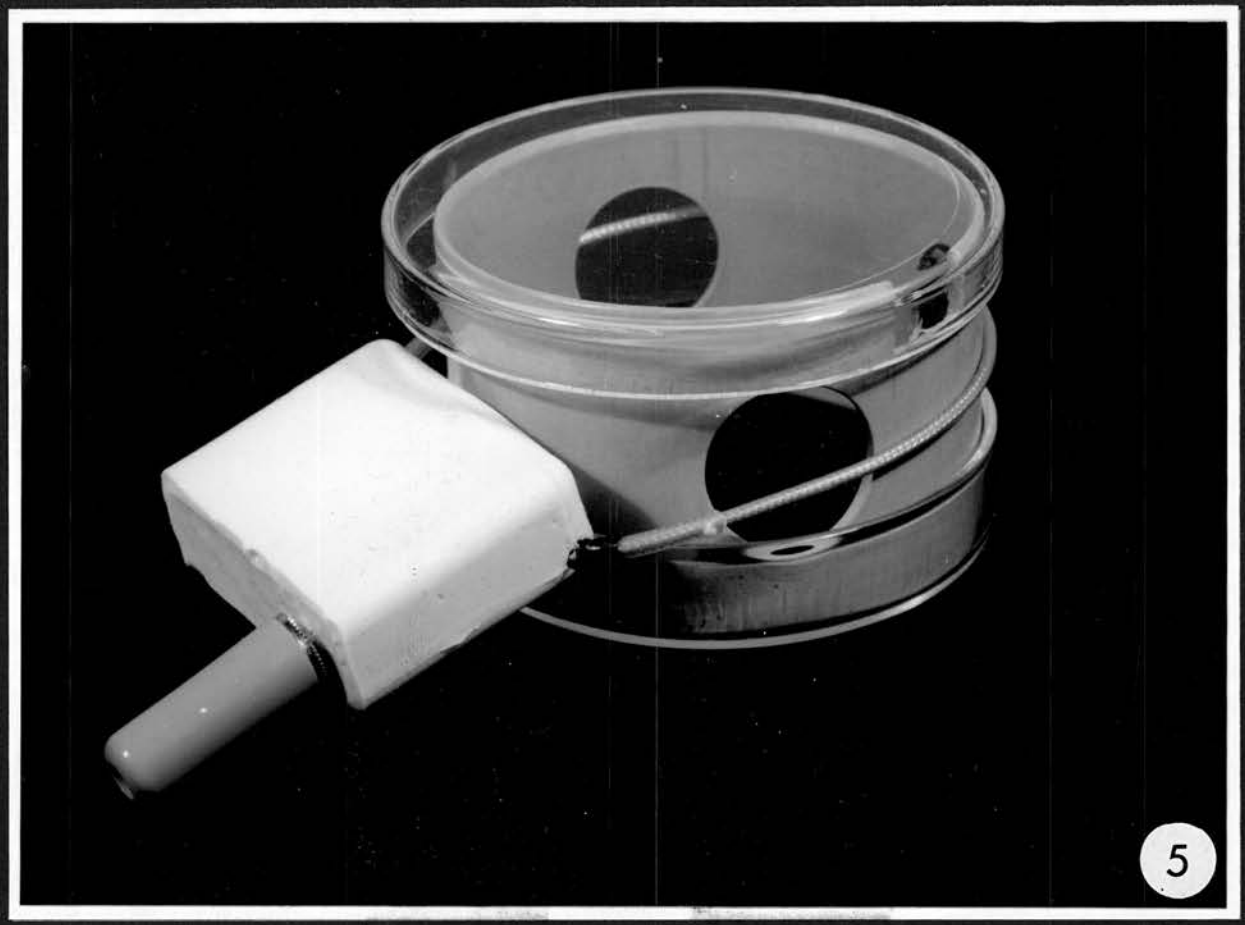
5

PLATE 6: Apparatus used for cracking the fertile eggs.

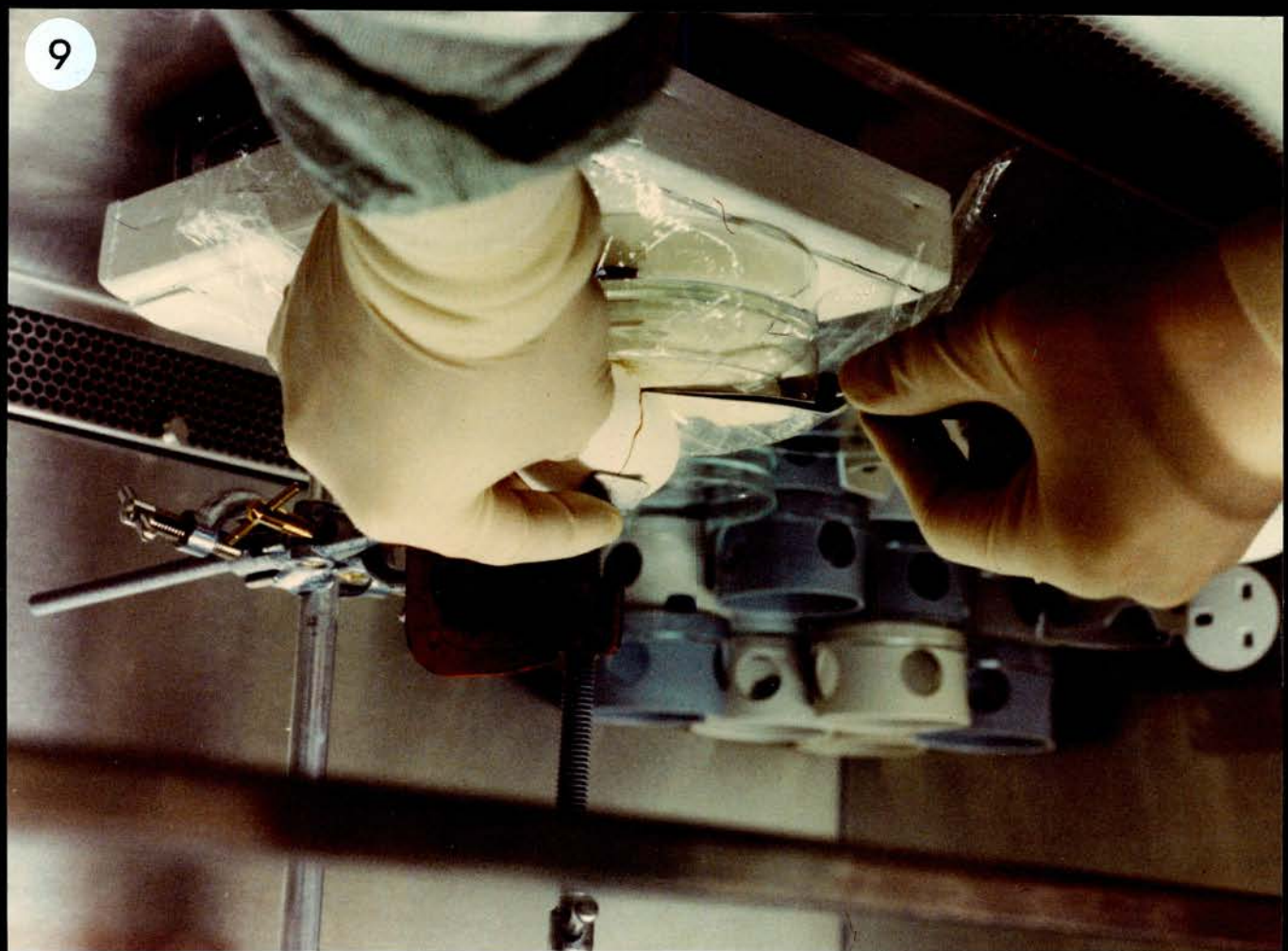
9

PLATE 7: Burning the CAM surface of 10.5 incubation day shell-less cultures.

PLATE 8: Growth line of BAES 90 hours after scraping. The thick arrow indicates an area of pallisading cells. The dotted line is the approximate position of the original growth line and the thin arrow indicates the direction of cell outgrowth (x700).

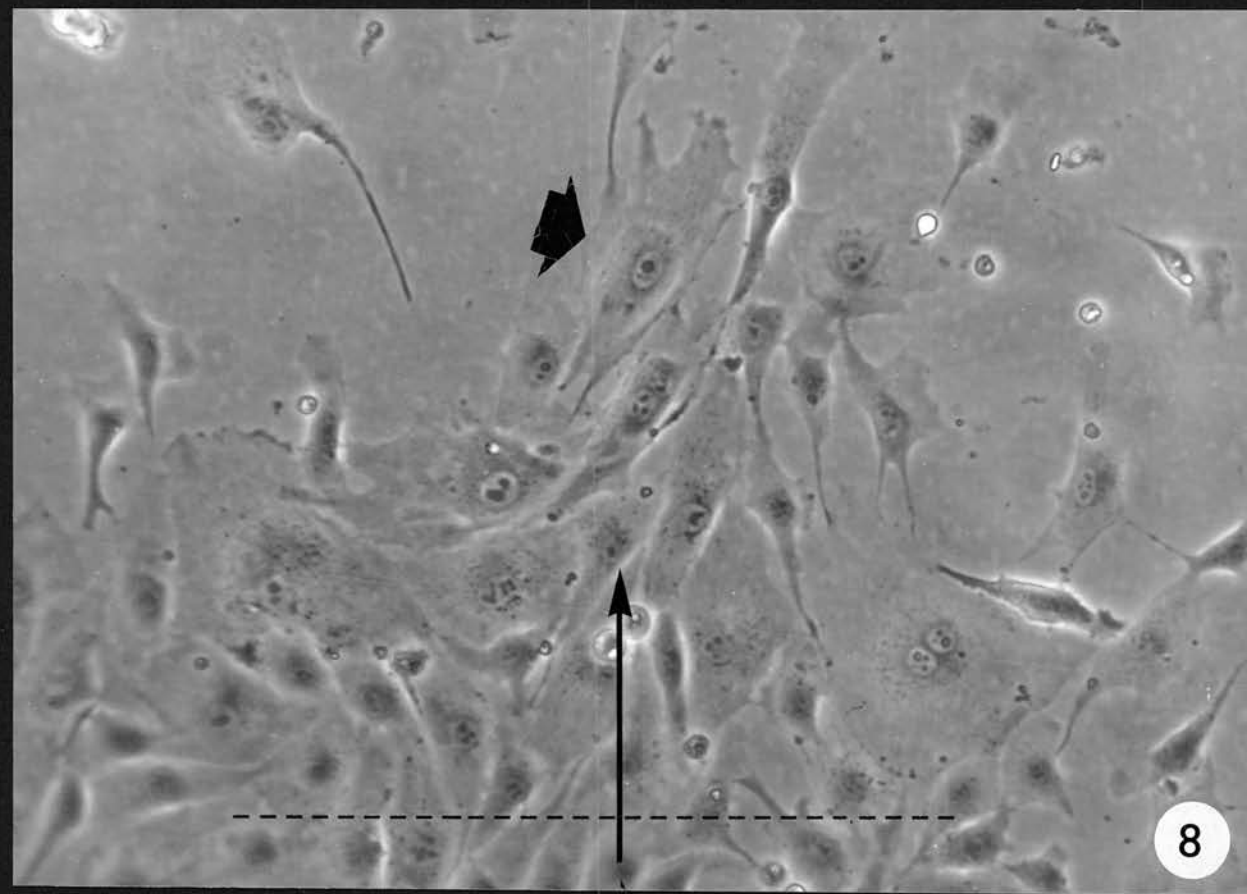
8

ABBREVIATIONS USED IN PLATES 9 - 14

C - wound associated capillaries
H - healthy CAM tissue
L - light reflection
N - necrotic tissue
P - petecheal haemorrhage
W - wound edge

PLATE 9: The CAM burn wound 1 hour after injury (x20).

PLATE 10: The CAM burn wound 13 hours after injury (x20).


P
W
H
9

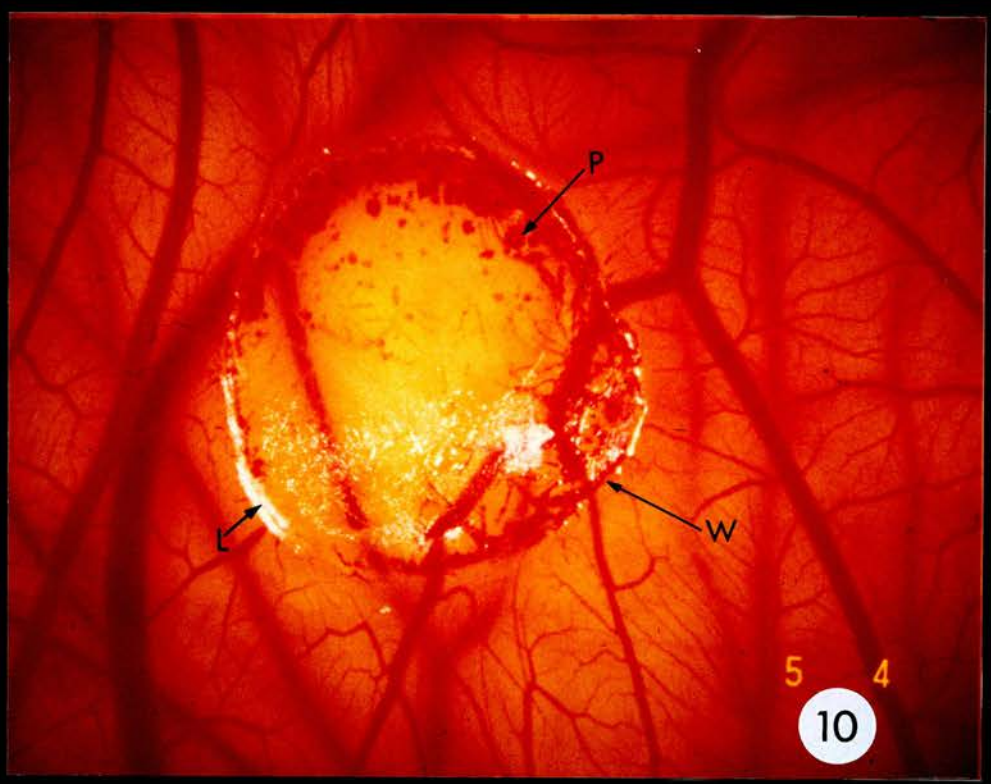
P
L
W
5 4
10

PLATE 11: The CAM burn wound 25 hours after injury (x20).

PLATE 12: The CAM burn wound 37 hours after injury (x20).

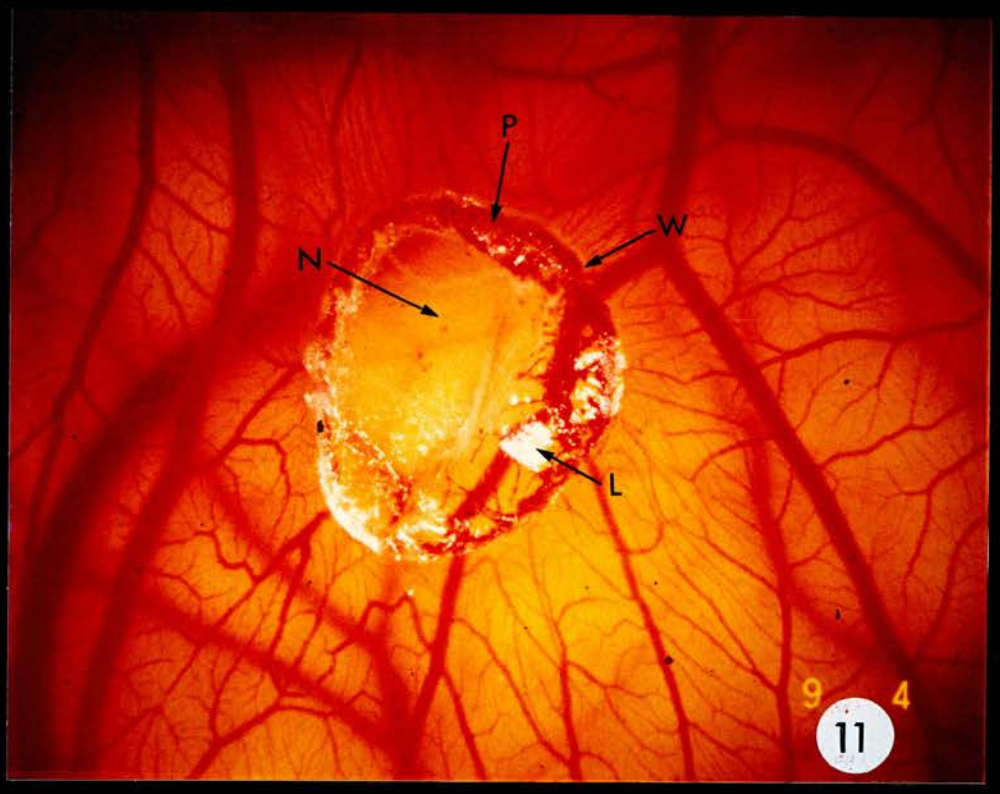
P
W
N
L
9 4
11

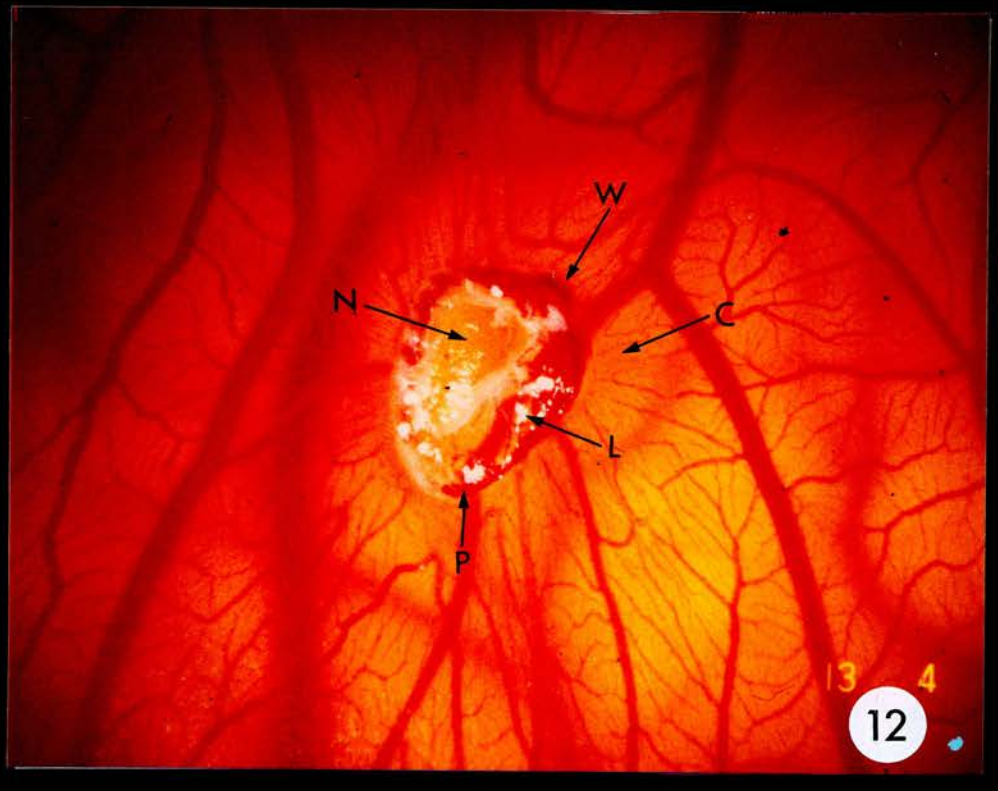
W
N
C
L
P
13 4
12

PLATE 13: The CAM burn wound 49 hours after injury (x20).

PLATE 14: The CAM burn wound 73 hours after injury (x20).

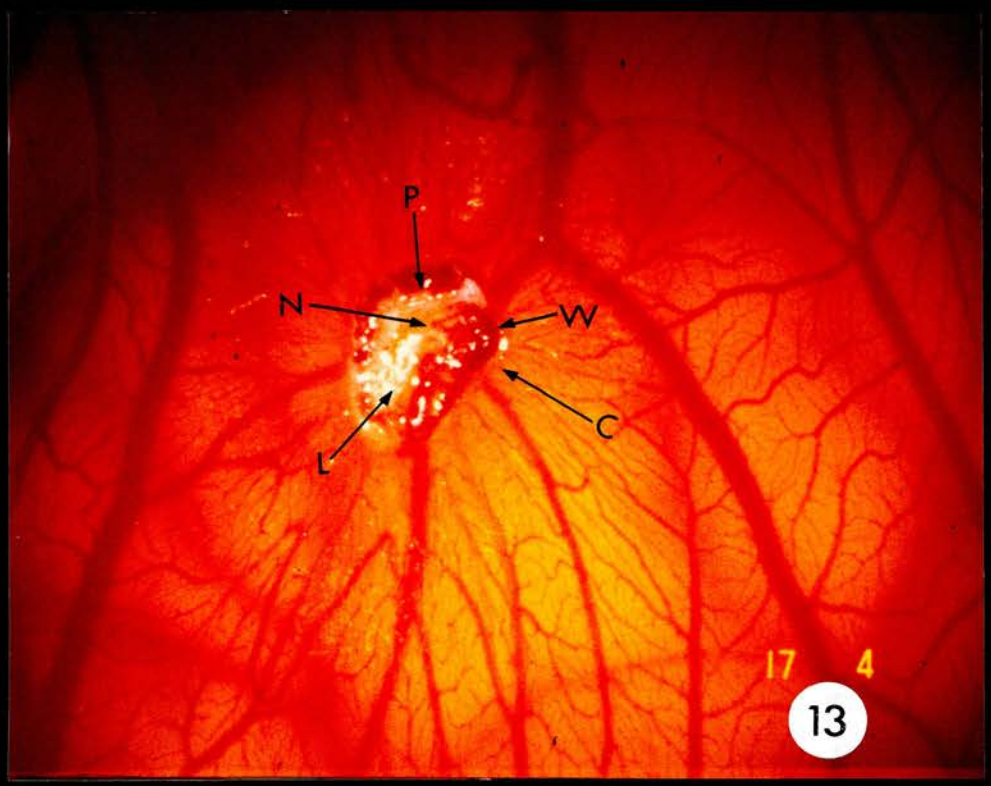
P
N
W
C
L
17 4
13

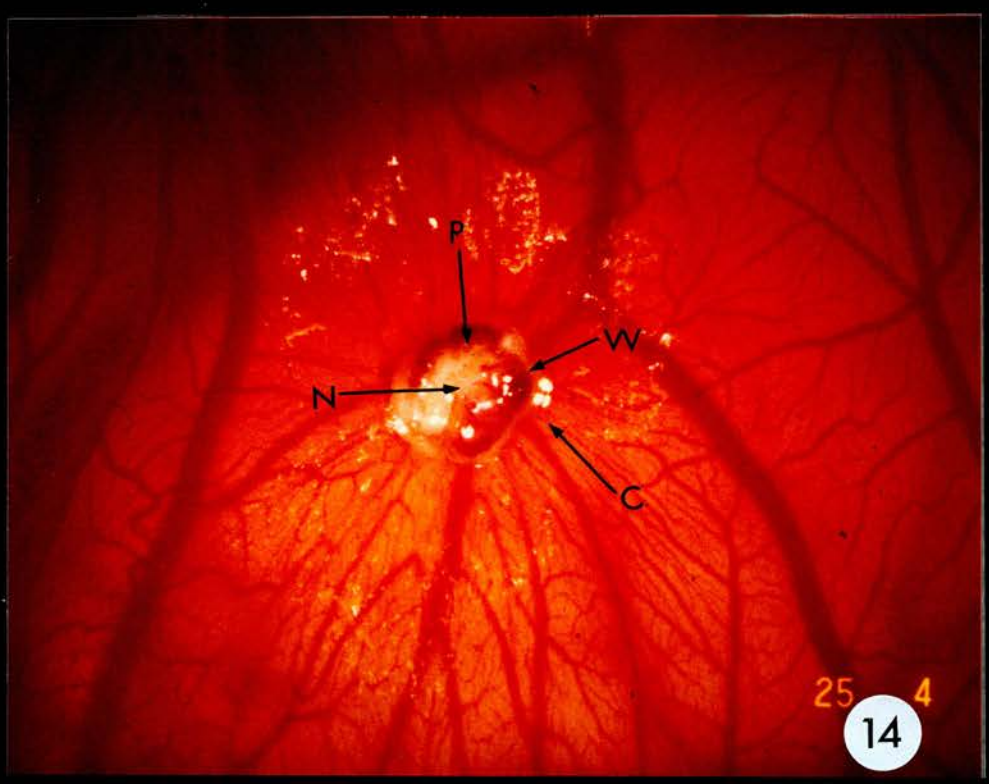
P
W
N
C
25 4
14

ABBREVIATIONS USED IN PLATES 15 - 21

AE - allantoic membrane
BV - blood vessel
C - wound associated capillaries
CB - coagulated blood
CE - chorionic epithelium
M - mesenchyme
WE - wound edge
→ - tissue above or below the heavy arrow is wounded

PLATE 15: Light Microscopy: Unwounded CAM at 10.5 incubation days, where X marks the probable position of a lymphatic vessel (x400)

PLATE 16: Light Microscopy: Wounded CAM 1 hour after injury where Y marks an area of haemorrhage (x550)

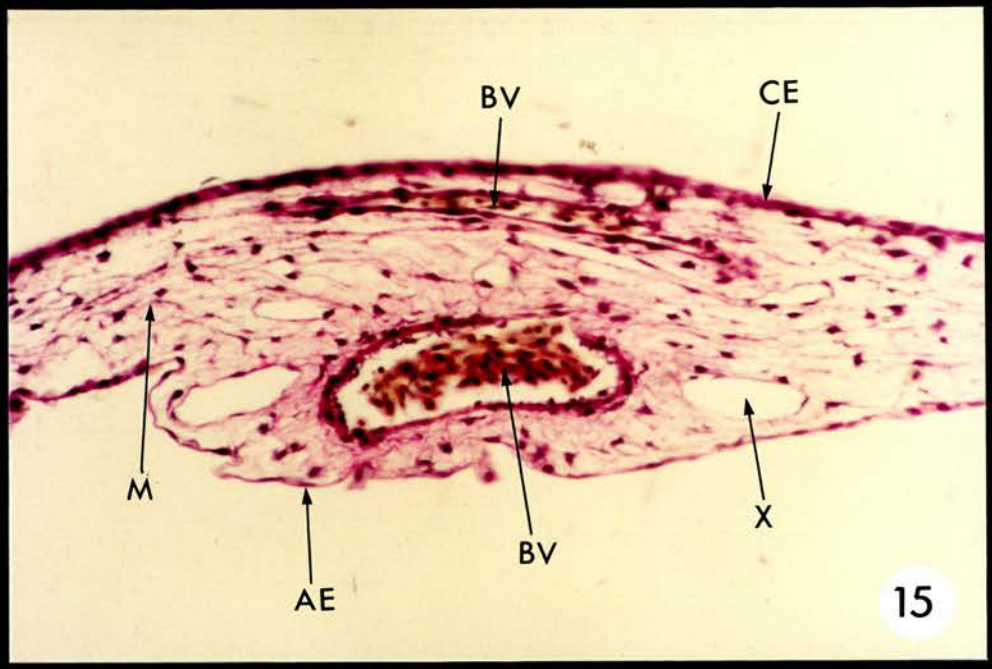
BV
CE
M
AE
BV
X
15

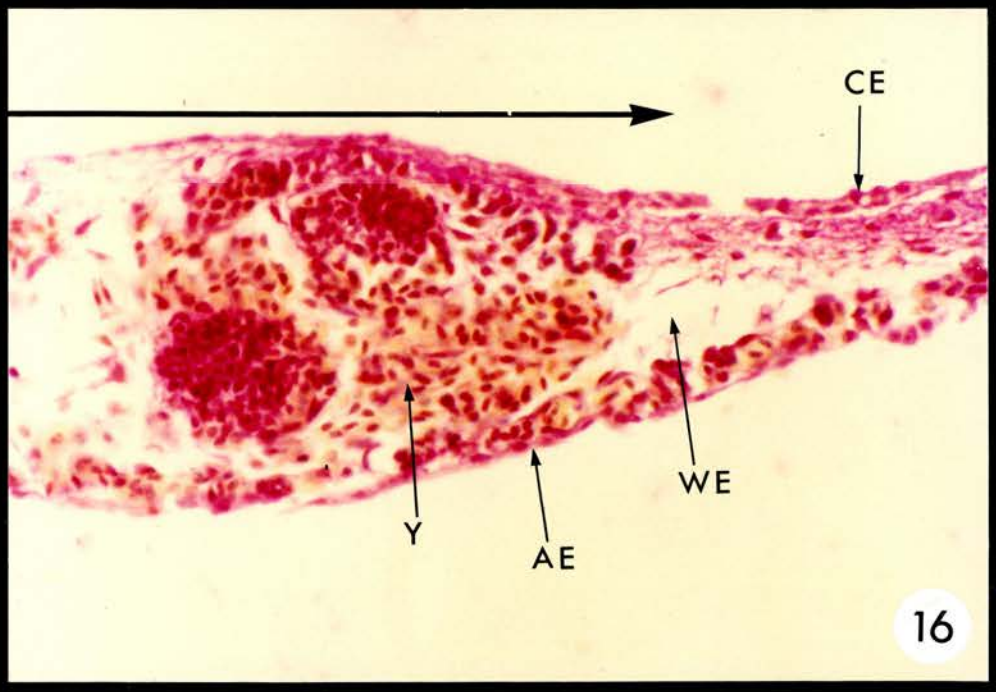
CE
Y
AE
WE
16

PLATE 17: Light Microscopy: Wounded CAM 24 hours after injury. Z marks an area where some cellular components are beginning to move towards the wound margin (x450)

PLATE 18: Light Microscopy: Wounded CAM 36 hours after injury where T marks the thickened chorionic epithelium (x450)

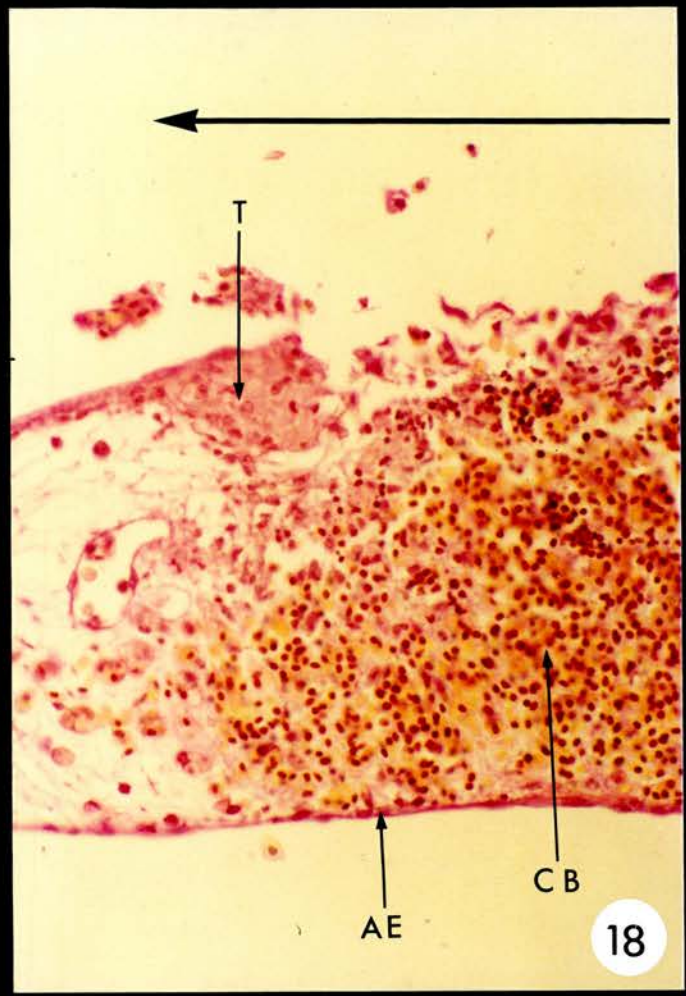
T
AE
C B
18


Z
C
AE
17

PLATE 19: Light Microscopy: Wounded CAM 48 hours after injury where T and Z are as given in Plates 17 and 18 (x250)

PLATE 20: Light Microscopy: Wounded CAM 48 hours after injury (wound centre x250)

20

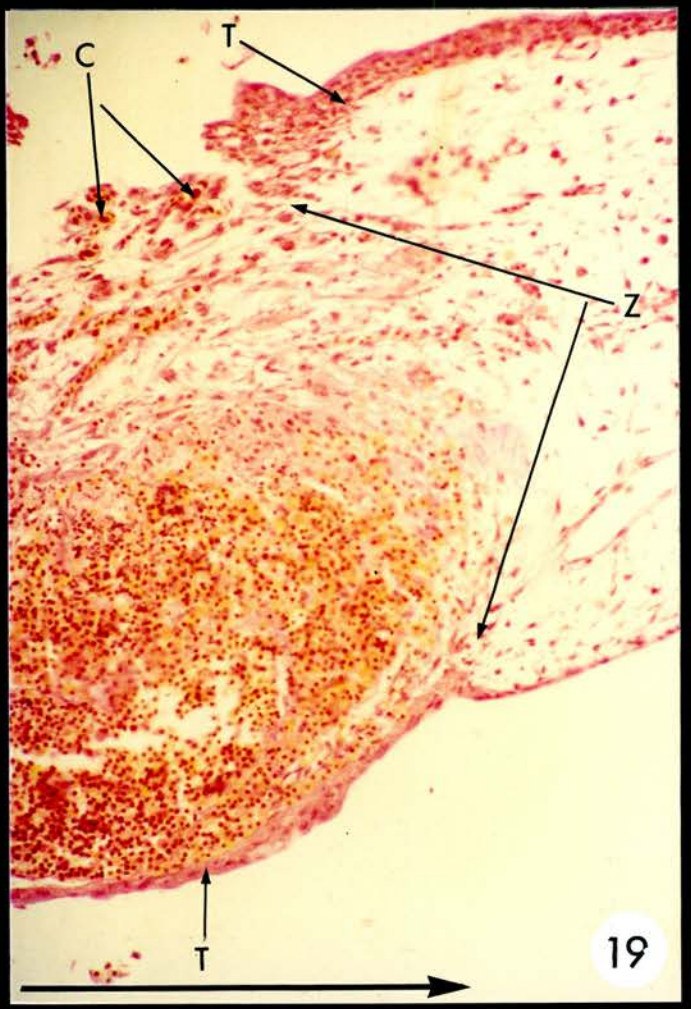

19

PLATE 21: Light Microscopy: Wounded CAM 73 hours after injury. Note the extensive inflammatory and necrotic material (purple area) (x250)

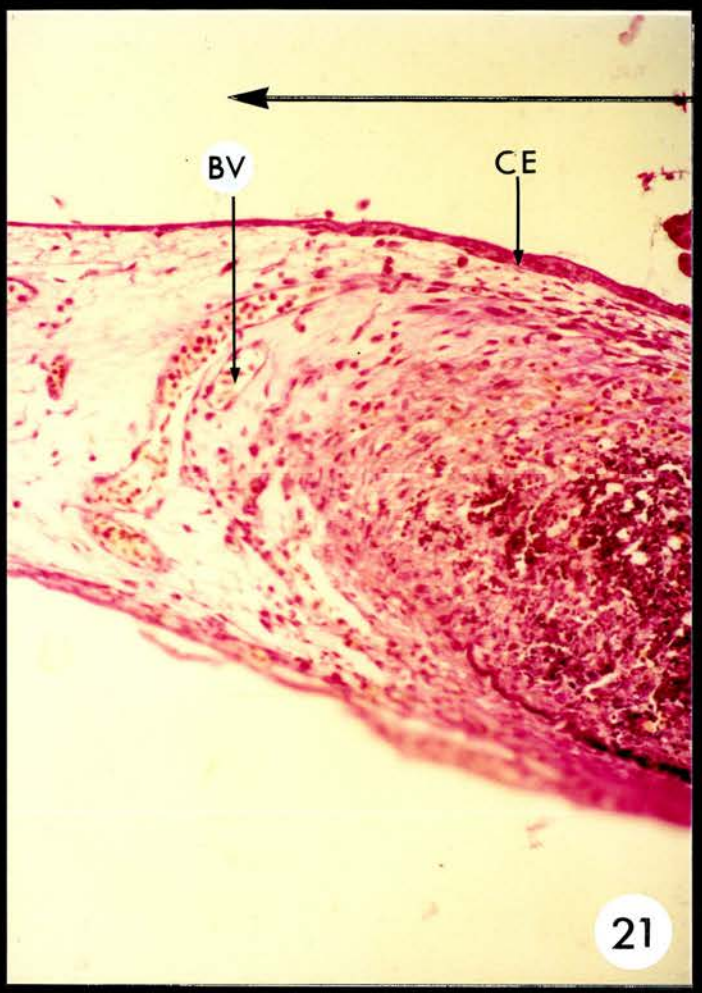
BV
CE
21

PLATE 22: Scanning Electron Microscopy: Wounded CAM 24 hours after injury (wound margin x700)

PLATE 23: Scanning Electron Microscopy: Wounded CAM 48 hours after injury (wound margin x700)

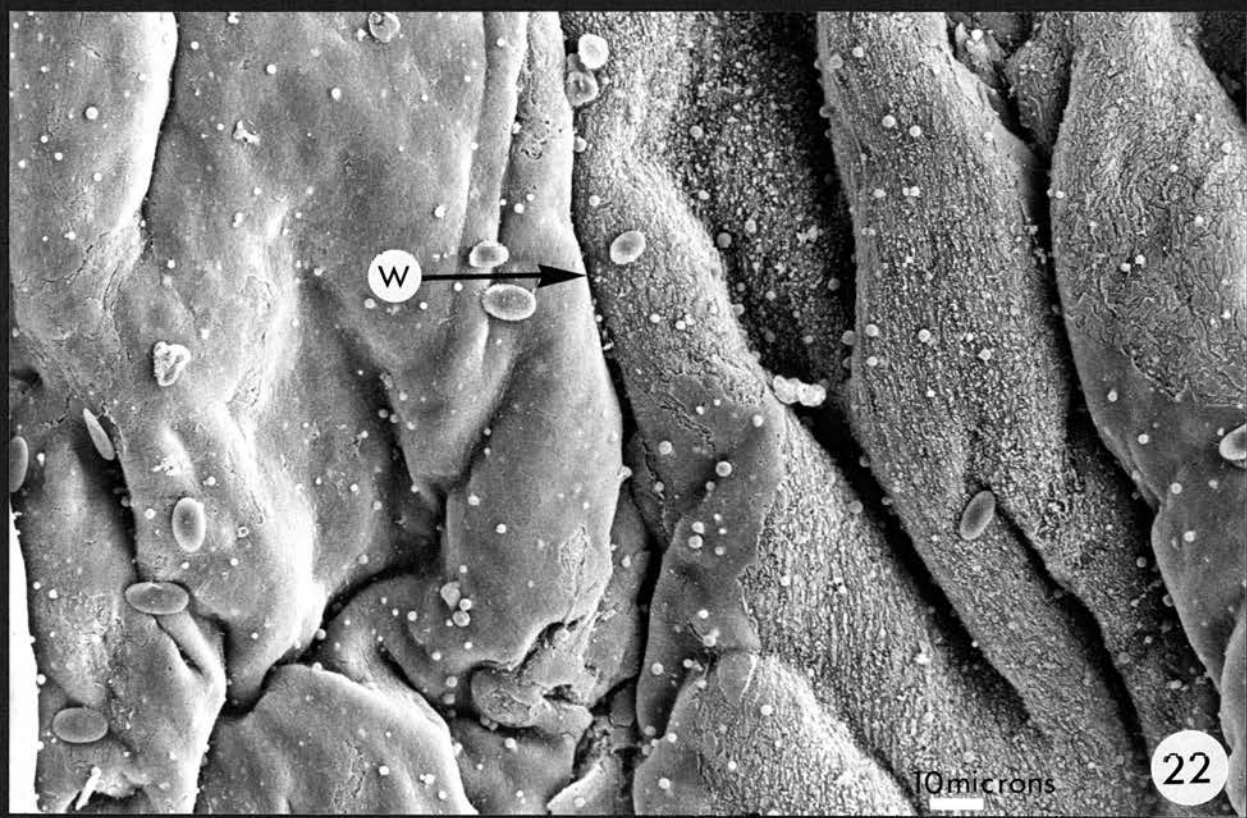
W
10microns
22

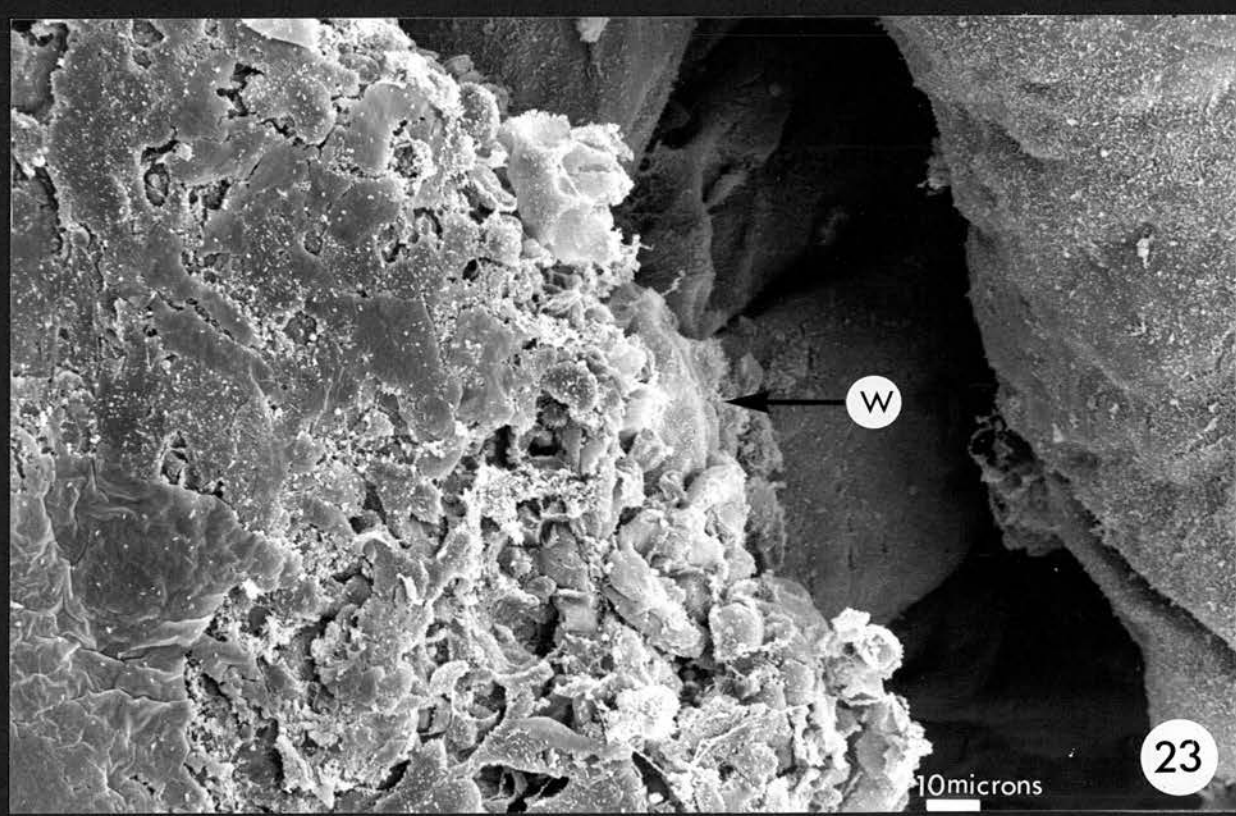
W
10microns
23

PLATE 24: Scanning Electron Microscopy: Wounded CAM 73 hours after injury (complete wound x45)

PLATE 25: Scanning Electron Microscopy: Wounded CAM 73 hours after injury (wound margin x700)

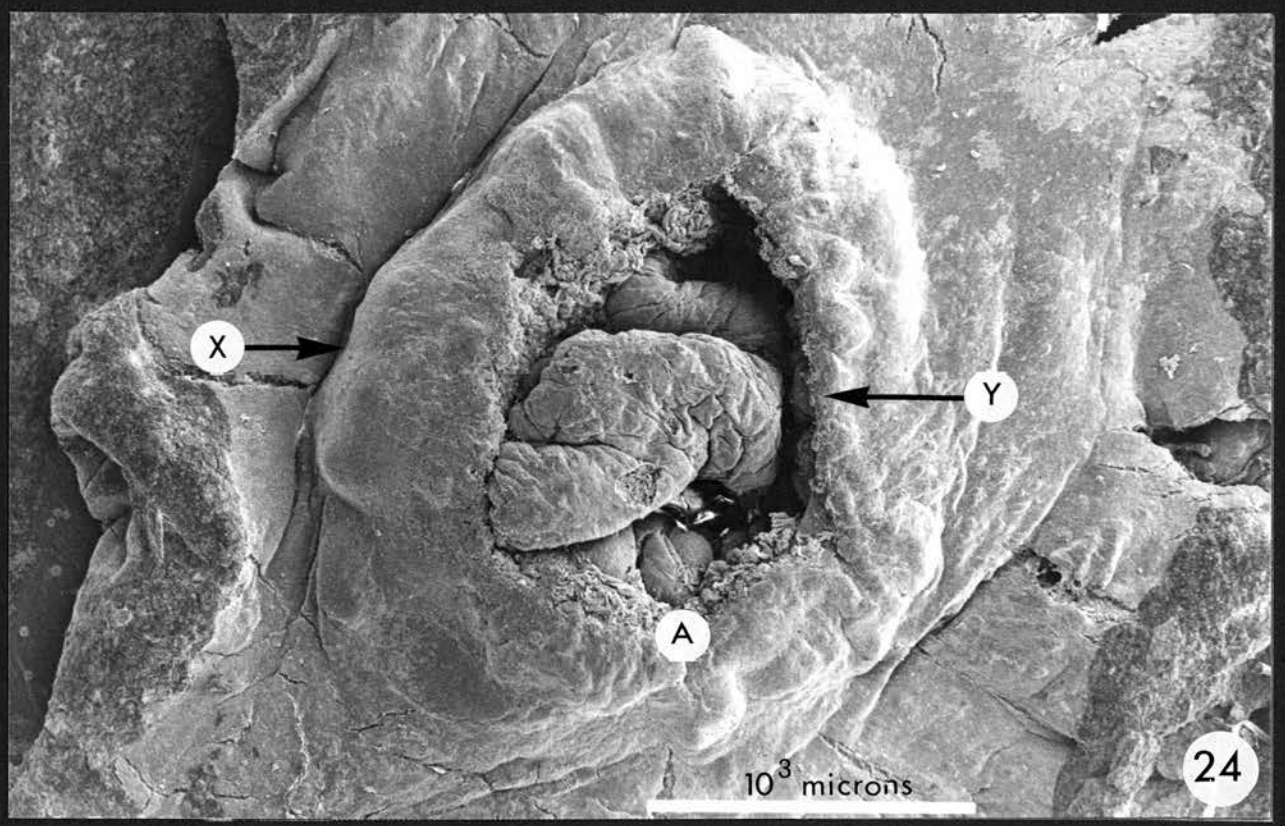
X
Y
A
10^3 microns
24

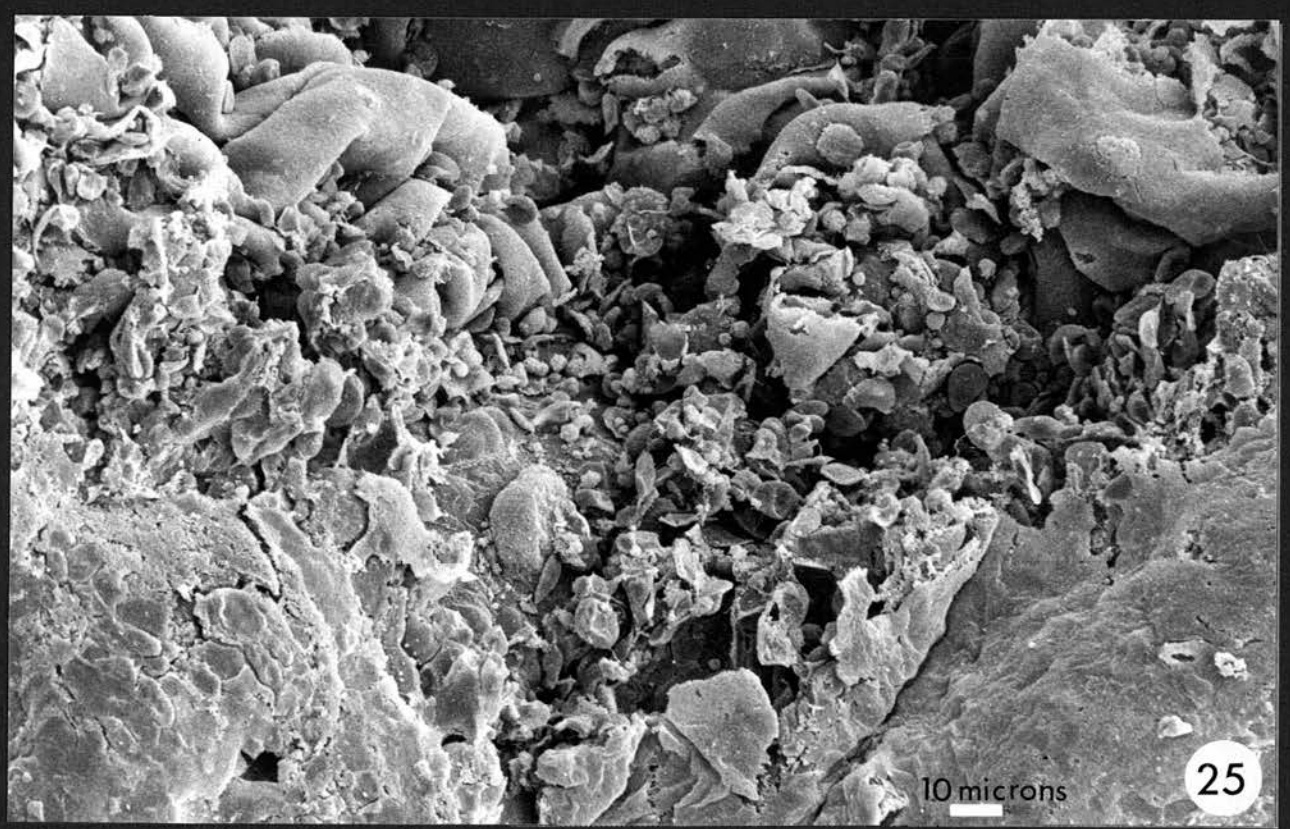
10 microns
25